



GNE-781, A Highly Advanced Potent and Selective Bromodomain Inhibitor of Cyclic Adenosine Monophosphate Response Element Binding Protein, Binding Protein (CBP)

F. Anthony Romero, Jeremy M. Murray, Kwong Wah Lai, Vickie Tsui, Brian K. Albrecht, Le An, Maureen H. Beresini, Gladys de Leon Boenig, Sarah M. Bronner, Emily W. Chan, Kevin X. Chen, Zhongguo Chen, Edna F. Choo, Kyle Clagg, Kevin Clark, Terry D. Crawford, Patrick Cyr, Denise De Almeida Nagata, Karen E. Gascoigne, Jane L. Grogan, Georgia Hatzivassiliou, Wei Huang, Thomas L. Hunsaker, Susan Kaufman, Stefan G. Koenig, Ruina Li, Yingjie Li, Xiaorong Liang, Jiangpeng Liao, Wenfeng Liu, Justin Q. Ly, Jonathan Maher, Colin Masui, Mark Merchant, Yingqing Ran, Alexander M. Taylor, John S. Wai, Fei Wang, Xiaocang Wei, Dong Yu, Bing-Yan Zhu, Xiaoyu Zhu, and Steven R. Magnuson

J. Med. Chem., **Just Accepted Manuscript** • DOI: 10.1021/acs.jmedchem.7b00796 • Publication Date (Web): 11 Sep 2017

Downloaded from <http://pubs.acs.org> on September 11, 2017

Just Accepted

“Just Accepted” manuscripts have been peer-reviewed and accepted for publication. They are posted online prior to technical editing, formatting for publication and author proofing. The American Chemical Society provides “Just Accepted” as a free service to the research community to expedite the dissemination of scientific material as soon as possible after acceptance. “Just Accepted” manuscripts appear in full in PDF format accompanied by an HTML abstract. “Just Accepted” manuscripts have been fully peer reviewed, but should not be considered the official version of record. They are accessible to all readers and citable by the Digital Object Identifier (DOI®). “Just Accepted” is an optional service offered to authors. Therefore, the “Just Accepted” Web site may not include all articles that will be published in the journal. After a manuscript is technically edited and formatted, it will be removed from the “Just Accepted” Web site and published as an ASAP article. Note that technical editing may introduce minor changes to the manuscript text and/or graphics which could affect content, and all legal disclaimers and ethical guidelines that apply to the journal pertain. ACS cannot be held responsible for errors or consequences arising from the use of information contained in these “Just Accepted” manuscripts.



1
2
3
4
5
6
7
8
9
10
11
12
13
14
15
16
17
18
19
20
21
22
23
24
25
26
27
28
29
30
31
32
33
34
35
36
37
38
39
40
41
42
43
44
45
46
47
48
49
50
51
52
53
54
55
56
57
58
59
60

	Wang, Fei; WuXi AppTec Wei, Xiaocang; WuXi AppTec, Yu, Dong; WuXi AppTec Zhu, Bing-Yan; Genentech Zhu, Xiaoyu; Wuxi AppTec Co., Ltd. Magnuson, Steven; Genentech, Discovery Chemistry
--	--

SCHOLARONE™
Manuscripts

1
2
3
4
5
6
7
8
9
10
11
12
13
14
15
16
17
18
19
20
21
22
23
24
25
26
27
28
29
30
31
32
33
34
35
36
37
38
39
40
41
42
43
44

GNE-781, A Highly Advanced Potent and Selective Bromodomain Inhibitor of Cyclic Adenosine Monophosphate Response Element Binding Protein, Binding Protein (CBP)

21
22
23
24
25
26
27
28
29
30
31
32
33
34
35
36
37
38
39
40
41
42
43
44

F. Anthony Romero,^{†} Jeremy Murray,[†] Kwong Wah Lai,[‡] Vickie Tsui,[†] Brian K. Albrecht,[§] Le An,[†] Maureen H. Beresini,[†] Gladys de Leon Boenig,[†] Sarah M. Bronner,[†] Emily W. Chan,[†] Kevin X. Chen,[‡] Zhongguo Chen,[‡] Edna F. Choo,[†] Kyle Clagg,[†] Kevin Clark,[†] Terry D. Crawford,[†] Patrick Cyr,[†] Denise de Almeida Nagata,[†] Karen E. Gascoigne,[†] Jane L. Grogan,[†] Georgia Hatzivassiliou,[†] Wei Huang,[‡] Thomas L. Hunsaker,[†] Susan Kaufman,[†] Stefan G. Koenig,[†] Ruina Li,[†] Yingjie Li,[‡] Xiaorong Liang,[†] Jiangpeng Liao,[‡] Wenfeng Liu,[‡] Justin Ly,[†] Jonathan Maher,[†] Colin Masui,[†] Mark Merchant,[†] Yingqing Ran,[†] Alexander M. Taylor,[§] John Wai,[‡] Fei Wang,[‡] Xiaocang Wei,[‡] Dong Yu,[‡] Bing-Yan Zhu,[†] Xiaoyu Zhu,[‡] Steven Magnuson^{*†}*

45
46
47
48

[†]Genentech, Inc. 1 DNA Way, South San Francisco, California 94080, United States

49
50
51
52
53

[‡]Wuxi Apptec Co., Ltd., 288 Fute Zhong Road, Waigaoqiao Free Trade Zone, Shanghai
200131, People's Republic of China

54
55
56
57
58
59
60

[§]Constellation Pharmaceuticals, Inc. 215 First Street, Suite 200, Cambridge, Massachusetts
02142, United States

Abstract

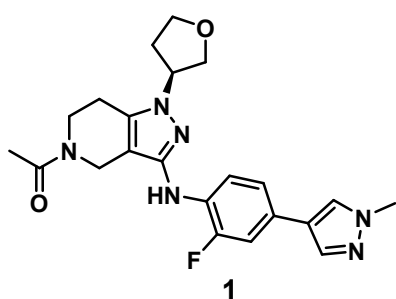
Inhibition of the bromodomain of the transcriptional regulator CBP/P300 is an especially interesting new therapeutic approach in oncology. We recently disclosed in vivo chemical tool **1** (GNE-272) for the bromodomain of CBP that was moderately potent and selective over BRD4(1). In pursuit of a more potent and selective CBP inhibitor we used structure-based design. Constraining the aniline of **1** into a tetrahydroquinoline motif maintained potency and increased selectivity 2-fold. Structure-activity relationship studies coupled with further structure-based design targeting the LPF shelf, BC loop and KAc regions allowed us to significantly increase potency and selectivity, resulting in the identification of non-CNS penetrant **19** (GNE-781; TR-FRET $IC_{50} = 0.94$ nM, BRET $IC_{50} = 6.2$ nM, BRD4(1) $IC_{50} = 5,100$ nM) that maintained good in vivo PK properties in multiple species. Compound **19** displays anti-tumor activity in an AML tumor model and was also shown to decrease Foxp3 transcript levels in a dose dependent manner.

Keywords: Epigenetics, CBP, CREBBP, P300, EP300, bromodomain, bromodomain inhibitor

Introduction

The histone acetyl transferase (HAT) cAMP response element binding protein, binding protein (CREBBP, CBP) and highly homologous paralog, adenoviral E1A binding protein of 300 kDa (EP300, P300) are large, multidomain proteins that each contain a single bromodomain and contribute to transcriptional regulation.¹⁻³ CBP/P300 (hereafter

1
2
3 together referred to as “CBP”) bind to chromatin via their bromodomain. Once associated
4
5 with chromatin, CBP modifies chromatin through its HAT activity, leading to the
6
7 recruitment of various transcriptional proteins to modulate gene expression. CBP has
8
9 been shown to bind non-histone proteins and to recognize acetylated p53 at K382
10
11 following DNA damage.³ There have been several studies that have implicated CBP in
12
13 the development, maintenance or progression of cancer and tumor immunity.⁴⁻⁸ Studies
14
15 have shown that inhibition of the bromodomain of CBP regulates *MYC*⁹ (a regulator gene
16
17 that plays a role in cell cycle progression and that is amplified in many cancers). Other
18
19 studies have demonstrated that CBP bromodomain inhibition impairs differentiation of
20
21 regulatory T cells (T_{regs}) and immunosuppressive function.¹⁰ To help understand the
22
23 physiological implications of CBP in disease states, much work has centered around
24
25 discovering novel chemical tools that inhibit the bromodomain of CBP.¹¹⁻¹⁹ These studies
26
27 have revealed that inhibition of the CBP bromodomain is a promising new therapeutic
28
29 approach in oncology and immuno-oncology.
30
31
32
33
34
35
36
37
38
39
40
41
42
43
44
45
46
47
48
49
50
51
52
53
54
55
56
57
58
59
60



1

CBP IC₅₀ = 20 nMBRD4(1) IC₅₀ = 13,000 nMBRD4(1) IC₅₀ / CBP IC₅₀ = 650CBP BRET IC₅₀ = 410 nM*MYC* EC₅₀ = 910 nM

Figure 1. In vivo chemical tool **1** and potency data.

1
2
3
4
5
6 We recently reported an in vivo chemical tool (**1**, GNE-272, Figure 1) as an inhibitor of
7
8 the bromodomain of CBP that was potent and 650-fold selective over the bromodomain 1
9
10 of the bromodomain-containing protein 4 [BRD4(1)] (BET bromodomain surrogate). We
11
12 demonstrated through in vivo studies that **1** is able to modulate CBP *MYC* expression that
13
14 corresponds with anti-tumor activity in a *MYC*-dependent acute myeloid leukemia (AML)
15
16 model. While **1** is a promising in vivo tool to investigate CBP biology, we wished to
17
18 extend our efforts to develop a more drug-like compound with improved cell potency and
19
20 increased bromodomain selectivity, particularly over the bromodomain and extra terminal
21
22 (BET) family.²⁰ Here we describe the design of **19** (GNE-781; 3-[7-(difluoromethyl)-6-
23
24 (1-methylpyrazol-4-yl)-3,4-dihydro-2*H*-quinolin-1-yl]-*N*-methyl-1-tetrahydropyran-4-yl-
25
26 6,7-dihydro-4*H*-pyrazolo[4,3-*c*]pyridine-5-carboxamide), a highly potent and selective
27
28 CBP inhibitor that is efficacious in a MOLM-16 AML xenograft model. Additionally, in
29
30 vitro studies show that **19** reduces FOXP3 (forkhead box P3) transcript levels, confirming
31
32 earlier studies¹⁰ with a less optimal chemical probe and suggesting that inhibition of the
33
34 CBP bromodomain may provide a novel small molecule therapeutic approach for cancer
35
36 immunotherapy.
37
38
39
40
41
42
43
44
45

46 **Results and Discussion**

47
48 Co-crystal structures of **1** bound to both CBP and BRD4(1) provided insight towards
49
50 understanding the selectivity preference of this compound for CBP over BRD4(1) (Figure
51
52 2).¹² Previously we have shown that **1** binds to CBP and BRD4(1) in different
53
54 conformations.¹² While **1** binds in a lower energy conformation in CBP, this compound
55
56
57
58
59
60

1
2
3 binds at a higher energy conformation in BRD4(1) due to a residue difference in the WPF
4 motif: Trp81, Pro82 and Phe83 for BRD4(1), and Leu1109, Pro1110 and Phe1111 for
5 CBP (Figure 2).²¹ Upon binding to BRD4(1), the fluorophenylpyrazole arm of **1** is
6 pushed into a strained conformation in-plane with the pyrazolopiperidine core to avoid
7 clashing with Trp81.¹² With this in mind, we hypothesized that selectivity could be
8 increased further on this scaffold by constraining the aniline nitrogen of **1** in a bicycle,
9 thus limiting the ability of the fluorophenylpyrazole to become co-planar with the
10 pyrazolopiperidine core in the BRD4(1) binding site. Accordingly, we explored three
11 saturated ring-size analogues (5, 6 or 7-membered) of **1**. While indoline **2** had a slight
12 decrease in CBP potency and selectivity compared to parent **1**, tetrahydroquinoline
13 (THQ) **3** maintained CBP potency and improved selectivity by nearly 2-fold. Expanding
14 the ring further to a seven-membered ring (**4**) resulted in a significant loss in CBP
15 potency indicating the preferred conformations of the 7-membered ring are not
16 accommodated in the binding site of CBP. We therefore used **3** as a template from which
17 to further improve potency and selectivity. Since inhibition of the BET family
18 bromodomains produces profound phenotypes we were particularly focused on
19 selectivity over BRD4(1) (our surrogate for BET bromodomains).
20
21
22
23
24
25
26
27
28
29
30
31
32
33
34
35
36
37
38
39
40
41
42
43
44
45
46
47
48
49
50
51
52
53
54
55
56
57
58
59
60

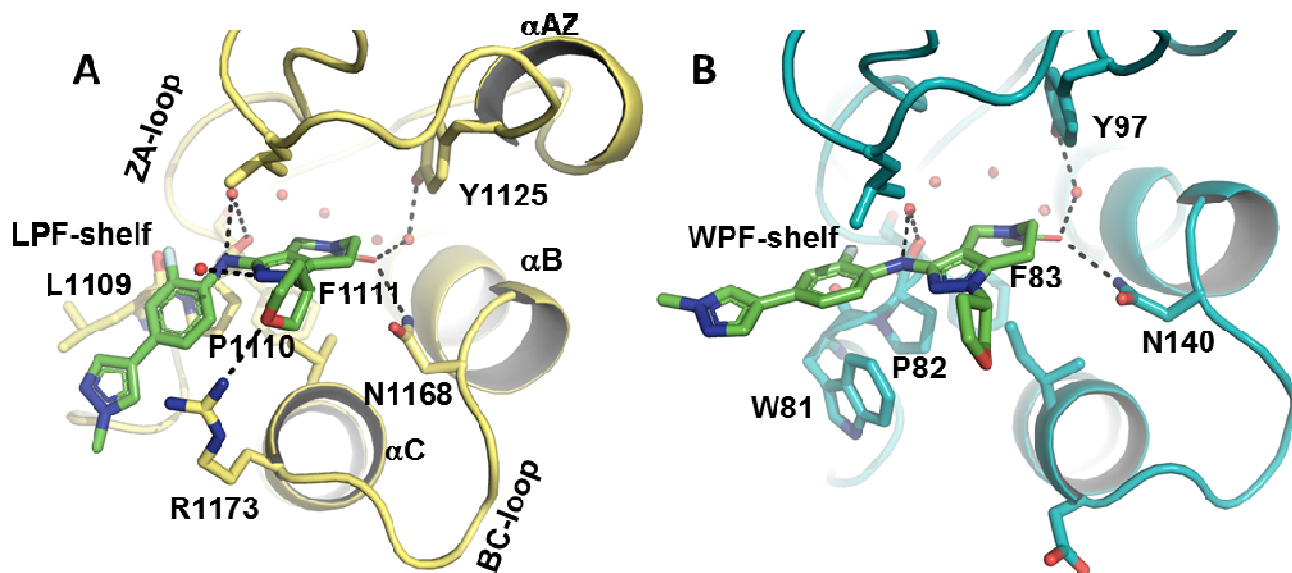
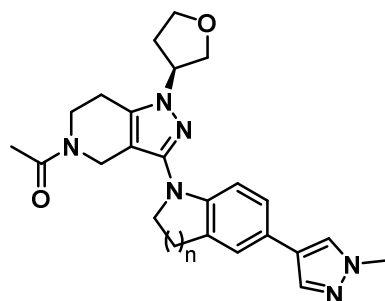


Figure 2. (A) A co-crystal structure of **1** (green) in the CBP bromodomain (yellow, 1.23 Å resolution, PDB code: 5KTX) highlighting hydrogen bond interactions between the ligand and receptor. Water molecules are shown as small red spheres. (B) A co-crystal structure of **1** (green) and BRD4(1) (cyan, 1.14 Å resolution, PDB code: 5KU3) highlighting hydrogen bond interactions between the ligand and receptor. Water molecules are shown as small red spheres.

Table 1. Constrained analogues of **1**



Cmpd	n	CBP	BRD4(1)	Fold Selectivity ^b
		IC ₅₀ (nM) ^a	IC ₅₀ (nM) ^a	
2	1	31	12,000	387
3	2	16	20,000	1,250
4	3	1,800	>20,000	>11

1
2
3
4
5
6
7
8
9
10
11
12
13
14
15
16
17
18
19
20
21
22
23
24
25
26
27
28
29
30
31
32
33
34
35
36
37
38
39
40
41
42
43
44
45
46
47
48
49
50
51
52
53
54
55
56
57
58
59
60

^aAll IC₅₀ values are reported as the geometric mean from at least two determinations. TR-FRET assay with the isolated CBP or BRD4(1) bromodomain. ^bFold selectivity is defined by [BRD4(1) IC₅₀ (nM) / CBP IC₅₀ (nM)]

We obtained a co-crystal structure of **3** with the bromodomain of CBP (Figure 3). As observed with **1**, the amide of **3** binds in the acetylated lysine (KAc) binding site, with the amide carbonyl making a canonical hydrogen bond to Asn1168 and additional water-mediated hydrogen bond interactions to Tyr1125. The pyrazolopiperidine core is sandwiched between the gatekeeper (Val1174) and Leu1120. The THQ ring makes van der Waals interactions with Pro1110 and Leu1120. The *N*-methylpyrazole packs along the lipophilic surface defined by the LPF shelf (Leu1109, Pro1110, Phe1111). Examination of the **3**-CBP co-crystal structure revealed several areas in the binding site that could be explored to potentially improve potency. Initially, we examined structure-activity relationships (SAR) targeting Arg1173, the BC loop, and the KAc binding pocket.

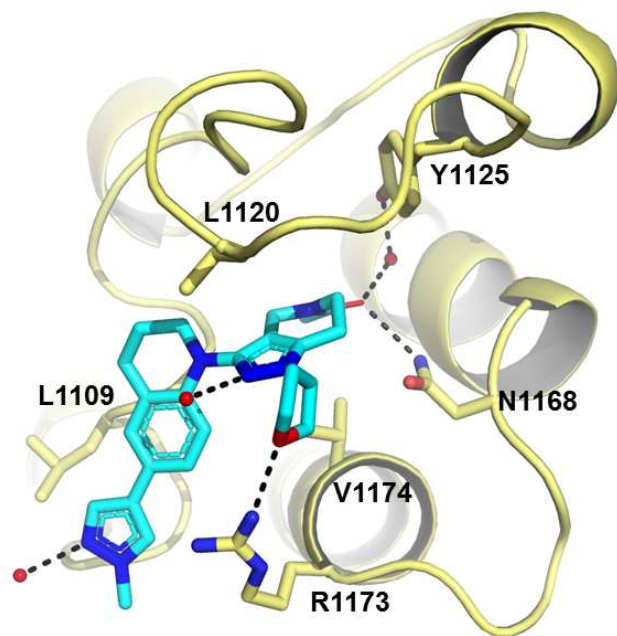
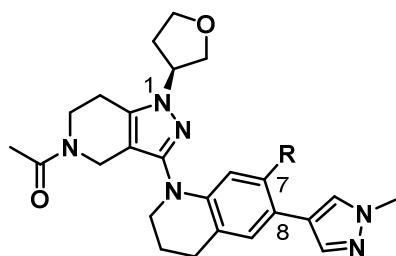


Figure 3. A co-crystal structure of **3** in the CBP (cyan) bromodomain (yellow, 1.6 Å resolution, PDB code: 5W0F) displaying important contacts between the ligand and receptor. Water molecules are shown as small red spheres.

We sought to improve the affinity of **3** by making favorable interactions with residues in the LPF shelf and Arg1173 through the introduction of various substituents to the 7-position of the THQ ring (Table 2).²² To explore potential hydrophobic interactions with the methylene side-chain of Arg1173 and to test the feasibility of disrupting the planarity between the *N*-methyl pyrazole and the phenyl ring of the THQ, methyl (**5**), chloro (**6**) and methoxy (**7**) substitutions were evaluated, resulting in each case in a 3.4–3.7-fold increase in CBP potency. The selectivity of **5** and **6** for CBP over BRD4(1) was comparable to parent **3** while **7** had reduced (~3-fold) selectivity for CBP. In order to further increase van der Waals interactions with residues in the LPF shelf and potentially interact with the guanidine atoms of Arg1173, fluorine atoms were added to the 7-methyl

1
2
3 of **5**. Notably, difluoro **8** demonstrated an 11-fold increase in CBP inhibitory potency
4 compared to **3** and exhibited selectivity (BRD4/CBP) substantially exceeding that of **3**.
5
6 Additionally, **8** had significantly improved cell potency (CBP BRET $IC_{50} = 37$ nM).
7
8 Trifluoro analogue **9** was also quite potent, but had lower selectivity compared to **8**.
9
10 While **9** was potentially an interesting compound itself to follow up, we choose **8** to
11 further examine SAR since it had a more favorable lipophilic ligand efficiency ($cLogP^{23}$
12 $= 2.1$; $LLE^{24} = 6.9$) compared to **9** ($cLogP = 3.6$; $LLE = 5.4$). To further understand the
13 increased CBP potency of **8** we obtained a co-crystal structure of **8** and the CBP
14 bromodomain (Figure 4). The crystal structure revealed that while **8** had a similar binding
15 mode compared to **3**, additional favorable dipolar interactions between the partial
16 negative charge on the fluorines of the 7-difluoromethyl and the positively charged
17 guanidine on Arg1173 were observed. Relative to **3**, the *N*-methylpyrazole is rotated and
18 lies out of plane by $\sim 30^\circ$, as expected due to the CF_2H substitution (see Supporting
19 Information for torsion scan plot). As a result, the *N*-methylpyrazole sits in a shallow
20 crevice on the surface of CBP that is formed by the side-chains of Leu1109, Val1174,
21 Phe1177 of the LPF shelf, and the $C\beta$ of Arg1173.
22
23
24
25
26
27
28
29
30
31
32
33
34
35
36
37
38
39
40
41
42

43 **Table 2.** Substitution at the 7-position of the THQ
44
45
46
47
48
49
50
51
52
53
54
55
56
57
58
59
60



Cmpd	R	CBP IC ₅₀ (nM) ^a	BRD4(1) IC ₅₀ (nM) ^a	CBP BRET IC ₅₀ (nM) ^b	Fold Selectivity ^c
3	H	16	20,000	320	1,250
5	CH ₃	4.4	7,300	120	1,659
6	Cl	4.3	4,800	68	1,116
7	OCH ₃	4.7	2,200	140	468
8	CF ₂ H	1.4	5,600	37	4,000
9	CF ₃	1.5	4,400	39	2,933

^aAll IC₅₀ values are reported as the geometric mean from at least two determinations. ^bBRET assay in HEK293 cells transiently transfected with CBP-Nanoluc and Histone H3.3-Halo tag constructs. ^cFold selectivity is defined by [BRD4(1) IC₅₀ (nM) / CBP IC₅₀ (nM)].

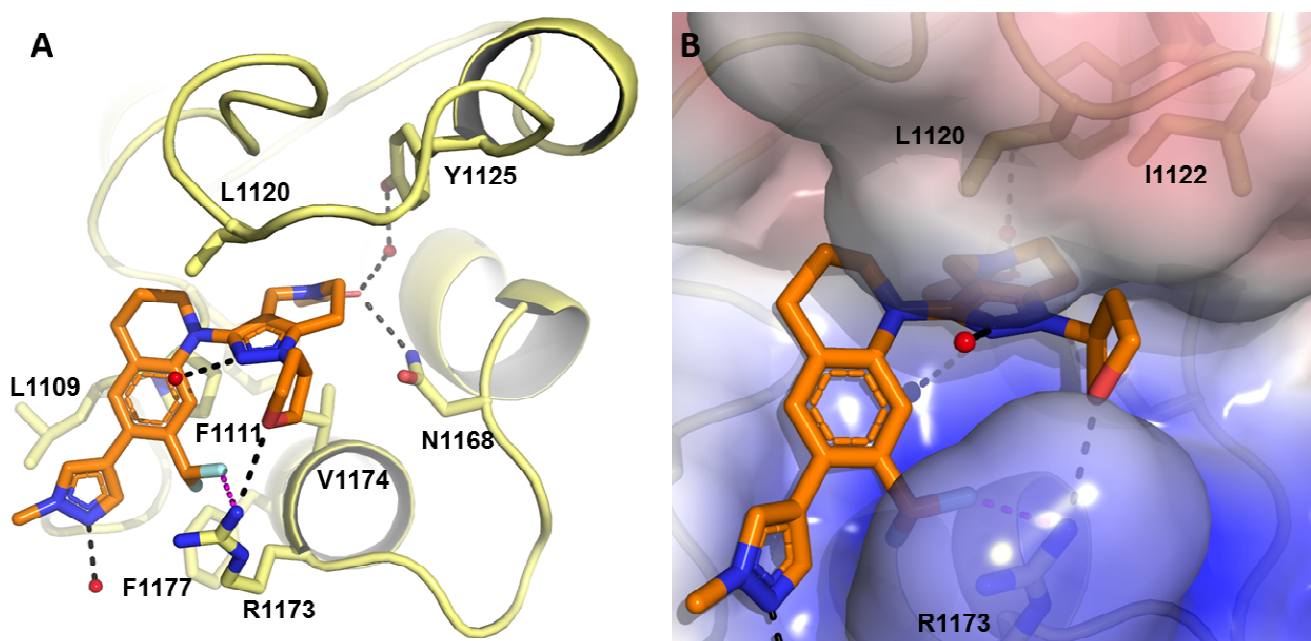


Figure 4. (A) Co-crystal structure of **8** (orange) in the CBP bromodomain (yellow, 1.43 Å

1
2
3 resolution, PDB code: 5W0I) displaying important contacts between the ligand and receptor.
4
5 Water molecules are shown as small red spheres. (B) The solvent accessible surface of the CBP
6
7 bromodomain colored to highlight hydrophobicity and charge where hydrocarbon groups are
8
9 white; atoms with a partial negative charge are red; atoms with partial positive charge are blue.
10
11 Bound ligand **8** is shown in stick representation (orange). Water molecules are shown as small
12
13 red spheres.
14
15
16
17
18
19

20
21 Further inspection of the co-crystal structure of **8** and CBP suggested that we could explore N1-
22
23 substitution of the pyrazolopiperidine might increase hydrophobic interactions with residues in
24
25 the BC and ZA loops. Figure 4B displays the surface of the protein around the THF moiety of **8**
26
27 and indicates that expanding the THF to a 6-membered ring could increase van der Waals
28
29 interactions with Leu1120 and Ile1122. Tetrahydropyran (THP) **10** resulted in an increase in both
30
31 biochemical and cell potency (Table 3; it should be noted that the effective lower limit of the
32
33 CBP TR-FRET assay is 1 nM, as the CBP concentration is 2 nM). Additionally, the stability of
34
35 **10** in liver microsomes (LM) increased compared to **8**. A co-crystal structure of **10** with CBP
36
37 shows similar interactions to those described for **3** and **8** with the exception of the THP ring
38
39 (Figure 5). Rather than pointing towards Arg1173 as observed with the THF moiety, the oxygen
40
41 atom of the THP pointed out towards solvent in the BC loop region and suggested that this
42
43 region would enable us to tune physicochemical properties. To reduce the $c\text{LogP}^{23}$ of **10** we
44
45 investigated the addition of polar substituents to this area of the binding site. The structure
46
47 suggested that these modifications would have minimal effect on the biochemical potency and
48
49 potentially would increase LM stability. Removing the oxygen atom of the THP ring of **10**
50
51 afforded cyclohexane **11** that had decreased CBP inhibitory potency. To further investigate polar
52
53
54
55
56
57
58
59
60

1
2
3 atoms in this area, the oxygen atom of **10** was replaced with a nitrogen to make piperidines **12**
4 and **13**. While the biochemical potency of **12** only decreased slightly compared to **10**, there was a
5
6 significant decrease in cell potency presumably that may indicate poor permeability of this
7
8 compound. The *N*-methyl piperidine **13** rescues the cell potency of **12**, but leads to increased
9
10 cLogP. The decrease in LM stability observed for **13** may be attributed to the increased cLogP.
11
12 To lower cLogP and increase LM stability, we evaluated analogues **14**, **15** and **16**. This afforded
13
14 compounds with reduced cellular potency compared to **10**, but limited increase in LM stability.
15
16 Ultimately, **10** (GNE-049) was selected for further profiling as it had the best balance of LM
17
18 stability, selectivity and cellular potency (Figure 6). Furthermore, **10** demonstrated acceptable
19
20 PK in mouse, rat, dog and monkey. Determination of potency versus a selection of
21
22 bromodomains revealed that this compound is selective for CBP/P300 (full bromodomain
23
24 selectivity profile provided in Supporting Information) and, importantly, quite selective (3,820-
25
26 fold) over BRD4(1). The compound had excellent potency in the BRET cellular assay and, in an
27
28 orthogonal measure of the target engagement, **10** was shown to inhibit the expression of *MYC*⁹
29
30 (MV4-11 cell line) with an EC₅₀ of 14 nM. Compound **10** was further evaluated in a rat single
31
32 dose (30–250 mg/kg QD) toxicokinetic study (data not shown). Adverse central nervous system
33
34 (CNS)-related signs (*e.g.*, marked hyperactivity and vocalization) were observed in several of the
35
36 rats at the 250 mg/kg dose level. Furthermore, at the 250 mg/kg dose level, the ratio of the
37
38 unbound drug concentration in brain to unbound drug concentration in plasma ($K_{p,uu}$) 3 hours
39
40 post dose was determined to be 0.43 indicating that compound was penetrating into the CNS, and
41
42 potentially resulting in the observed toxicity.
43
44
45
46
47
48
49
50
51
52
53
54

55 **Table 3.** Exploration of SAR in the BC loop region of CBP
56
57
58
59
60



Cmpd	R	CBP ^a IC ₅₀ (nM)	BRD4(1) ^a IC ₅₀ (nM)	CBP BRET ^a IC ₅₀ (nM)	Fold Selectivity ^b	LM Cl _{hep} ^c M / R / H	cLogP
8		1.4	5,600	37	4,000	55 / 24 / 13	2.1
10		1.1	4,200	12	3,820	29 / 21 / 9.4	2.5
11		3.1	9,500	45	3,070	62 / 45 / 19	4.0
12		1.5	3,100	690	2,070	<18 / <7.7 / <4.8	2.2
13		2.0	4,200	98	2,100	54 / 22 / 17	2.8
14		1.0	4,100	53	4,100	39 / <6.1 / 10	2.1
15		1.2	4,000	46	3,300	25 / 23 / 6.2	1.7
16		1.2	5,400	41	4500	31 / 18 / 5.3	0.99

^aAll IC₅₀ values are reported as the geometric mean from at least two determinations. ^bFold selectivity is defined by [BRD4(1) IC₅₀ (nM) / CBP IC₅₀ (nM)]. ^cMouse (M), rat (R) and human (H) liver microsome-predicted hepatic clearance (mL/min/kg).

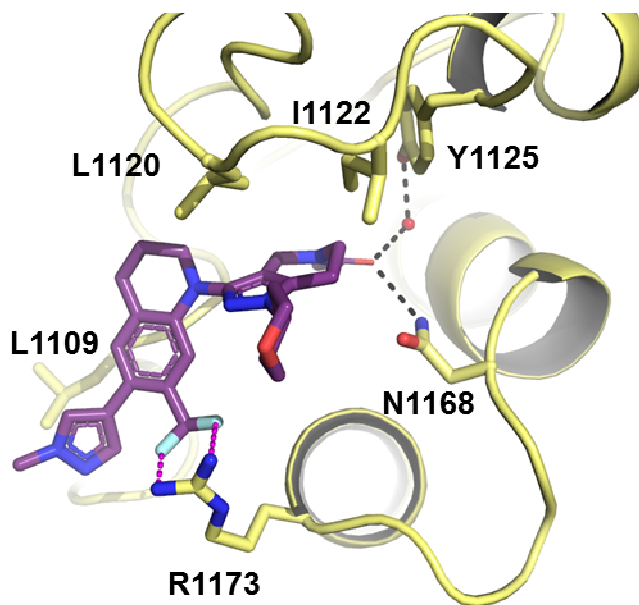
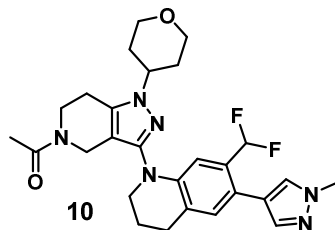


Figure 5. (A) Co-crystal structure of **10** (purple) in the CBP bromodomain (yellow, 1.55 Å resolution, PDB code: 5W0L) displaying important contacts between the ligand and receptor. Water molecules are shown as small red spheres.



							Selectivity	
							Bromodomain	IC ₅₀ (nM) ^a
CBP	P300	CBP BRET		Myc			BAZ2B	>20,000
IC₅₀ (nM)^a	IC₅₀ (nM)^a	IC₅₀ (nM)^a		EC₅₀ (nM)^a			BPTF	>20,000
1.1	1.3	12		14			BRD4(1)	4,200
<i>In vitro</i> stability & binding							BRD4(2)	>20,000
Papp	PPB (%)^c	LM Cl_{hep}^d		Hep Cl_{hep}^e			BRD8(1)	>20,000
(A to B)^b	M/R/D/C/H	M/R/D/C/H		M/R/D/C/H			BRD9	>20,000
15	92/88/81/79/84	32/21/16/22/10		<21/15/<7.8/<8.8/<6.2			BRPF1	>20,000
PK Parameters							CECR2	14,000
Species	CL	t_{1/2}	F	V_{ss}	C_{max}	AUC_{last}	GCN5L	>20,000
	(mL/min/kg)	(h)	(%)	(L/kg)	(μM)	(hr*μM)	PCAF	>20,000
Mouse ^f	8.8	1.1	72	0.81	4.2	13.7	TAF1(1)	>20,000
Rat ^f	16	0.66	93	0.81	3.2	9.4	TAF1(2)	>20,000
Dog ^g	4.6	4.2	94	1.0	5.1	31		
Cyno ^g	7.4	2.8	39	1.4	1.6	8.5		

cLogP: 2.5

Kinetic Solubility: 76 μM

^aAll IC₅₀ values are reported as the geometric mean from at least two determinations. ^bMDCK cell line; apical-to-basolateral; units = ×10⁻⁶ cm s⁻¹. ^cMouse (M), rat (R), dog (D), cynomolgus monkey (C) and human (H) plasma protein binding. ^dLiver microsome-predicted hepatic clearance (mL/min/kg). ^eHepatocyte-predicted hepatic clearance (mL/min/kg). ^fCompound was dosed i.v. (1 mg/kg) as PEG400/H₂O (35/65) solution and p.o. (5 mg/kg) as an aqueous suspension with 0.5% methylcellulose and 0.2% Tween 80. ^gCompound was dosed i.v. (1 mg/kg) as EtOH/PEG400/H₂O (20/15/65) solution and p.o. (5 mg/kg) as an aqueous suspension with 0.5% methylcellulose and 0.2% Tween 80.

Figure 6. Summary of potency, selectivity and DMPK properties of **10**.

In pursuit of a more drug-like CBP inhibitor, we sought a compound with a similar profile to **10**, but with limited CNS penetration. To do this we targeted a molecule with increased total polar

1
2
3 surface area (*t*PSA) (**10** *t*PSA = 68) and containing an additional H-bond donor. Previously, as
4 part of our screening efforts, we had run a high-concentration fragment screen attempting to find
5 alternative and novel Asn1168 binding chemotypes (not shown) and identified a highly ligand
6 efficient²⁵ fragment, **17** (CBP IC₅₀ = 18 μM, LE = 0.41), that displayed >6-fold selectivity for
7 CBP over BRD4 (Figure 7A). A co-crystal structure of this compound bound to the CBP
8 bromodomain (Figure 7B) revealed the methyl urea moiety to be occupying the KAc binding
9 pocket. The NH of the urea makes a hydrogen bond with the backbone of Pro1110, and the
10 methyl group of the urea making van der Waals interactions with Phe1111. Interestingly, the
11 phenyl ring of Phe1111 is rotated slightly such that the Cδ1 and Cε1 atoms are 0.8 Å and 0.9 Å
12 from their positions when bound to **10** (Figure 7C). From the structure of **10** overlaid with **17**, it
13 appeared that the key Asn-binding acetamide of **10** could be replaced with a urea moiety. We
14 therefore explored a small set of substituted urea analogues of **10** (Table 4). Primary urea **18**
15 matched the biochemical potency of **10** and displayed a remarkable 9,600-fold selectivity for
16 CBP over BRD4(1). Methyl urea **19**, the same group present in fragment hit **17**, afforded
17 subnanomolar biochemical potency, 5,425-fold selectivity for CBP over BRD4(1) and <10 nM
18 cellular potency. To further probe the KAc pocket we made ethyl urea **20** and *N,N*-dimethyl urea
19 **21**, but these resulted in 33-fold and 330-fold losses in potency, respectively, compared to **19**.
20 The significant loss in potency observed with **21** was expected since it was assumed that the NH
21 of the urea was participating in a H-bond with the backbone of Pro1110 similar to that observed
22 with the **17**-CBP crystal structure.
23
24
25
26
27
28
29
30
31
32
33
34
35
36
37
38
39
40
41
42
43
44
45
46
47
48
49
50
51
52
53
54
55
56
57
58
59
60

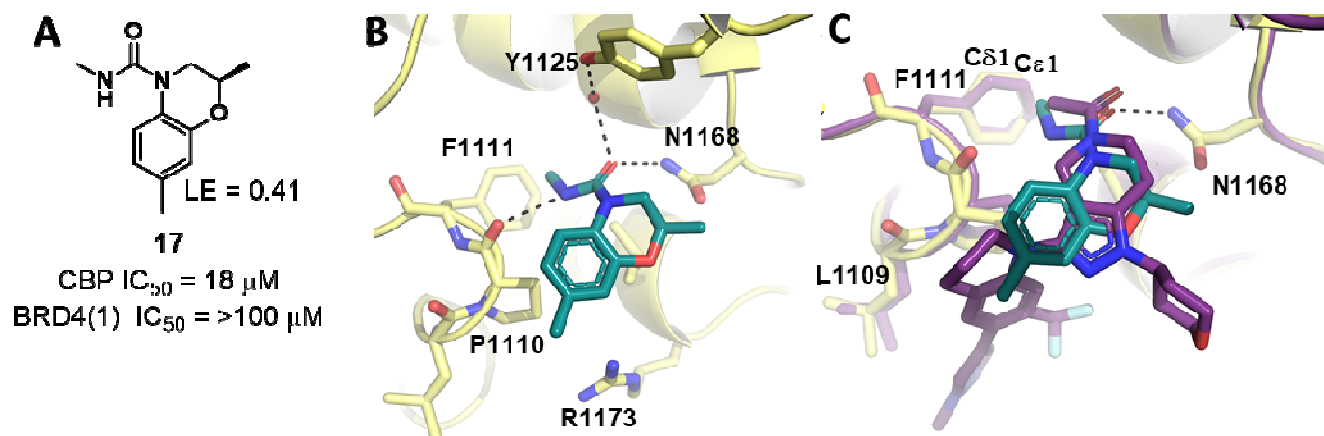


Figure 7. (A) CBP-selective fragment screening hit **17**. (B) Co-crystal structure of **17** (aqua) and the CBP bromodomain (yellow, 1.7 Å resolution; PDB code: 5W0Q). Residues engaging in important contacts between the ligand and receptor are shown in stick representation. Water molecules are shown as small red spheres. (C) Compound **17** (aqua) overlaid with **10** (purple) in the CBP binding site (yellow).

Table 4. Exploring the KAc binding site with urea substitution

Cmpd	R	CBP ^a IC ₅₀ (nM)	BRD4(1) ^a IC ₅₀ (nM)	CBP BRET ^a IC ₅₀ (nM)	Fold Selectivity ^b
10	CH ₃	1.1	4,200	12	3,818
18	NH ₂	1	9,600	28	8,727
19	NHCH ₃	0.94	5,100	6.2	5,425
20	NHCH ₂ CH ₃	31	>20,000	530	>645
21	N(CH ₃) ₂	310	15,000	3,700	48

1
2
3 ^aAll IC₅₀ values are reported as the geometric mean from at least two determinations. ^bFold
4
5
6 selectivity is defined by [BRD4(1) IC₅₀ (nM) / CBP IC₅₀ (nM)]
7
8
9

10
11 To further understand the selectivity of **19** we obtained co-crystal structures of this compound
12
13 with CBP and BRD4(1) (Figure 8). In the **19**-CBP co-crystal structure, similar interactions with
14
15 the binding site are observed as seen in the **10**-CBP co-crystal crystal structure, with an
16
17 additional interaction provided by the methyl urea of **19** (Figure 8A). As observed in the **17**-CBP
18
19 co-crystal structure, the urea NH of **19** makes a hydrogen bond with the backbone of Pro1110
20
21 and the methyl group of the urea makes van der Waals interactions with Phe1111.
22
23 Unsurprisingly, the C δ 1 and C ϵ 1 atoms of Phe1111 shifted by 0.8 Å and 1.0 Å, respectively,
24
25 relative to the **10** structure, consistent with the shifts observed in the **17**-CBP co-crystal structure.
26
27 In BRD4, Trp81 from the WPF shelf served as a lipophilic “protrusion” compared to CBP’s LPF
28
29 “wall” (Figure 8B). As a result, the THQ of **19** is rotated in BRD4(1) such that the phenyl ring
30
31 makes van der Waals contacts with Leu92 from the BC loop while the *N*-methylpyrazole is
32
33 completely solvent-exposed. The ligand-receptor complementarity of **19** in BRD4 is less optimal
34
35 relative to **19** bound to CBP, providing an explanation for the selectivity.
36
37
38
39
40
41
42
43
44
45
46
47
48
49
50
51
52
53
54
55
56
57
58
59
60

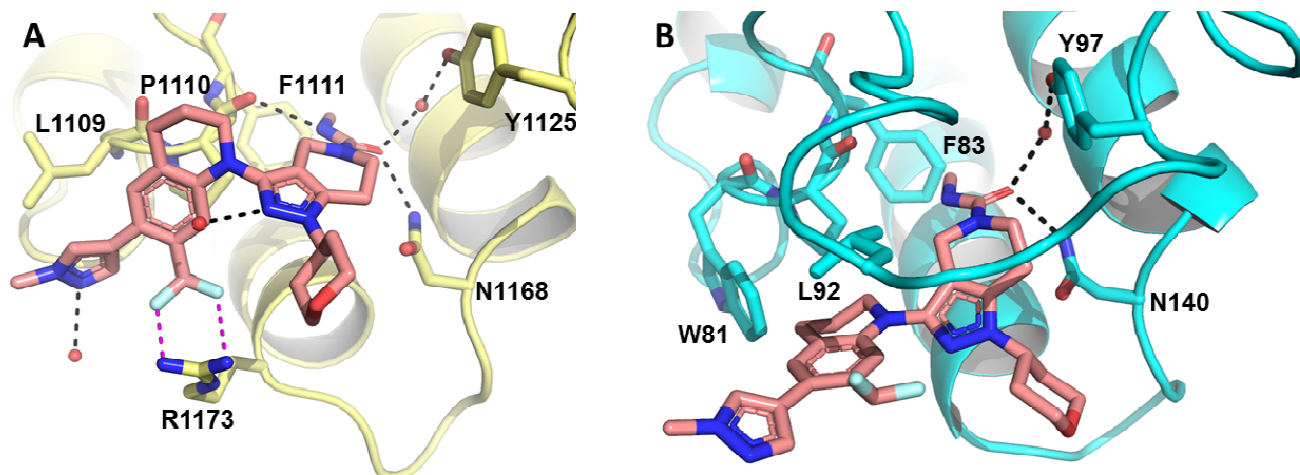
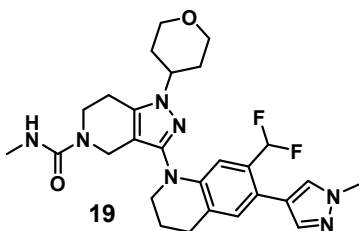


Figure 8. (A) Co-crystal structure of **19** (pink) and the CBP bromodomain (yellow, 1.41 Å resolution; PDB code: 5W0E). Residues engaging in important contacts between the ligand and receptor are shown in stick representation. Water molecules are shown as small red spheres. (B) Co-crystal structure of **19** (pink) and the BRD4(1) bromodomain (cyan, 1.71 Å resolution; PDB code: 5VZS). Residues engaging in important contacts between the ligand and receptor are shown in stick representation. Water molecules are shown as small red spheres.

Based on the cell potency and selectivity of **19**, we further profiled this compound (Figure 9). Compound **19** showed moderate to low clearance in vivo in all species evaluated, with acceptable oral bioavailability. Examination of a subset of bromodomains revealed that this compound is exquisitely selective for CBP/P300 (full bromodomain selectivity profile provided in Supporting Information) and is remarkably selective for CBP (5,425-fold) and P300 (4,250-fold). When tested (full details in Supporting Information) in an Invitrogen kinase panel (1 μM, 220 kinases) **19** did not inhibit any target at >10%, and in a Cerep off-target screening panel (10 μM, 43 receptors), **19** did not inhibit any target at >39%. In addition, **19** did not inhibit (>10 μM,

top concentration) several cytochrome P450s (3A4, 1A2, 2C9, 2C19, 2D6). The compound had excellent and comparable potency (<10 nM) between the BRET and MYC cellular assays. Furthermore, when **19** was dosed in a rat at 250 mg/kg, the $K_{p,uu}$ (3 hours post dose) was determined to be 0.02 (compared to 0.43 for **10**), indicating that there was little brain penetration of this compound, and no adverse CNS-related signs were observed.



				Selectivity		
CBP	P300	CBP BRET	Myc	Bromodomain	IC ₅₀ (nM) ^a	
IC ₅₀ (nM) ^a	IC ₅₀ (nM) ^a	IC ₅₀ (nM) ^a	EC ₅₀ (nM) ^a			
0.94	1.2	6.2	6.6	BAZ2B	>18,000	
<i>In vitro</i> stability & binding				BPTF	>20,000	
Papp	PPB (%) ^c	LM Cl _{hep} ^d	Hep Cl _{hep} ^e	BRD4(1)	5,100	
(A to B) ^b	M/R/D/C/H	M/R/D/C/H	M/R/D/C/H	BRD4(2)	12,000	
19	94/94/77/78/84	35/18/17/23/10	<21/<10/<7.8/24/<6.2	BRD8(1)	>20,000	
PK Parameters				BRD9	>20,000	
Species	CL (mL/min/kg)	t _{1/2} (h)	F (%)	V _{ss} (L/kg)	C _{max} (μM)	AUC _{last} (hr*μM)
Mouse ^f	5.2	1.4	73	0.60	23	6.5
Rat ^f	3.8	3.7	37	0.64	4.1	16
Dog ^g	4.8	4.7	100	1.5	8.3	44
Cyno ^g	18	0.72	28	1.0	1.9	2.5

cLogP: 2.4
Kinetic Solubility: 95 μM

^aAll IC₅₀ values are reported as the geometric mean from at least two determinations. ^bMDCK cell line; apical-to-basolateral; units = ×10⁻⁶ cm s⁻¹. ^cMouse (M), rat (R), dog (D), cynomolgus monkey (C) and human (H) plasma protein binding. ^dLiver microsome-predicted hepatic clearance (mL/min/kg). ^eHepatic clearance (mL/min/kg). ^fCompound was dosed i.v. (1 mg/kg) as PEG400/H₂O (35/65) solution and p.o. (5 mg/kg) as an aqueous suspension with 0.5% methylcellulose and 0.2% Tween 80. ^gCompound was dosed i.v. (1 mg/kg) as

1
2
3 EtOH/PEG400/H₂O (20/15/65) solution and p.o. (5 mg/kg) as an aqueous suspension with 0.5%
4
5 methylcellulose and 0.2% Tween 80.
6
7

8 **Figure 9.** Summary of potency, selectivity and DMPK properties of **19**.
9
10

11
12 We next determined the effect of **19** in an in vivo PK/PD experiment using a MOLM-16 (adult
13 AML cell line) xenograft mouse model. Single doses of **19** were given at dose levels between 3
14 and 30 mg/kg in MOLM-16 tumor-bearing animals, and samples were collected at time points
15 covering 2 to 24 hours. Tumor RNA was generated and used to assess *MYC* transcript by
16 quantitative RT-PCR relative to vehicle-treated animals. Suppression of *MYC* was observed at
17 doses as low as 3 mg/kg at 2 and 8 h, with maximal suppression observed at 10 and 30 mg/kg at
18 2 hours (87% and 88% inhibition, respectively; Figure 10A). It should be noted that suppression
19 of *MYC* at the 3, 10 and 30 mg/kg doses was seen without tumor or plasma levels of **19** reaching
20 the BRD4(1) IC₅₀ (5.1 μM) and thus results observed are clearly not from BET inhibition.
21
22 Consistent with previous results,¹² inhibition of *MYC*-transcript was transient over the 24-hour
23 window with an apparent rebound effect at the 3 mg/kg dose level, rising to about 150% of
24 vehicle control at the 16 h time point. Increasing suppression of *MYC*-transcript level correlated
25 with increasing plasma and tumor drug levels (Figure 10A).
26
27
28
29
30
31
32
33
34
35
36
37
38
39
40
41
42

43 To evaluate the in vivo efficacy of **19**, MOLM-16 AML xenografts were established in SCID
44 beige mice. Upon tumor establishment, dosing of compound **19** was initiated with p.o. doses of
45 3–30 mg/kg, twice daily (BID). Single-agent efficacy was observed at all doses, as evidenced by
46 inhibition of MOLM-16 tumor growth (Figure 10B). Tumor growth inhibition (%TGI) was 73%,
47 71%, and 89% at 3, 10 and 30 mg/kg, respectively. All doses of **19** were well tolerated over the
48 21-day dosing window, with a maximal body weight loss of 3.7%. There was a lack of dose
49
50
51
52
53
54
55
56
57
58
59
60

proportionality observed between the 3 mg/kg and 10 mg/kg doses for **19**, resulting in comparable exposures and suppression of *MYC* transcript levels, corresponding to comparable efficacy for these two doses in the efficacy study. At a dose of 30 mg/kg we observed higher exposures of **19** resulting in more durable suppression of *MYC* transcript levels, which corresponded to an increase in anti-tumor activity. These data suggest that there is a dose-proportional PK-PD-efficacy relationship where more durable suppression of *MYC* transcript results in better suppression of MOLM-16 tumor growth. Previously we had evaluated **1** in this same xenograft model.¹² Compound **19**, possessing greater cell potency than **1**, exhibited approximately the same %TGI at 3 mg/kg as **1** does at 25 mg/kg (65% TGI). Taken together these results demonstrate that **19** is highly active in vivo and capable of modulating CBP-dependent *MYC* transcription, which corresponds with anti-tumor activity in a *MYC*-dependent AML tumor model.

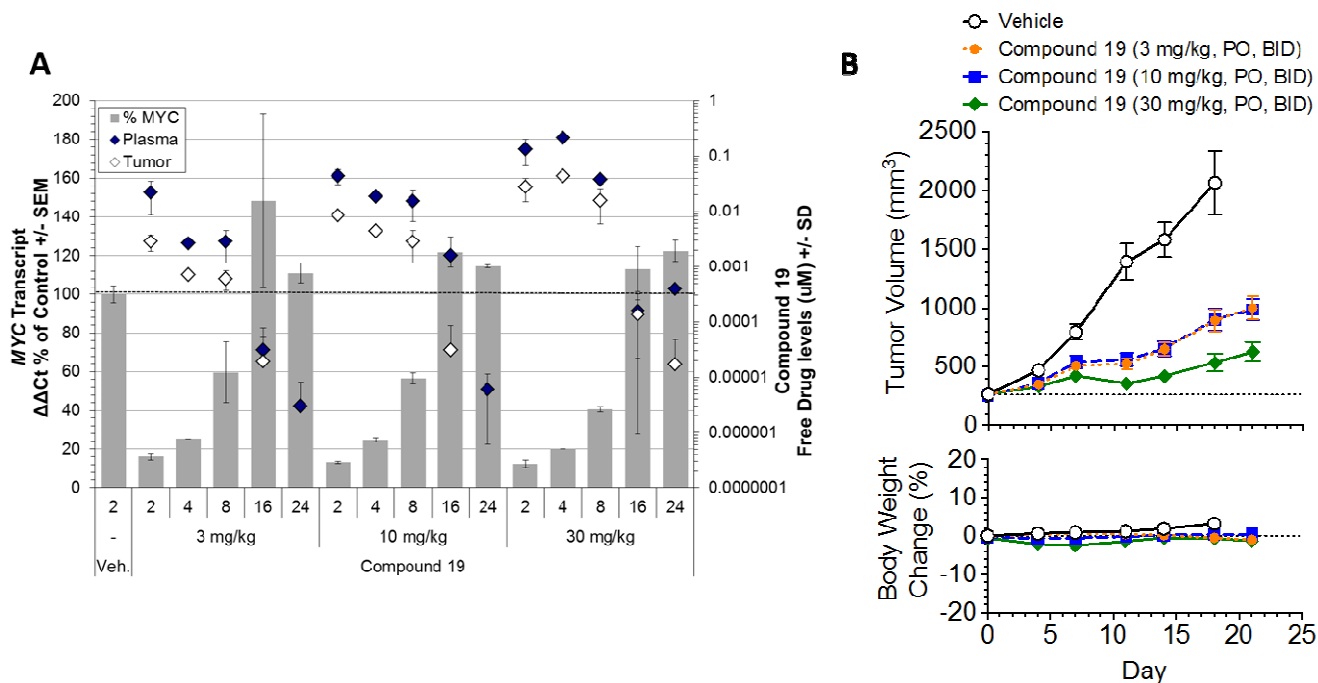


Figure 10. In vivo evaluation of **19** (A) Effect on **19** treatment on *MYC* transcript levels in

1
2
3 MOLM-16 xenograft tumors with single doses of **19** (n=3/group; mean \pm SEM plotted). Plasma
4 and tumor levels were adjusted for PPB and tissue binding, respectively, and mean plasma and
5 tumor unbound drug levels (\pm SD) are displayed. (B) Anti-tumor efficacy of **19** at 3, 10 and 30
6 mg/kg in the MOLM-16 AML xenograft tumor model and effect on body weight (n=10/group;
7 tumor volume - mean \pm SEM plotted; body weight - group fitted % body weight loss plotted).
8
9
10
11
12
13
14
15
16

17
18 In addition to studying the effect of **19** in a hematologic anti-tumor xenograft model, we also
19 explored the ability of this compound to impair T_{reg} differentiation and immunosuppressive
20 function. CBP can interact with multiple transcription factors.²⁶ One of them is FOXP3, the
21 master transcription factor defining T_{regs} . FOXP3 is essential for immune homeostasis,
22 preventing autoimmunity, limiting chronic inflammation, and hampering effective immunity
23 against tumors.²⁷⁻³⁰ Inhibition of the histone acetyltransferase domain of CBP has been shown to
24 decrease the expression of FOXP3, leading to reduced tumor growth in mouse models of
25 cancer.^{8,31} More recently, inhibition of the CBP bromodomain was also reported to impair
26 *FOXP3* expression and T_{reg} function, suggesting that bromodomain inhibition could impact
27 optimal acetylation of chromatin associated transcription factors, including FOXP3 itself.¹⁰ To
28 determine whether **19** would affect in vitro generation of inducible T_{regs} (iT_{regs}) and *FOXP3*
29 expression, human naïve CD4+T cells were differentiated towards T_{regs} using anti-CD3, anti-
30 CD28, rIL-2 and rTGF β in the presence of increasing concentrations of **19** (0.001 to 2 μ M),
31 using DMSO as a control. At day 4 post-differentiation, cells were harvested, mRNA was
32 extracted, and *FOXP3* gene expression was assessed by quantitative reverse transcriptase
33 polymerase chain reaction (q-RT-PCR). Figure 11A shows that **19** decreases *FOXP3* transcripts
34 in a dose-dependent manner (IC_{50} = 17 nM) consistent with the cellular potency in our *MYC* RNA
35
36
37
38
39
40
41
42
43
44
45
46
47
48
49
50
51
52
53
54
55
56
57
58
59
60

1
2
3 assay. Moreover the reduction in *FOXP3* mRNA corresponded to a reduction in FOXP3 protein
4 as determined in fixed and permeabilized CD4⁺CD25⁺ cells by fluorescence-activated cell
5 sorting. Compound **19** did not affect cell viability (Figure 11B), and a dose-dependent decrease
6 in FOXP3 staining was observed (Figure 11C), corroborating the gene expression data. Taken
7 together with our previous work,¹⁰ these data suggest that inhibition of the CBP bromodomain
8 may provide a novel small molecule approach for cancer immunotherapy.
9
10
11
12
13
14
15
16
17
18
19
20
21
22
23
24
25
26
27
28
29
30
31
32
33
34
35
36
37
38
39
40
41
42
43
44
45
46
47
48
49
50
51
52
53
54
55
56
57
58
59
60

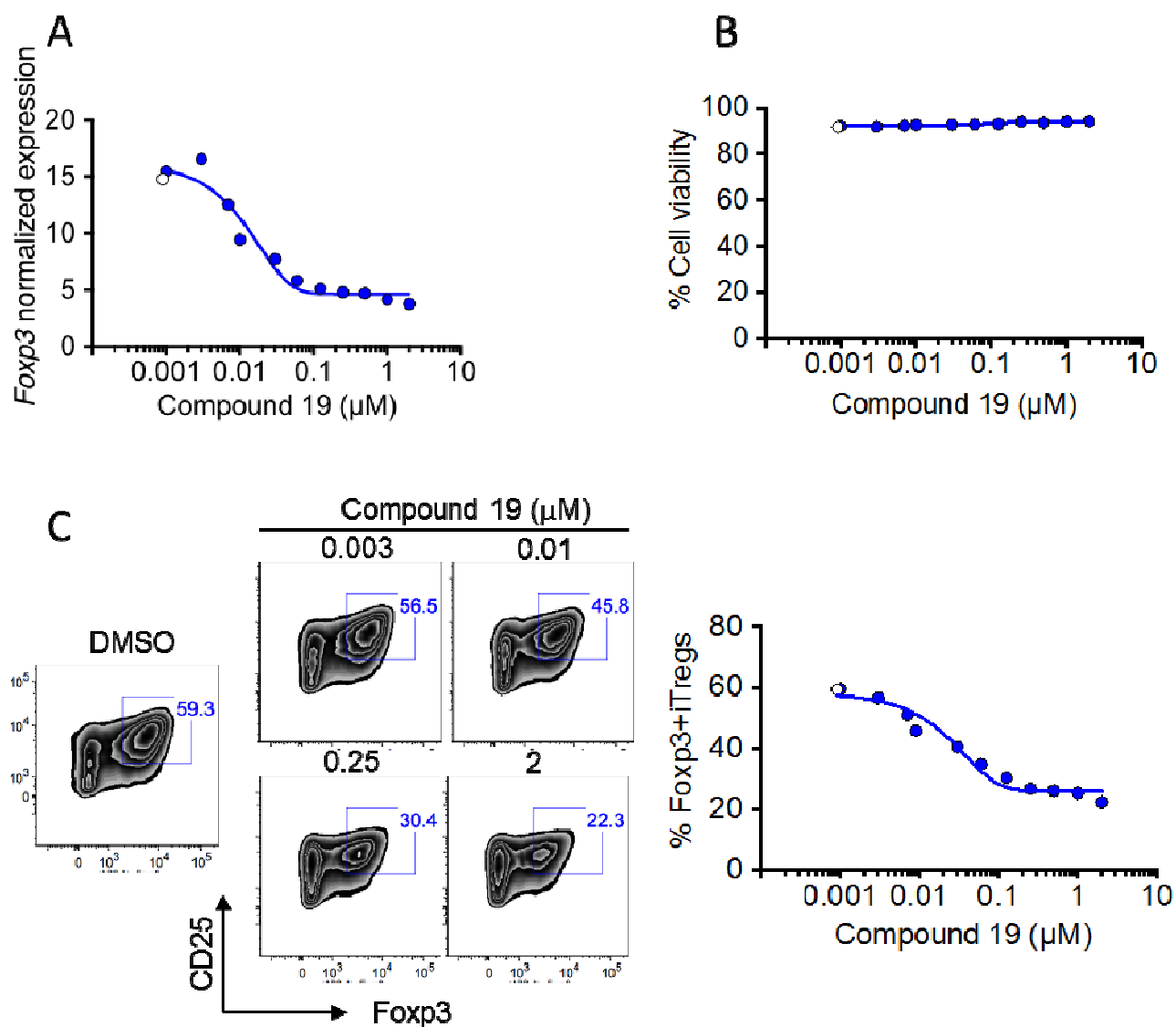


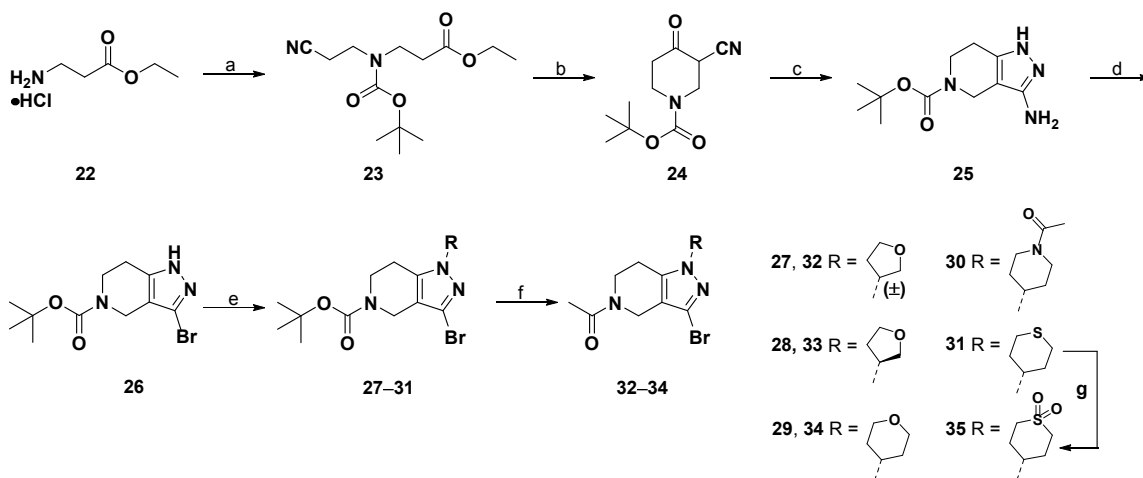
Figure 11. Compound **19** decreased the generation of iT_{regs} in vitro without affecting cell

1
2
3 viability. Human iT_{reg} cells were differentiated in vitro from naïve CD4⁺T cells derived from
4
5
6 Peripheral blood mononuclear cells (PBMCs) of a healthy donor in the presence of **19** or DMSO
7
8 as control. On day 4, cells were harvested. (A) *FOXP3* expression was assessed by q-RT-PCR
9
10 and normalized with *B2M*. (B) Cell viability was assessed by flow cytometry using a fixable
11
12 viability dye. (C) T_{reg} cells were also fixed, permeabilized and intracellular FOXP3 protein
13
14 assessed in CD4⁺CD25⁺ by flow cytometry. Graph shows % FOXP3⁺iTregs cells out of total
15
16 CD4⁺T cells. Data are representative of three independent experiments.
17
18
19
20
21

22 Chemistry

23
24 Intermediates **27–35** were prepared according to Scheme 1. Conjugate addition of ethyl 3-
25
26 aminopropanoate (**22**) to acrylonitrile followed by Boc protection yielded **23**. Compound **23** was
27
28 treated with sodium hydride and cyclized to give **24**. The pyrazolopiperidine core (**25**) was
29
30 formed by treatment of **24** with hydrazine, and subsequent conversion of the amino function of
31
32 **25** to the bromide under Sandmeyer conditions afforded **26**. Alkylation of the pyrazole **26** with
33
34 the appropriate alkyl methanesulfonate yielded **27–31**. Deprotection of the Boc group with TFA
35
36 followed by acylation with acetic anhydride afforded **32–34**. Intermediate sulfone **35** was formed
37
38
39
40
41 by oxidation of thioether **31** with Oxone®.
42
43
44
45

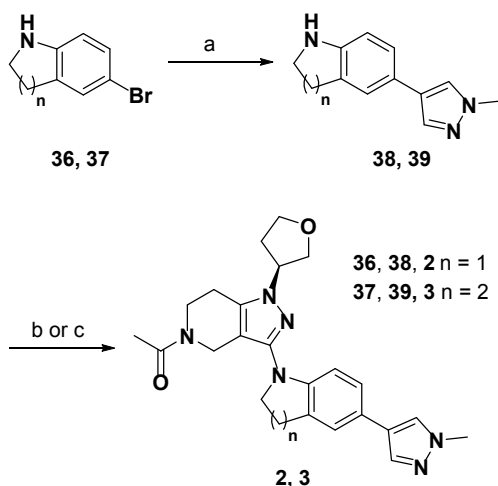
46 **Scheme 1.** Synthesis of Intermediates **27–35**^a
47
48
49
50
51
52
53
54
55
56
57
58
59
60



^aReagents and conditions: (a) i. NaOH, acrylonitrile, MeOH, 70 °C ii. di-*tert*-butyl dicarbonate, 0 °C, 99%; (b) NaH, toluene, 100 °C, 100%; (c) hydrazine monohydrate, EtOH, 60 °C, 70%; (d) isopentyl nitrite, MeCN, CuBr₂, 60 °C, 34%; (e) R-OMs, Cs₂CO₃, DMF, 80 °C, 28–71%; (f) i. TFA, DCM, rt, ii. Ac₂O, TEA, DMF, rt, 77–87%; (g) Oxone, THF, H₂O, rt, 98%.

The synthesis of **2** and **3** is outlined in Scheme 2. Suzuki coupling of 1-methyl-4-(4,4,5,5-tetramethyl-1,3,2-dioxaborolan-2-yl)-1*H*-pyrazole with commercially-available **36** or **37** afforded **38** and **39**, respectively. Buchwald coupling of racemate **32** and **38** followed by chiral chromatography yielded **2**. (We have observed from evaluating analogues from the synthesis of enantiopure starting material that the (*R*)-isomer is always less potent than the (*S*)-isomer. Compound **2** was assumed to be the (*S*)-isomer as this was more potent than the (*R*)-isomer.) Buchwald coupling of optically pure **33** with **39** afforded **3**.

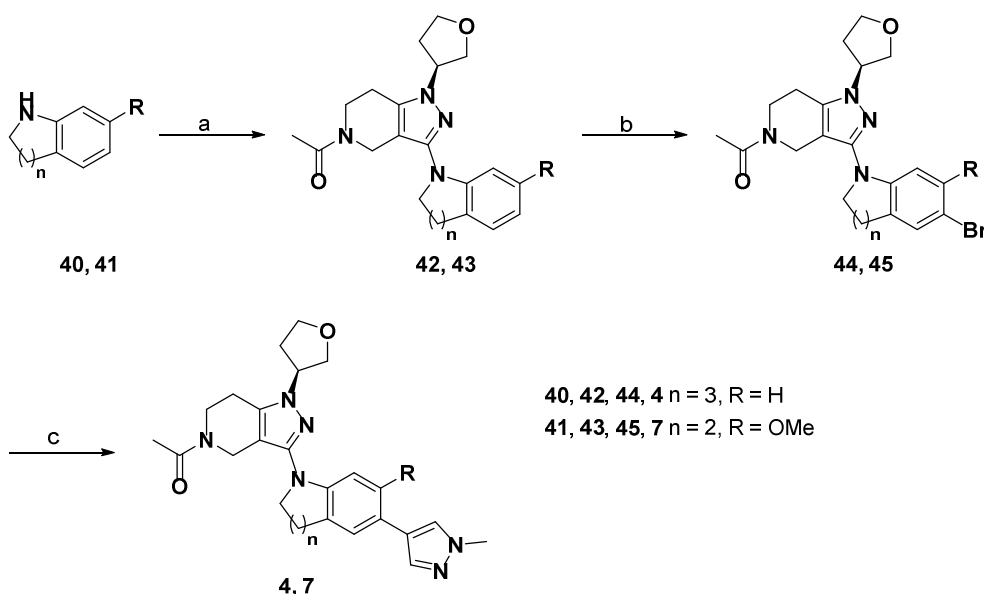
Scheme 2. Synthesis of Compounds **2** and **3**^a



^aReagents and conditions: (a) 1-methyl-4-(4,4,5,5-tetramethyl-1,3,2-dioxaborolan-2-yl)-1*H*-pyrazole, Pd(dppf)Cl₂, Na₂CO₃ or K₂CO₃, dioxane, H₂O, 120 °C, 47–86%; (b) **32**, RuPhos Pd G1, RuPhos, *t*-BuONa, dioxane, 120 °C, Supercritical Fluid Chromatography (SFC) chiral resolution, 16%; (c) **33**, RuPhos Pd G1, RuPhos, *t*-BuONa, dioxane, 120 °C, 34%

Buchwald coupling of commercially-available **40** or **41** with intermediate **33** yielded **42** and **43**, respectively (Scheme 3). Bromination of **42** and **43** with *N*-bromosuccinimide (NBS) gave bromides **44** and **45**, respectively. Subsequent Suzuki coupling with 1-methyl-4-(4,4,5,5-tetramethyl-1,3,2-dioxaborolan-2-yl)pyrazole provided analogues **4** and **7**, respectively.

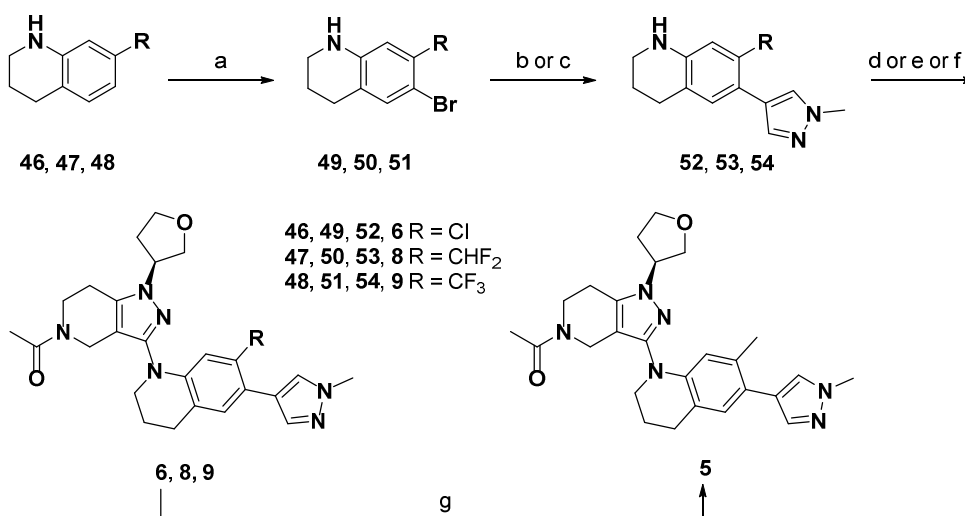
Scheme 3. Synthesis of Compounds **4** and **7**^a



^aReagents and conditions: (a) **33**, RuPhos Pd G1, RuPhos, *t*-BuONa, dioxane, 120 °C, 26–39%; (b) NBS, DCM, 0 °C to rt 90–97%; (c) 1-methyl-4-(4,4,5,5-tetramethyl-1,3,2-dioxaborolan-2-yl)-1*H*-pyrazole, Pd(dppf)Cl₂, K₂CO₃, dioxane, H₂O, 110 °C, 23–24%.

Scheme 4 shows the synthesis of compounds **5**, **6**, **8** and **9**. Appropriately substituted THQs (**46**–**48**) were treated with NBS yielding the brominated intermediates **49**–**51**. Suzuki coupling of **49**–**51** with 1-methyl-4-(4,4,5,5-tetramethyl-1,3,2-dioxaborolan-2-yl)-1*H*-pyrazole provided **52**–**54**. Buchwald coupling of intermediate **33** with **52** or **54** provided compounds **6** and **9**, respectively. Buchwald coupling of racemic intermediate **32** with **53** followed by chiral chromatography yielded **8**. Chloride **6** was converted directly to methyl analogue **5** via palladium coupling with potassium methyltrifluoroborate.

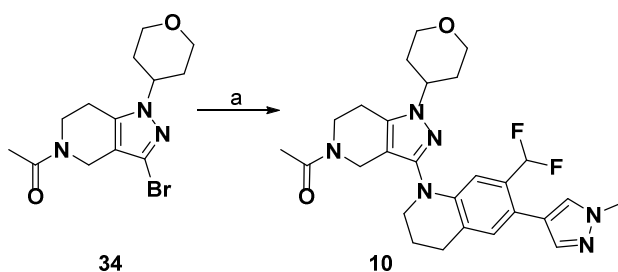
Scheme 4. Synthesis of Compounds **5**, **6**, **8** and **9**^a



^aReagents and conditions: (a) NBS, DCM, 0 °C to rt, 36–60%; (b) 1-methyl-4-(4,4,5,5-tetramethyl-1,3,2-dioxaborolan-2-yl)-1*H*-pyrazole, Pd(dppf)Cl₂, K₂CO₃ or Na₂CO₃, dioxane, H₂O, 110 °C, 86–95%; (c) 1-methyl-4-(4,4,5,5-tetramethyl-1,3,2-dioxaborolan-2-yl)-1*H*-pyrazole, XPhos Pd G2, XPhos, Na₂CO₃, THF, H₂O, 80 °C, 70%; (d) **33**, Pd₂(dba)₃, XantPhos, *t*-BuONa, dioxane, toluene, 90 °C, 50%; (e) **32**, RuPhos Pd G1, RuPhos, *t*-BuONa, dioxane, 130 °C, SFC chiral resolution, 16%; (f) **33**, Pd-PEPPSI-IPent, *t*-BuONa, dioxane, 150 °C, 21%; (g) **6**, Ad₂PBu, MeBF₃K, Pd(OAc)₂, Cs₂CO₃, toluene, H₂O, 100 °C, 15%.

Buchwald coupling of intermediate **34** with THQ **53** afforded **10** (Scheme 5).

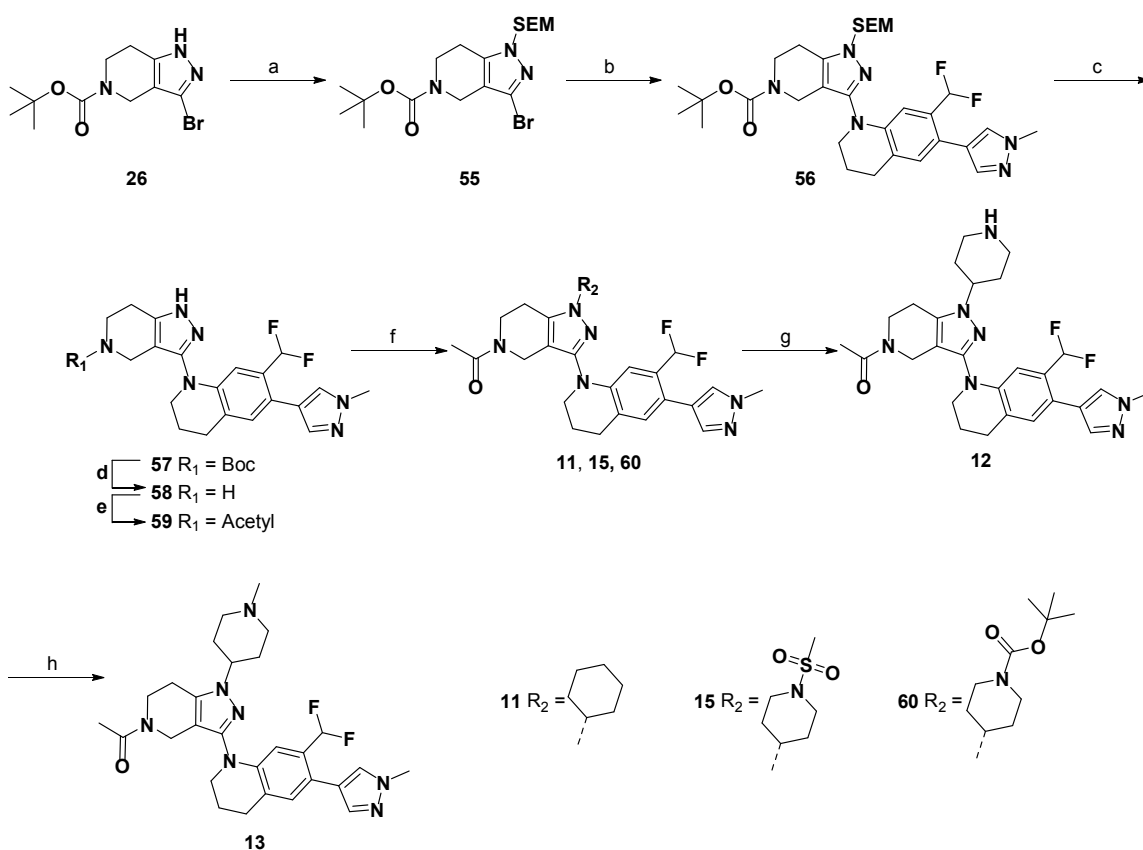
Scheme 5. Synthesis of Compound **10**^a



^aReagents and conditions: (a) **53**, XPhos Pd G3, K₃PO₄, *t*-amyl alcohol, 95 °C, 74%.

The syntheses of **11–13** and **15** are shown in Scheme 6. Treatment of intermediate **26** with SEM-Cl followed by Buchwald coupling with **53** provided **56**. Removal of the SEM and Boc protecting groups yielded **58**. Acetylation of the piperidine with acetic anhydride afforded the key intermediate **59**. Alkylation of **59** with the corresponding bromide or mesylate yielded **11**, **15** and **60**. Compound **60** was further converted to **13** by first removing the Boc group followed by reductive amination with formaldehyde.

Scheme 6. Synthesis of Compounds **11–13** and **15**^a

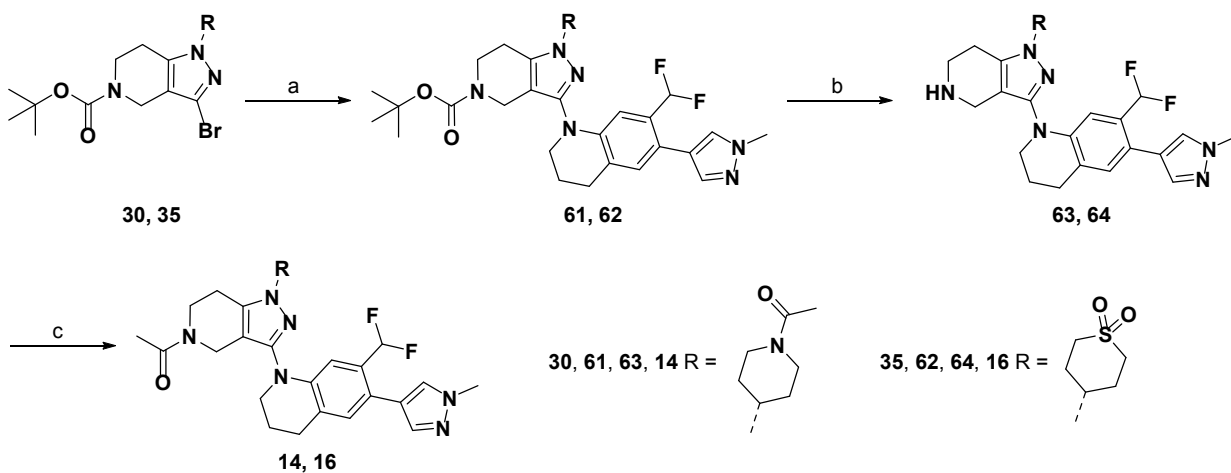


^aReagents and conditions: (a) NaH, SEM-Cl, THF, 0 °C to rt, 83%; (b) **53**, RuPhos Pd G2, RuPhos, *t*-BuONa, dioxane, 120 °C, 20%; (c) TBAF, THF, 60 °C, 66%; (d) TFA, DCM, rt, 100%; (e) Ac₂O, TEA, DMF, rt, 14%; (f), R₂-Br or R₂-OMs, Cs₂CO₃, DMF, 80 °C, 5–17%; (g)

60, TFA, DCM, 0 °C to rt, 49%; (h) aq. CH₂O, CH₃CO₂H, NaBh(OAc)₃, DCE, rt, 23%.

Outlined in Scheme 7 is the synthesis of **14** and **16**. Buchwald coupling of **30** or **35** with THQ **53** provided **61** and **62**, respectively. Deprotection of the Boc group with TFA followed by acetylation with acetic anhydride afforded candidate compounds **14** and **16**.

Scheme 7. Synthesis of Compounds **14** and **16**^a

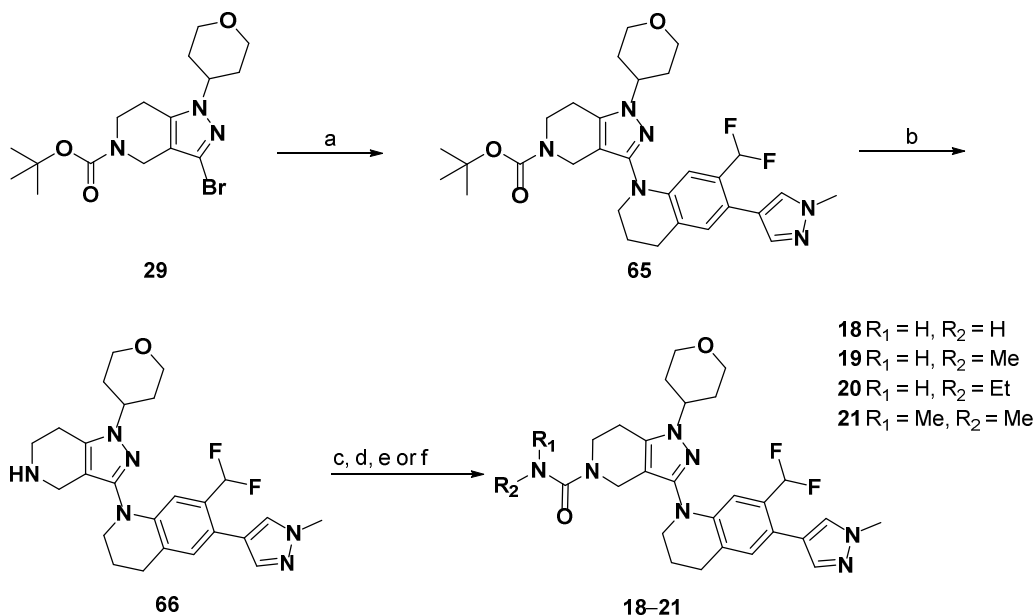


^aReagents and conditions: (a) **53**, Pd-PEPPSi-IPent, *t*-BuONa, dioxane, 120 °C, 42–46%; (b) TFA, DCM, rt, 100%; (c) Ac₂O, TEA, DCM, 0 °C to rt, 40–52%.

Buchwald coupling of THQ **53** with **29** to form **65**, followed by deprotection of the Boc group with TFA yielded key intermediate **66** from which urea analogues **18–21** could be synthesized (Scheme 8). Compound **66** was treated with (trimethylsilyl)isocyanate to afford the unsubstituted urea **18**. Monomethyl urea **19** was formed from treatment of **66** with *N*-methyl-1*H*-imidazole-1-carboxamide. Intermediate **66** was first treated with 4-nitrophenyl chloroformate then with ethylamine to yield **20**. Dimethyl urea **21** was synthesized by treatment of **66** with

dimethylcarbamoyl chloride.

Scheme 8. Synthesis of Compounds **18–21**^a



^aReagents and conditions: (a) **53**, RuPhos Pd G1, RuPhos, *t*-BuONa, dioxane, 120 °C, 73%; (b) TFA, DCM, rt; (c) TMSNCO, DCM, rt, 20%; (d) *N*-methyl-1*H*-imidazole-1-carboxamide, DCM, rt, 22%; (e) i. 4-nitrophenyl chloroformate, pyridine, DMF, rt, ii. EtNH₂, THF, rt, 14%; (f) dimethylcarbamyl chloride, TEA, DMF, rt, 22%.

Conclusion

We have identified a highly potent and selective in vivo probe (**19**) of the CBP bromodomain that is suitable to interrogate the biology of CBP without the complication of BET inhibition. Our studies began with recently disclosed **1** (TR-FRET IC₅₀ = 20 nM, BRET IC₅₀ = 410 nM, BRD4(1) IC₅₀ = 13,000 nM) that was moderately potent for the bromodomain of CBP and 650-fold selective over BRD4(1). Constraining the aniline of **1** into tetrahydroquinoline **3** maintained potency and increased selectivity by 2-fold over **1**. Structure-activity relationship studies coupled

1
2
3 with structure-based design targeting the LPF shelf, BC loop and KAc regions allowed us to
4 identify **10** (TR-FRET IC_{50} = 1.1 nM, BRET IC_{50} = 12 nM, BRD4(1) IC_{50} = 4,200 nM). Further
5
6
7
8 profiling of this compound revealed that it penetrated into the CNS resulting in adverse CNS
9 effects. Subsequent optimization focused on increasing *t*PSA with the addition of a hydrogen
10 bond donor. This was accomplished with conversion of the Asn-binding acetamide of **10** to a
11 methyl urea, enabling identification of non-CNS penetrant **19** (TR-FRET IC_{50} = 0.94 nM, BRET
12
13
14
15
16
17
18
19
20
21
22
23
24
25
26
27
28
29
30
31
32
33
34
35
36
37
38
39
40
41
42
43
44
45
46
47
48
49
50
51
52
53
54
55
56
57
58
59
60
compound **19** (TR-FRET IC_{50} = 0.94 nM, BRET IC_{50} = 6.2 nM, BRD4(1) IC_{50} = 5,100 nM) that demonstrated an appropriate balance of cell
potency, selectivity (5,425-fold over BRD4(1)) and in vivo PK. The exquisite potency and
selectivity of **19** enables the clear delineation of pharmacological effects from the inhibition of
CBP over the BET bromodomains. In vivo, **19** modulates *MYC* expression that corresponds with
anti-tumor activity in an AML tumor model. Additional in vitro studies with **19** showed that this
compound impaired *FOXP3* expression and T_{reg} function, further suggesting CBP bromodomain
inhibition as a novel small molecule approach for cancer immunotherapy.

Experimental Procedures

General Methods. All solvents and reagents were used as obtained. NMR analysis performed in a deuterated solvent with a Varian Avance 300-MHz or Bruker Avance 400- or 500-MHz NMR spectrometers, referenced to trimethylsilane (TMS). Chemical shifts are expressed as δ units using TMS as the external standard (in NMR description, s = singlet, d = doublet, t = triplet, q = quartet, m = multiplet, and br = broad peak). All coupling constants (*J*) are reported in Hertz. Compounds with the acetamide moiety (e.g., compound **10**) exhibited rotamers in the NMR and thus in many cases coupling constants were not reported and generally characterized as multiplets. In addition, the ^{13}C of

1
2
3 compound **10** was run at elevated temperature in order to coalesce the multiple rotamer
4 peaks into a single peak. Mass spectra were measured with a Finnigan SSQ710C
5 spectrometer using an ESI source coupled to a Waters 600MS high performance liquid
6 chromatography (HPLC) system operating in reverse-phase mode with an X-bridge
7 Phenyl column of dimensions 150 mm by 2.6 mm, with 5 μm sized particles.
8 Preparatory-scale silica gel chromatography was performed using medium-pressure
9 liquid chromatography (MPLC) on a CombiFlash Companion (Teledyne ISCO) with
10 RediSep normal phase silica gel (35–60 μm) columns and UV detection at 254 nm.
11 Reverse-phase (HPLC) was used to purify compounds as needed by elution from a
12 Phenomenex Gemini-NX C18 column (20.2 \times 50 mm, 5 micron) as stationary phase
13 using mobile phase indicated, and operating at a 35 mL/min flow rate on a Waters 3100
14 mass-directed prep instrument. Chemical purities were >95% for all final compounds as
15 assessed by LC/MS analysis. The following analytical method was used to determine
16 chemical purity of final compounds: HPLC-Agilent 1200, water with 0.05% TFA,
17 acetonitrile with 0.05% TFA (buffer B), Agilent SB-C18, 1.8 μm , 2.1 \times 30 mm, 25 $^{\circ}\text{C}$, 3–
18 95% buffer B in 8.5 min, 95% in 2.5 min, 400 $\mu\text{L}/\text{min}$, 220 nm and 254 nm, equipped
19 with Agilent quadrupole 6140, ESI positive, 90–1300 amu.
20
21
22
23
24
25
26
27
28
29
30
31
32
33
34
35
36
37
38
39
40
41
42
43
44

45
46 ***tert*-butyl 3-bromo-1-(tetrahydrofuran-3-yl)-6,7-dihydro-1*H*-pyrazolo[4,3-
47 *c*]pyridine-5(4*H*)-carboxylate (27)**
48

49
50
51
52 **Step 1:**
53

54
55 **ethyl 3-((*tert*-butoxycarbonyl)(2-cyanoethyl)amino)propanoate (23)**
56
57
58
59
60

1
2
3 To a solution of ethyl 3-aminopropanoate hydrochloride (**22**, 367 g, 2.39 mol) in MeOH
4 (1.2 L) at room temperature was added NaOH (95.6 g, 2.39 mol) in portion-wise. The
5
6 mixture was heated to 70 °C, acrylonitrile (158 g, 2.98 mol) was added dropwise and the
7
8 reaction mixture stirred for 6 h. The solution was cooled to 0 °C before di-*tert*-butyl
9
10 dicarbonate (521 g, 2.39 mol) was added. The reaction was stirred at room temperature
11
12 for 6 h, filtered, and washed with MeOH (200 mL). The filtrate was concentrated in
13
14 vacuo to give a yellow oily residue that was re-dissolved in EtOAc and water (500 mL).
15
16 The aqueous layer was extracted with EtOAc (800 mL). The combined organic layers
17
18 were dried over anhydrous Na₂SO₄, filtered and concentrated in vacuo to give the title
19
20 compound (**23**, 638 g, 99%) as a light yellow oil that required no further purification. ¹H
21
22 NMR (400 MHz, CDCl₃) δ 4.17 (q, *J* = 7.2 Hz, 2H), 3.68–3.62 (m, 4H), 2.57–2.53 (m,
23
24 4H), 1.49 (s, 9H), 1.29 (t, *J* = 7.2 Hz, 3H).
25
26
27
28
29
30
31
32
33
34
35

36 Step 2:

37 *tert*-butyl 3-cyano-4-oxopiperidine-1-carboxylate (**24**)

38
39 To toluene (2.7 L) at 25 °C was added NaH (80 g, 2.0 mol) portion-wise and the
40
41 suspension was heated to 80 °C. Ethyl 3-((*tert*-butoxycarbonyl)(2-
42
43 cyanoethyl)amino)propanoate (**23**, 270 g, 1.00 mol) in anhydrous toluene (270 mL) was
44
45 added dropwise. The mixture was heated to 100 °C and stirred for 5 h. The mixture was
46
47 cooled to room temperature, quenched with sat. aq. ammonium chloride (800 mL) and
48
49 washed with hexanes (800 mL). The aqueous phase was acidified with HCl (2N) to pH 6
50
51 and the mixture was extracted with EtOAc (1 L x 2). The combined organic layers were
52
53
54
55
56
57
58
59
60

1
2
3 dried over anhydrous Na₂SO₄, filtered and concentrated in vacuo to give *tert*-butyl 3-
4 cyano-4-oxopiperidine-1-carboxylate (**24**, 310 g, 100%) as yellow oil that required no
5 further purification. ¹H NMR (400 MHz, CDCl₃) δ 4.17–4.14 (m, 1H), 3.59–3.56 (m,
6 2H), 3.43–3.41 (m, 2H), 2.70–2.66 (m, 2H), 1.51 (s, 9H).
7
8
9
10
11
12
13
14
15
16

17 **Step 3:**

18
19
20 ***tert*-butyl 3-amino-6,7-dihydro-1*H*-pyrazolo[4,3-*c*]pyridine-5(4*H*)-carboxylate (**25**)**

21
22
23 A mixture of *tert*-butyl 3-cyano-4-oxopiperidine-1-carboxylate (**24**, 310 g, 1.38 mol) and
24 hydrazine monohydrate (140 mL, 2.08 mol) in EtOH (1.5 L) was heated to 60 °C for 2 h.
25
26 The mixture was concentrated in vacuo to give the crude product that was dissolved in
27 EtOAc (1 L) and washed with water (1 L x 2). The organic layer was dried over
28 anhydrous Na₂SO₄, filtered and concentrated in vacuo to afford *tert*-butyl 3-amino-6,7-
29 dihydro-1*H*-pyrazolo[4,3-*c*]pyridine-5(4*H*)-carboxylate (**25**, 230 g, 70%) as a colorless
30 solid. ¹H NMR (400 MHz, CD₃OD) δ 4.28 (s, 2H), 3.66–3.63 (m, 2H), 2.62–2.59 (m,
31 2H), 1.49 (s, 9H).
32
33
34
35
36
37
38
39
40
41
42
43
44
45

46 **Step 4:**

47
48
49 ***tert*-butyl 3-bromo-6,7-dihydro-1*H*-pyrazolo[4,3-*c*]pyridine-5(4*H*)-carboxylate (**26**)**

50
51
52 To a stirred mixture of *tert*-butyl 3-amino-6,7-dihydro-1*H*-pyrazolo[4,3-*c*]pyridine-
53 5(4*H*)-carboxylate (**25**, 120 g, 504 mmol), CuBr₂ (112.5 g, 503.6 mmol) and MeCN (1.2
54 L) at 0 °C was added isopentyl nitrite (76.7 g, 655 mmol) and the reaction mixture stirred
55
56
57
58
59
60

1
2
3 for 20 min. The temperature was raised to 60 °C and the reaction mixture was stirred for
4
5 an additional 5 h. After cooling the reaction to room temperature, the reaction mixture
6
7 was quenched with water (1 L) and the mixture was extracted with EtOAc (1 L x 2). The
8
9 combined organic layers were dried over anhydrous Na₂SO₄, filtered and concentrated in
10
11 vacuo. The crude residue was purified by silica gel chromatography (petroleum
12
13 ether/EtOAc = 4:1) to afford *tert*-butyl 3-bromo-6,7-dihydro-1*H*-pyrazolo[4,3-*c*]pyridine-
14
15 5(4*H*)-carboxylate (**26**, 52 g, 34%) as light yellow solid. LCMS M/Z (M+H) 302.
16
17
18
19
20
21
22

23 **Step 5:**

24
25
26 ***tert*-butyl 3-bromo-1-(tetrahydrofuran-3-yl)-6,7-dihydro-1*H*-pyrazolo[4,3-
27
28 *c*]pyridine-5(4*H*)-carboxylate (**27**)**

29
30
31 To a solution of *tert*-butyl 3-bromo-6,7-dihydro-1*H*-pyrazolo[4,3-*c*]pyridine-5(4*H*)-
32
33 carboxylate (**26**, 20.0 g, 66.0 mmol) in DMF (100 mL) was added Cs₂CO₃ (40.0 g, 123
34
35 mmol) and tetrahydrofuran-3-yl methanesulfonate (16.0 g, 98.0 mmol). The mixture was
36
37 heated to 80 °C for 12 h. The solution was concentrated in vacuo and the crude residue
38
39 was purified by silica gel chromatography (eluent from petroleum ether/EtOAc = 10:1 to
40
41 3:1) to give the title compound (**27**, 17 g, 69 %) as a yellow oil. ¹H NMR (400 MHz,
42
43 CDCl₃) δ 4.78–4.69 (m, 1 H), 4.26 (s, 2 H), 4.18–3.86 (m, 4 H), 3.72 (s, 2 H), 2.72–2.62
44
45 (m, 2H), 2.44–2.22 (m, 2H), 1.48 (s, 9H).
46
47
48
49
50
51
52
53
54

55 **(*S*)-*tert*-butyl 3-bromo-1-(tetrahydrofuran-3-yl)-6,7-dihydro-1*H*-pyrazolo[4,3-
56
57 *c*]pyridine-5(4*H*)-carboxylate (**28**)**

1
2
3 In a similar manner to **27**, compound **28** was prepared from (*R*)-tetrahydrofuran-3-yl
4 methanesulfonate to provide the title compound (71 %) as a yellow oil. ¹H NMR (400
5 MHz, DMSO-*d*₆) δ 4.97–4.78 (m, 1H), 4.13 (s, 2H), 3.98–3.86 (m, 2H), 3.81–3.67 (m,
6 2H), 3.56 (t, *J* = 5.6 Hz, 2H), 2.68 (t, *J* = 5.6 Hz, 2H), 2.33–2.08 (m, 2H), 1.38 (s, 9H).
7
8
9
10
11
12
13
14
15
16

17 ***tert*-butyl 3-bromo-1-(tetrahydro-2*H*-pyran-4-yl)-6,7-dihydro-1*H*-pyrazolo[4,3-
18 *c*]pyridine-5(4*H*)-carboxylate (29)**
19
20
21

22 In a similar manner to **27**, compound **29** was prepared from tetrahydro-2*H*-pyran-4-yl
23 methanesulfonate to provide the title compound (47%) as a colorless oil. ¹H NMR (400
24 MHz, DMSO-*d*₆) δ 4.35–4.25 (m, 1H), 4.17 (s, 2H), 3.95–3.93 (m, 2H), 3.62–3.57 (m,
25 2H), 3.42 (t, *J* = 11.2 Hz, 2H), 2.74–2.73 (m, 2H), 1.98–1.89 (m, 2H), 1.80–1.77 (m, 2H),
26 1.41 (s, 9H).
27
28
29
30
31
32
33
34
35
36
37

38 ***tert*-butyl 1-(1-acetylpiperidin-4-yl)-3-bromo-6,7-dihydro-1*H*-pyrazolo[4,3-
39 *c*]pyridine-5(4*H*)-carboxylate (30)**
40
41
42
43

44 In a similar manner to **27**, compound **30** was prepared from 1-acetylpiperidin-4-yl
45 methanesulfonate to provide the title compound (28%) as a yellow solid. ¹H NMR (400
46 MHz, DMSO-*d*₆) δ 4.50–4.41 (m, 1H), 4.38–4.29 (m, 1H), 4.16 (s, 2H), 3.94–3.85 (m,
47 1H), 3.64–3.57 (m, 2H), 3.21–3.09 (m, 1H), 2.75–2.58 (m, 3H), 2.03 (s, 3H), 1.91–1.80
48 (m, 3H), 1.73–1.61 (m, 1H), 1.41 (s, 9H).
49
50
51
52
53
54
55
56
57
58
59
60

***tert*-butyl 3-bromo-1-(1,1-dioxidotetrahydro-2*H*-thiopyran-4-yl)-6,7-dihydro-1*H*-
pyrazolo[4,3-*c*]pyridine-5(4*H*)-carboxylate (35)**

Step 1:

***tert*-butyl 3-bromo-1-(tetrahydro-2*H*-thiopyran-4-yl)-6,7-dihydro-1*H*-pyrazolo[4,3-
c]pyridine-5(4*H*)-carboxylate (31)**

To a solution of *tert*-butyl 3-bromo-6,7-dihydro-1*H*-pyrazolo[4,3-*c*]pyridine-5(4*H*)-carboxylate (**26**, 10.0 g, 33.1 mmol) in DMF (50 mL) was added Cs₂CO₃ (27.0 g, 82.7 mmol) and tetrahydro-2*H*-thiopyran-4-yl methanesulfonate (8.4 g, 43.0 mmol). The mixture was heated to 80 °C for 16 h under a nitrogen atmosphere. After cooling the reaction to room temperature, the mixture was filtered. The mixture was diluted with EtOAc (100 mL) and washed with brine (100 mL x 2). The organic layer was dried over anhydrous Na₂SO₄, filtered and concentrated in vacuo. The crude residue was purified by silica gel chromatography (eluent from petroleum ether : *tert*-butyl methyl ether : THF = from 10 : 1 : 1 to 3 : 1 : 1) to give the title compound (**31**, 5.9 g, 44%) as a white solid. ¹H NMR (400 MHz, DMSO-*d*₆) δ 4.17 (s, 2H), 4.09–4.04 (m, 1H), 3.62–3.59 (m, 2H), 2.83–2.77 (m, 2H), 2.71–2.68 (m, 4H), 2.13–2.10 (m, 2H), 2.03–1.93 (m, 2H), 1.44 (s, 9H).

Step 2:

***tert*-butyl 3-bromo-1-(1,1-dioxidotetrahydro-2*H*-thiopyran-4-yl)-6,7-dihydro-1*H*-
pyrazolo[4,3-*c*]pyridine-5(4*H*)-carboxylate (35)**

1
2
3 To a solution of *tert*-butyl 3-bromo-1-(tetrahydro-2*H*-thiopyran-4-yl)-6,7-dihydro-1*H*-
4 pyrazolo[4,3-*c*]pyridine-5(4*H*)-carboxylate (**31**, 2.0 g, 5.0 mmol) in THF (10 mL) and
5
6 water (2 mL) at 0 °C was added Oxone (3.1 g, 5 mmol) portionwise. The mixture was
7
8 stirred at room temperature for 2 h. The reaction was quenched by sat. aq. Na₂SO₃ and
9
10 extracted with DCM (20 mL x 3). The combined organic layers were dried over
11
12 anhydrous Na₂SO₄, filtered and concentrated in vacuo to give the title compound (**35**, 2.1
13
14 g, 98%) as a white solid that required no further purification. LCMS M/Z (M+H) 436.
15
16
17
18
19
20
21
22
23

24 **1-(3-bromo-1-(tetrahydrofuran-3-yl)-6,7-dihydro-1*H*-pyrazolo[4,3-*c*]pyridin-5(4*H*)-**
25
26 **yl)ethanone (**32**)**
27
28

29 To a solution of *tert*-butyl 3-bromo-1-(tetrahydrofuran-3-yl)-6,7-dihydro-1*H*-pyrazolo
30 [4,3-*c*]pyridine-5(4*H*)-carboxylate (**27**, 17.0 g, 45.0 mmol) in DCM (60 mL) was added
31
32 TFA (30 mL) dropwise. The reaction solution was stirred at room temperature for 2 h.
33
34 The solvent was removed by evaporation and the crude product was re-dissolved in DMF
35
36 (50 mL). The mixture was cooled to 0 °C before TEA (41.0 g, 40.5 mmol) and acetic
37
38 anhydride (7.00 g, 68.0 mmol) were added dropwise. The ice bath was removed and the
39
40 reaction was stirred at room temperature for additional 2 h. Water (50 mL) was added and
41
42 the solution was extracted with EtOAc (150 mL x 3). The combined organic layers were
43
44 dried over anhydrous Na₂SO₄, filtered and concentrated in vacuo. The crude residue was
45
46 purified by silica gel chromatography (DCM / MeOH = 30 : 1) to give the title compound
47
48 (**32**, 12.0 g, 82%) as a white solid. ¹H NMR (400 MHz, DMSO-*d*₆) δ 4.96–4.92 (m 1H),
49
50
51
52
53
54
55
56
57
58
59
60

1
2
3 4.28 (s, 2H), 3.99–3.95 (m, 2H), 3.80–3.68 (m, 4H), 2.82–2.70 (m, 2H), 2.29–2.19 (m,
4
5
6 2H), 2.10–2.08 (m, 3H).
7
8
9

10
11
12 **(S)-1-(3-bromo-1-(tetrahydrofuran-3-yl)-6,7-dihydro-1H-pyrazolo[4,3-c]pyridin-**
13
14 **5(4H)-yl)ethanone (33)**
15
16

17
18 In a similar manner to **32**, compound **33** was prepared from (*S*)-*tert*-butyl 3-bromo-1-
19
20 (tetrahydrofuran-3-yl)-6,7-dihydro-1H-pyrazolo[4,3-*c*]pyridine-5(4H)-carboxylate (**28**) to
21
22 provide the title compound (87%) as a white solid. ¹H NMR (400 MHz, CDCl₃) δ 4.78–
23
24 4.67 (m, 1H), 4.45–4.29 (m, 2H), 4.15–4.06 (m, 2H), 3.96–3.92 (m, 2H), 3.88–3.70 (m,
25
26 2H), 2.71–2.67 (m, 2H), 2.38–2.34 (m, 2H), 2.16 (s, 3H).
27
28
29
30
31
32

33
34 **1-(3-bromo-1-(tetrahydro-2H-pyran-4-yl)-6,7-dihydro-1H-pyrazolo[4,3-c]pyridin-**
35
36 **5(4H)-yl)ethanone (34)**
37
38

39
40 In a similar manner to **32**, compound **34** was prepared from *tert*-butyl 3-bromo-1-
41
42 (tetrahydro-2H-pyran-4-yl)-6,7-dihydro-1H- pyrazolo[4,3-*c*]pyridine-5(4H)-carboxylate
43
44 (**29**) to provide the title compound (77%) as a light yellow solid. ¹H NMR (400 MHz,
45
46 DMSO-*d*₆) δ 4.33–4.29 (m, 1H), 4.28 (s 2H), 3.95–3.92 (m, 2H), 3.70–3.67 (m, 2H),
47
48 3.43–3.36 (m, 2H), 2.84–2.69 (m, 2H), 2.09–2.08 (m, 3H), 1.96–1.91 (m, 2H), 1.80–1.76
49
50 (m, 2H).
51
52
53
54
55
56
57
58
59
60

1
2
3
4
5
6
7
8
9
10
11
12
13
14
15
16
17
18
19
20
21
22
23
24
25
26
27
28
29
30
31
32
33
34
35
36
37
38
39
40
41
42
43
44
45
46
47
48
49
50
51
52
53
54
55
56
57
58
59
60

1-[3-[5-(1-methylpyrazol-4-yl)indolin-1-yl]-1-[(3*S*)-tetrahydrofuran-3-yl]-6,7-dihydro-4*H*-pyrazolo[4,3-*c*]pyridin-5-yl]ethanone (2)

Step 1:

5-(1-methyl-1*H*-pyrazol-4-yl)indoline (38)

To a solution of 5-bromoindoline (**36**, 500 mg, 2.52 mmol), 1-methyl-4-(4,4,5,5-tetramethyl-1,3,2-dioxaborolan-2-yl)-1*H*-pyrazole (630 mg, 3.03 mmol) and Na₂CO₃ (535 mg, 5.05 mmol) in dioxane (20 mL) and H₂O (5 mL) was added [1,1'-bis(diphenylphosphino)ferrocene]dichloropalladium(II) (184 mg, 0.250 mmol). The mixture was heated to 120 °C for 12 h under a nitrogen atmosphere. After cooling to room temperature, the mixture was filtered and the filtrate was concentrated in vacuo. The crude residue was purified by silica gel chromatography (petroleum ether / EtOAc = 1 : 1) to give the presumed title compound (**38**, 430 mg, 86%) as a light yellow solid.

Step 2:

1-[3-[5-(1-methylpyrazol-4-yl)indolin-1-yl]-1-tetrahydrofuran-3-yl]-6,7-dihydro-4*H*-pyrazolo[4,3-*c*]pyridin-5-yl]ethanone

To a solution of 1-(3-bromo-1-(tetrahydrofuran-3-yl)-6,7-dihydro-1*H*-pyrazolo[4,3-*c*]pyridin-5(4*H*)-yl)ethanone (**32**, 500 mg, 1.59 mmol), 5-(1-methyl-1*H*-pyrazol-4-yl)indoline (**38**, 371 mg, 1.59 mmol) and *t*-BuONa (458 mg, 4.77 mmol) in 1,4-dioxane (10 mL) was added chloro(2-dicyclohexylphosphino-2',6'-di-*i*-propoxy-1,1'-biphenyl)[2-(2-aminoethylphenyl)]palladium(II), methyl-*tert*-butylether adduct (130 mg, 0.160 mmol) and 2-dicyclohexylphosphino-2',6'-di-*i*-propoxy-1,1'-biphenyl (74 mg, 0.16 mmol). The

1
2
3 mixture was heated to 120 °C for 12 h under a nitrogen atmosphere. After cooling to
4 room temperature, the mixture was filtered and the filtrate was concentrated in vacuo.
5
6 The crude residue was purified by reverse phase chromatography (acetonitrile 32–62% /
7
8 0.1% NH₄OH in water) to give the title compound (112 mg, 16%) as a white solid. ¹H
9
10 NMR (400 MHz, CDCl₃) δ 7.69 (s, 1H), 7.51 (s, 1H), 7.41–7.13 (m, 3H), 4.74–4.71 (m,
11
12 1H), 4.68–4.48 (m, 2H), 4.12–4.06 (m, 2H), 4.04–4.01 (m, 4H), 3.99 (s, 3H), 3.93–3.75
13
14 (m, 2H), 3.21–3.17 (m, 2H), 2.73–2.70 (m, 2H), 2.45–2.32 (m, 2H), 2.20–2.15 (m, 3).
15
16 LCMS M/Z (M+H) 433.
17
18
19
20
21
22
23
24
25
26

27 **Step 3:**

28
29 **1-[3-[5-(1-methylpyrazol-4-yl)indolin-1-yl]-1-[(3*S*)-tetrahydrofuran-3-yl]-6,7-**
30
31 **dihydro-4*H*-pyrazolo[4,3-*c*]pyridin-5-yl]ethanone (2)**
32
33

34 Racemic 1-[3-[5-(1-methylpyrazol-4-yl)indolin-1-yl]-1-tetrahydrofuran-3-yl]-6,7-dihydro-
35
36 4*H*-pyrazolo[4,3-*c*]pyridin-5-yl]ethanone (100 mg) was separated by using chiral SFC
37
38 (Chiralcel OJ 250×30mm I.D., 10um; Supercritical CO₂/ MeOH (0.1% NH₃ H₂O) =
39
40 50/50 at 70 mL/min) to give 1-[3-[5-(1-methylpyrazol-4-yl)indolin-1-yl]-1-[(3*R*)-
41
42 tetrahydrofuran-3-yl]-6,7-dihydro-4*H*-pyrazolo[4,3-*c*]pyridin-5-yl]ethanone (26 mg, first
43
44 peak) and 1-[3-[5-(1-methylpyrazol-4-yl)indolin-1-yl]-1-[(3*S*)-tetrahydrofuran-3-yl]-6,7-
45
46 dihydro-4*H*-pyrazolo[4,3-*c*]pyridin-5-yl]ethanone (29 mg, second peak). Absolute
47
48 configuration was arbitrarily assigned to each enantiomer. Isomer A: ¹H NMR (400 MHz,
49
50 DMSO-*d*₆) δ 7.94 (s, 1H), 7.72 (s, 1H), 7.42–7.32 (m, 2H), 7.26–7.23 (m, 1H), 4.89–4.83
51
52 (m, 1H), 4.55–4.53 (m, 2H), 4.05–3.97 (m, 4H), 3.86–3.70 (m, 7H), 3.14–3.10 (m, 2H),
53
54
55
56
57
58
59
60

1
2
3 2.80–2.67 (m, 2H), 2.26–2.23 (m, 2H), 2.10–2.28 (m, 3H). LCMS M/Z (M+H) 433.
4
5 Isomer B (2): ¹H NMR (400 MHz, DMSO-*d*₆) δ 7.94 (s, 1H), 7.72 (s, 1H), 7.42–7.32 (m,
6 2H), 7.26–7.23 (m, 1H), 4.88–4.86 (m, 1H), 4.55–4.53 (m, 2H), 4.03–3.96 (m, 4H), 3.86–
7 3.70 (m, 7H), 3.14–3.10 (m, 2H), 2.80–2.67 (m, 2H), 2.26–2.24 (m, 2H), 2.10–2.28 (m,
8 3H). LCMS M/Z (M+H) 433.
9
10
11
12
13
14
15
16
17
18
19

20 **1-[3-[6-(1-methylpyrazol-4-yl)-3,4-dihydro-2H-quinolin-1-yl]-1-(3S)-**
21 **tetrahydrofuran-3-yl]-6,7-dihydro-4H-pyrazolo[4,3-*c*]pyridin-5-yl]ethanone (3)**
22
23
24

25 **Step 1:**
26

27 **6-(1-methyl-1H-pyrazol-4-yl)-1,2,3,4-tetrahydroquinoline (39)**
28

29 To a solution of 6-bromo-1,2,3,4-tetrahydroquinoline (**37**, 17.0 g, 80.2 mmol), 1-methyl-
30 4-(4,4,5,5-tetramethyl-1,3,2-dioxaborolan-2-yl)-1H-pyrazole (25.0 g, 120.2 mmol) and
31 K₂CO₃ (33.2 g, 240 mmol) in dioxane / H₂O (5:1, 150 mL) was added [1,1'-
32 bis(diphenylphosphino)ferrocene]dichloropalladium(II) (5.80 g, 8.02 mmol). The mixture
33 was heated to 120 °C for 16 h under a nitrogen atmosphere. After cooling the reaction to
34 room temperature, the mixture was filtered and the filtrate was concentrated in vacuo.
35 The crude residue was purified by silica gel chromatography (petroleum ether / EtOAc =
36 1 : 1) to give the title compound (**39**, 8.0 g, 47%) as a yellow solid. ¹H NMR (400 MHz,
37 CD₃OD) δ 7.71 (s, 1H), 7.62 (s, 1H), 7.07 (d, *J* = 6.0 Hz, 2H), 6.50 (d, *J* = 8.4 Hz, 1H),
38 3.87 (s, 3H), 3.23 (t, *J* = 5.2 Hz, 2H), 2.75 (t, *J* = 6.4 Hz, 2H), 1.94–1.88 (m, 2H).
39
40
41
42
43
44
45
46
47
48
49
50
51
52
53
54
55

56 **Step 2:**
57
58
59
60

1
2
3
4
5
6
7
8
9
10
11
12
13
14
15
16
17
18
19
20
21
22
23
24
25
26
27
28
29
30
31
32
33
34
35
36
37
38
39
40
41
42
43
44
45

**1-[3-[6-(1-methylpyrazol-4-yl)-3,4-dihydro-2H-quinolin-1-yl]-1-[(3S)-
tetrahydrofuran-3-yl]-6,7-dihydro-4H-pyrazolo[4,3-c]pyridin-5-yl]ethanone (3)**

To a solution of (*S*)-1-(3-bromo-1-(tetrahydrofuran-3-yl)-6,7-dihydro-1*H*-pyrazolo[4,3-*c*]pyridin-5(4*H*)-yl)ethanone (**33**, 300 mg, 0.96 mmol), 6-(1-methyl-1*H*-pyrazol-4-yl)-1,2,3,4-tetrahydroquinoline (**39**, 127 mg, 0.960 mmol) and *t*-BuONa (123 mg, 1.28 mmol) in 1,4-dioxane (3.0 mL) was added chloro(2-dicyclohexylphosphino-2',6'-di-*i*-propoxy-1,1'-biphenyl)[2-(2-aminoethylphenyl)]palladium(ii), methyl-*tert*-butylether adduct (78 mg, 0.096 mmol) and 2-dicyclohexylphosphino-2',6'-di-*i*-propoxy-1,1'-biphenyl (45 mg, 0.096 mmol). The mixture was heated to 120 °C for 12 h under a nitrogen atmosphere. After cooling the reaction to room temperature, the mixture was filtered and the filtrate was concentrated in vacuo. The crude residue was purified by reverse phase chromatography (acetonitrile 38–68% / 0.2% formic acid in water) to give the title compound (**3**, 145 mg, 34%) as a white solid. ¹H NMR (400 MHz, DMSO-*d*₆) δ 7.92 (s, 1H), 7.68 (s, 1H), 7.20 (s, 1H), 7.15–7.06 (m, 1H), 6.49–6.37 (m, 1H), 4.93–4.85 (m, 1H), 4.14–4.06 (m, 2H), 4.05–3.92 (m, 2H), 3.87–3.65 (m, 7H), 3.62–3.48 (m, 2H), 2.83–2.78 (m, 4H), 2.37–2.18 (m, 2H), 2.06–1.94 (m, 5H). LCMS M/Z (M+H) 447.

46
47
48
49
50
51
52
53
54
55
56
57
58
59
60

**1-[3-[7-(1-methylpyrazol-4-yl)-2,3,4,5-tetrahydro-1-benzazepin-1-yl]-1-[(3S)-
tetrahydrofuran-3-yl]-6,7-dihydro-4H-pyrazolo[4,3-c]pyridin-5-yl]ethanone (4)**

Step 1:

**(S)-1-(3-(2,3,4,5-tetrahydro-1*H*-benzo[*b*]azepin-1-yl)-1-(tetrahydrofuran-3-yl)-6,7-
dihydro-1*H*-pyrazolo[4,3-*c*]pyridin-5(4*H*)-yl)ethanone (42)**

To a solution of (*S*)-1-(3-bromo-1-(tetrahydrofuran-3-yl)-6,7-dihydro-1*H*-pyrazolo[4,3-*c*]pyridin-5(4*H*)-yl)ethanone (**33**, 500 mg, 1.6 mmol), 2,3,4,5-tetrahydro-1*H*-benzo[*b*]azepine (**40**, 235 mg, 1.60 mmol) and *t*-BuONa (461 mg, 4.80 mmol) in 1,4-dioxane (5.0 mL) was added chloro(2-dicyclohexylphosphino-2',6'-di-*i*-propoxy-1,1'-biphenyl)[2-(2-aminoethylphenyl)]palladium(ii), methyl-*tert*-butylether adduct (131 mg, 0.160 mmol) and 2-dicyclohexylphosphino-2',6'-di-*i*-propoxy-1,1'-biphenyl (75 mg, 0.16 mmol). The mixture was heated to 110 °C for 16 h under a nitrogen atmosphere. After cooling the reaction to room temperature, the mixture was filtered and the filtrate was concentrated in vacuo. The crude residue was purified by Prep-TLC (DCM / MeOH = 25 : 1) to give the presumed title compound (**42**, 400 mg, 60% purity) as a light yellow solid.

Step 2:

(*S*)-1-(3-(7-bromo-2,3,4,5-tetrahydro-1*H*-benzo[*b*]azepin-1-yl)-1-(tetrahydrofuran-3-yl)-6,7-dihydro-1*H*-pyrazolo[4,3-*c*]pyridin-5(4*H*)-yl)ethanone (**44**)

To a solution of (*S*)-1-(3-(2,3,4,5-tetrahydro-1*H*-benzo[*b*]azepin-1-yl)-1-(tetrahydrofuran-3-yl)-6,7-dihydro-1*H*-pyrazolo[4,3-*c*]pyridin-5(4*H*)-yl)ethanone (**42**, 400 mg, 60% purity) in DCM (3 mL) at 0 °C was added *N*-bromosuccinimide (154 mg, 0.860 mmol) portionwise. The mixture was stirred at room temperature for 16 h. The mixture was washed with water (40 mL x 2). The organic layer was dried over anhydrous Na₂SO₄, filtered and concentrated in vacuo. The crude residue was purified by silica gel chromatography (DCM / MeOH = 20 : 1) to give the title compound (**44**, 280 mg, 97%) as a yellow solid. LCMS M/Z (M+H) 459.

Step 3:**1-[3-[7-(1-methylpyrazol-4-yl)-2,3,4,5-tetrahydro-1-benzazepin-1-yl]-1-(3*S*-tetrahydrofuran-3-yl)]-6,7-dihydro-4*H*-pyrazolo[4,3-*c*]pyridin-5-yl]ethanone (4)**

To a solution of (*S*)-1-(3-(7-bromo-2,3,4,5-tetrahydro-1*H*-benzo[*b*]azepin-1-yl)-1-(tetrahydrofuran-3-yl)-6,7-dihydro-1*H*-pyrazolo[4,3-*c*]pyridin-5(4*H*)-yl)ethanone (**44**, 350 mg, 0.760 mmol) in dioxane (5 mL) and water (3 mL) was added 1-methyl-4-(4,4,5,5-tetramethyl-1,3,2-dioxaborolan-2-yl)-1*H*-pyrazole (175 mg, 0.840 mmol), K₂CO₃ (210 mg, 1.52 mmol) and [1,1'-bis(diphenylphosphino)ferrocene]dichloropalladium(II) (56 mg, 0.076 mmol). The mixture was heated to 110 °C for 18 h under a nitrogen atmosphere. After cooling the reaction to room temperature, the mixture was concentrated in vacuo. The residue was purified by reverse phase chromatography (acetonitrile 23–53% / 0.2% formic acid in water) to give the title compound (**4**, 82 mg, 23%) as a white solid. ¹H NMR (400 MHz, DMSO-*d*₆) δ 8.06–8.05 (m, 1H), 8.00–7.79 (m, 1H), 7.44–7.42 (m, 1H), 7.31–7.26 (m, 1H), 6.90–6.77 (m, 1H), 4.81–4.78 (m, 1H), 4.03–3.98 (m, 2H), 3.84–3.78 (m, 5H), 3.55–3.43 (m, 6H), 2.77–2.55 (m, 4H), 2.25–2.22 (m, 2H), 1.97–1.62 (m, 7H). LCMS M/Z (M+H) 483.

1-[3-[7-methoxy-6-(1-methylpyrazol-4-yl)-3,4-dihydro-2*H*-quinolin-1-yl]-1-(3*S*-tetrahydrofuran-3-yl)]-6,7-dihydro-4*H*-pyrazolo[4,3-*c*]pyridin-5-yl]ethanone (7)

1
2
3 In a similar manner to **4**, compound **7** was prepared from 7-methoxy-1,2,3,4-
4 tetrahydroquinoline (**41**) to provide the title compound (**7**, 24%) as a white solid. ¹H
5 NMR (400 MHz, DMSO-*d*₆) δ 7.90 (s, 1H), 7.72 (s, 1H), 7.19 (s, 1H), 6.29 (s, 1H), 4.95–
6 4.86 (m, 1H), 4.19–4.22 (m, 2H), 4.00–3.92 (m, 2H), 3.82–3.55 (m, 6H), 3.80 (s, 3H),
7 3.61 (s, 3H), 2.83–2.72 (m, 4H), 2.38–2.12 (m, 2H), 2.07–1.91 (m, 5H). LCMS M/Z
8 (M+H) 477.
9
10
11
12
13
14
15
16
17
18
19
20
21

22 **1-[3-[7-chloro-6-(1-methylpyrazol-4-yl)-3,4-dihydro-2H-quinolin-1-yl]-1-[(3S)-**
23 **tetrahydrofuran-3-yl]-6,7-dihydro-4H-pyrazolo[4,3-*c*]pyridin-5-yl]ethanone (6)**
24
25
26

27 **Step 1:**
28
29

30 **6-bromo-7-chloro-1,2,3,4-tetrahydroquinoline (49)**
31
32

33 To a solution of 7-chloro-1,2,3,4-tetrahydroquinoline (**46**, 14 g, 80 mmol) in DCM (100
34 mL) at 0 °C was added *N*-bromosuccinimide (14.8 g, 80.0 mmol). The mixture was
35 stirred at room temperature for 1 h. Water (100 mL) was added and the mixture was
36 extracted with DCM (100 mL x 2). The combined organic layers were dried over
37 anhydrous Na₂SO₄, filtered and concentrated in vacuo. The crude residue was purified by
38 silica gel chromatography (petroleum ether / EtOAc = 100 : 1) to give the title compound
39 (**49**, 7.1 g, 36%) as a light yellow solid. LCMS M/Z (M+H) 246.
40
41
42
43
44
45
46
47
48
49
50
51
52

53 **Step 2:**
54
55

56 **7-chloro-6-(1-methyl-1H-pyrazol-4-yl)-1,2,3,4-tetrahydroquinoline (52)**
57
58
59
60

To a solution of 6-bromo-7-chloro-1,2,3,4-tetrahydroquinoline (**49**, 2.1 g, 8.5 mmol) in dioxane/H₂O (60 mL, 5 : 1) was added 1-methyl-4-(4,4,5,5-tetramethyl-1,3,2-dioxaborolan-2-yl)-1*H*-pyrazole (1.9 g, 9.4 mmol), Na₂CO₃ (1.8 g, 17 mmol) and [1,1'-bis(diphenylphosphino)ferrocene]dichloropalladium(II) (622 mg, 0.900 mmol). The mixture was heated to 110 °C for 12 h under a nitrogen atmosphere. After cooling the reaction to room temperature, the mixture was concentrated in vacuo. The crude residue was purified by silica gel chromatography (petroleum ether / EtOAc = 4 : 1) to give the title compound (**52**, 2.0 g, 95%) as yellow solid. ¹H NMR (400 MHz, DMSO-*d*₆) δ 7.88–7.85 (m, 1H), 7.61 (s, 1H), 7.01 (s, 1H), 6.53 (s, 1H), 5.95 (s, 1H), 3.86–3.84 (m, 3H), 3.38–3.16 (m, 2 H), 2.65–2.62 (m, 2 H), 1.80–1.74 (m, 2 H).

Step 3:

1-[3-[7-chloro-6-(1-methylpyrazol-4-yl)-3,4-dihydro-2*H*-quinolin-1-yl]-1-(3*S*)-tetrahydrofuran-3-yl]-6,7-dihydro-4*H*-pyrazolo[4,3-*c*]pyridin-5-yl]ethanone (6**)**

To a solution of 7-chloro-6-(1-methyl-1*H*-pyrazol-4-yl)-1,2,3,4-tetrahydroquinoline (**52**, 247 mg, 1.0 mmol) in dioxane (3 mL) and toluene (3 mL) was added *t*-BuONa (288 mg, 3.00 mmol), tris(dibenzylideneacetone)dipalladium (46 mg, 0.050 mmol), 4,5-bis(diphenylphosphino)-9,9-dimethylxanthene (59 mg, 0.10 mmol) and (*S*)-1-(3-bromo-1-(tetrahydrofuran-3-yl)-6,7-dihydro-1*H*-pyrazolo[4,3-*c*]pyridin-5(4*H*)-yl)ethanone (**33**, 313 mg, 1.00 mmol). The mixture was heated to 90 °C for 16 h under a nitrogen atmosphere. After cooling the reaction to room temperature, the mixture was concentrated in vacuo. The crude residue was purified by Prep-TLC (DCM / MeOH = 20

1
2
3 : 1) to give the title compound (**6**, 240 mg, 50%) as a light yellow solid. ¹H NMR (400
4 MHz, DMSO-*d*₆) δ 7.97 (s, 1H), 7.68 (s, 1H), 7.21–7.20 (m, 1H), 6.54–6.50 (m, 1H),
5
6 4.95–4.89 (m, 1H), 4.18–4.15 (m, 2H), 4.03–3.98 (m, 2H), 3.85–3.71 (m, 7H), 3.54–3.50
7
8 (m, 2H), 2.86–2.77 (m, 4H), 2.33–2.27 (m, 2H), 2.08–1.94 (m, 5H). LCMS M/Z (M+H)
9
10
11 481.
12
13
14
15
16
17
18
19

20 **1-[3-[7-(difluoromethyl)-6-(1-methylpyrazol-4-yl)-3,4-dihydro-2*H*-quinolin-1-yl]-1-**
21 **[(3*S*)-tetrahydrofuran-3-yl]-6,7-dihydro-4*H*-pyrazolo[4,3-*c*]pyridin-5-yl]ethanone**
22
23
24 **(8)**
25
26

27 **Step 1:**
28

29
30 **quinoline-7-carbaldehyde**
31
32

33 To a solution of 7-methylquinoline (27.0 g, 189 mmol) at 160 °C was added SeO₂ (21.0
34 g, 189 mmol) portionwise over 5 min. The mixture was stirred at 160 °C for 8 h. After
35 cooling the reaction to room temperature, DCM (400 mL) was added and the mixture was
36 filtered through celite. The organic layer was concentrated in vacuo. The crude residue
37 was purified by silica gel chromatography (petroleum ether / EtOAc = 10 : 1) to give the
38 title compound (14.0 g, 47%) as yellow oil. ¹H NMR (400 MHz, CDCl₃) δ 10.23 (s, 1H),
39 9.03 (d, *J* = 2.8 Hz, 1H), 8.56 (s, 1H), 8.22 (d, *J* = 8.4 Hz, 1H), 8.04 (d, *J* = 8.4 Hz, 1H),
40 7.93 (d, *J* = 8.4 Hz, 1H), 7.55–7.52 (m, 1H).
41
42
43
44
45
46
47
48
49
50
51
52
53
54
55
56

57 **Step 2:**
58
59
60

7-(difluoromethyl)quinoline

To a solution of quinoline-7-carbaldehyde (14.0 g, 89.2 mmol) in DCM (150 mL) 0 °C was added diethylaminosulfurtrifluoride (65.0 g, 446 mmol) dropwise over 20 min. The mixture was stirred at room temperature for 16 h. The mixture was poured into sat. aq. NaHCO₃ (1 L) at 0 °C and extracted with DCM (200 mL x 2). The combined organic layers were dried over anhydrous Na₂SO₄, filtered and concentrated in vacuo. The crude residue was purified by silica gel chromatography (petroleum ether / EtOAc = 5 : 1) to give the title compound (13.0 g, 81%) as yellow oil. ¹H NMR (400 MHz, CDCl₃) δ 8.92 (d, *J* = 2.8 Hz, 1H), 8.15 (d, *J* = 8.4 Hz, 2H), 7.86 (d, *J* = 8.4 Hz, 1H), 7.63 (d, *J* = 8.8 Hz, 1H), 7.44–7.41 (m, 1H), 6.78 (t, *J* = 56.0 Hz, 1H).

Step 3:**7-(difluoromethyl)-1,2,3,4-tetrahydroquinoline (47)**

To a solution of 7-(difluoromethyl)quinoline (13.0 g, 72.6 mmol) and NaBH₃CN (23.0 g, 363 mmol) in MeOH (150 mL) at 0 °C was added boron trifluoride diethyl etherate (17.9 mL, 145 mmol) dropwise over 20 min. The mixture was heated to 90 °C for 24 h. After cooling the reaction to room temperature, the mixture was poured into sat. aq. NaHCO₃ (1 L) at 0 °C and extracted with DCM (200 mL x 2). The combined organic layers were dried over Na₂SO₄, filtered and concentrated in vacuo. The crude residue was purified by silica gel chromatography (petroleum ether / EtOAc = 20 : 1) to give the title compound (**47**, 8.0 g, 56%) as brown oil. ¹H NMR (400 MHz, CDCl₃) δ 7.00 (d, *J* = 7.2 Hz, 1H),

1
2
3 6.71 (d, $J = 8.0$ Hz, 1H), 6.59 (s, 1H), 6.50 (t, $J = 56.8$ Hz, 1H), 3.33 (t, $J = 5.6$ Hz, 2H),
4
5 2.79 (t, $J = 6.4$ Hz, 2H), 1.98–1.92 (m, 2H).
6
7
8
9

10
11
12 **Step 4:**
13

14
15 **6-bromo-7-(difluoromethyl)-1,2,3,4-tetrahydroquinoline (50)**
16

17
18 To a solution of 7-(difluoromethyl)-1,2,3,4-tetrahydroquinoline (**47**, 7.00 g, 38.3 mmol)
19 in DCM (100 mL) at 0 °C was added *N*-bromosuccinimide (6.90 g, 38.3 mmol)
20 portionwise over 20 min. The mixture was stirred at room temperature for 16 h. The
21 mixture was poured into water (100 mL) and extracted with DCM (200 mL x 2). The
22 combined organic layers were dried over Na₂SO₄, filtered and concentrated in vacuo. The
23 crude residue was purified by silica gel chromatography (petroleum ether / EtOAc = 300 :
24 1) to give the title compound (**50**, 6.0 g, 60%) as light yellow oil. ¹H NMR (400 MHz,
25 CDCl₃) δ 7.13 (s, 1H), 6.78 (t, $J = 55.2$ Hz, 1H), 6.72 (s, 1H), 3.31 (t, $J = 5.2$ Hz, 2H),
26 2.74 (t, $J = 6.0$ Hz, 2H), 1.95–1.87 (m, 2H).
27
28
29
30
31
32
33
34
35
36
37
38
39
40
41
42
43

44 **Step 5:**
45

46
47 **7-(difluoromethyl)-6-(1-methyl-1*H*-pyrazol-4-yl)-1,2,3,4-tetrahydroquinoline (53)**
48

49
50 To a solution of 6-bromo-7-(difluoromethyl)-1,2,3,4-tetrahydroquinoline (**50**, 600 mg,
51 2.30 mmol) in dioxane (8 mL) and H₂O (2 mL) was added K₂CO₃ (635 mg, 4.6 mmol),
52 [1,1'-bis(diphenylphosphino)ferrocene]dichloropalladium(II) (169 mg, 0.23 mmol) and 1-
53 methyl-4-(4,4,5,5-tetramethyl-1,3,2-dioxaborolan-2-yl)-1*H*-pyrazole (478 mg, 2.30
54
55
56
57
58
59
60

1
2
3 mmol). The mixture was heated to 110 °C for 18 h under a nitrogen atmosphere. After
4
5 cooling the reaction to room temperature, the mixture was concentrated in vacuo. The
6
7 crude residue was purified by silica gel chromatography (petroleum ether / EtOAc = 40 :
8
9 1) to give the title compound (**53**, 520 mg, 86%) as yellow oil. LCMS M/Z (M+H) 264.

16
17 **Step 6:**

18
19
20 **1-[3-[7-(difluoromethyl)-6-(1-methylpyrazol-4-yl)-3,4-dihydro-2H-quinolin-1-yl]-1-**
21
22 **tetrahydrofuran-3-yl-6,7-dihydro-4H-pyrazolo[4,3-c]pyridin-5-yl]ethanone**

23
24
25 To a solution of 1-(3-bromo-1-(tetrahydrofuran-3-yl)-6,7-dihydro-1H-pyrazolo[4,3-
26
27 c]pyridin-5(4H)-yl)ethanone (**32**, 313 mg, 1.0 mmol), 7-(difluoromethyl)-6-(1-methyl-
28
29 1H-pyrazol-4-yl)-1,2,3,4-tetrahydroquinoline (**53**, 263 mg, 1.0 mmol) and *t*-BuONa (288
30
31 mg, 3.0 mmol) in 1,4-dioxane (10 mL) was added chloro(2-dicyclohexylphosphino-2',6'-
32
33 di-*i*-propoxy-1,1'-biphenyl)[2-(2-aminoethylphenyl)]palladium(II), methyl-*tert*-
34
35 butylether adduct (82 mg, 0.10 mmol) and 2-dicyclohexylphosphino-2',6'-di-*i*-propoxy-
36
37 1,1'-biphenyl (47 mg, 0.10 mmol). The mixture was irradiated in a microwave at 130 °C
38
39 for 45 min. After cooling to room temperature, the mixture was filtered and the filtrate
40
41 was concentrated in vacuo. The crude residue was purified by Prep-TLC (DCM / MeOH
42
43 = 20 : 1) to give the title compound (76 mg, 16%) as a light yellow solid. ¹H NMR (400
44
45 MHz, DMSO-*d*₆) δ 7.76 (s, 1H), 7.50 (s, 1H), 7.11 (s, 1H), 6.94–6.65 (m, 2H), 4.94–4.88
46
47 (m, 1H), 4.16–4.12 (m, 2H), 4.03–3.90 (m, 2H), 3.86 (s, 3H), 3.82–3.79 (m, 4H), 3.70–
48
49 3.56 (m, 2H), 2.86–2.74 (m, 4H), 2.29–2.22 (m, 2H), 2.07–1.96 (m, 5H). LCMS M/Z
50
51 (M+H) 497.

Step 7:

1-**[3-[7-(difluoromethyl)-6-(1-methylpyrazol-4-yl)-3,4-dihydro-2*H*-quinolin-1-yl]-1-
[(3*S*)-tetrahydrofuran-3-yl]-6,7-dihydro-4*H*-pyrazolo[4,3-*c*]pyridin-5-yl]ethanone**
(8)

Racemic 1-[3-[7-(difluoromethyl)-6-(1-methylpyrazol-4-yl)-3,4-dihydro-2*H*-quinolin-1-yl]-1-tetrahydrofuran-3-yl]-6,7-dihydro-4*H*-pyrazolo[4,3-*c*]pyridin-5-yl]ethanone (50 mg) was separated by using chiral SFC (Cellulose-3 150×21.2mm I.D.; Supercritical CO₂ / MeOH (0.1% NH₄OH) = 20/80 at 70 mL/min) to give 1-[3-[7-(difluoromethyl)-6-(1-methylpyrazol-4-yl)-3,4-dihydro-2*H*-quinolin-1-yl]-1-[(3*R*)-tetrahydrofuran-3-yl]-6,7-dihydro-4*H*-pyrazolo[4,3-*c*]pyridin-5-yl]ethanone (22 mg, second peak) and 1-[3-[7-(difluoromethyl)-6-(1-methylpyrazol-4-yl)-3,4-dihydro-2*H*-quinolin-1-yl]-1-[(3*S*)-tetrahydrofuran-3-yl]-6,7-dihydro-4*H*-pyrazolo[4,3-*c*]pyridin-5-yl]ethanone (**8**, 17 mg, first peak). *R*-isomer: ¹H NMR (400 MHz, DMSO-*d*₆) δ 7.75 (s, 1H), 7.51 (s, 1H), 7.11 (s, 1H), 6.94–6.64 (m, 2H), 4.95–4.88 (m, 1H), 4.17–4.12 (m, 2H), 4.04–3.91 (m, 2H), 3.86 (s, 3H), 3.82–3.80 (m, 4H), 3.70–3.56 (m, 2H), 2.87–2.74 (m, 4H), 2.29–2.22 (m, 2H), 2.07–1.97 (m, 5H). LCMS M/Z (M+H) 497. *S*-isomer (**8**): ¹H NMR (400 MHz, DMSO-*d*₆) δ 7.76 (s, 1H), 7.49 (s, 1H), 7.10 (s, 1H), 6.93–6.64 (m, 2H), 4.94–4.88 (m, 1H), 4.16–4.12 (m, 2H), 4.03–3.90 (m, 2H), 3.86 (s, 3H), 3.82–3.79 (m, 4H), 3.69–3.56 (m, 2H), 2.86–2.73 (m, 4H), 2.30–2.20 (m, 2H), 2.06–1.96 (m, 5H). LCMS M/Z (M+H) 497.

1
2
3
4
5
6
7
8
9
10

**1-[3-[6-(1-methylpyrazol-4-yl)-7-(trifluoromethyl)-3,4-dihydro-2*H*-quinolin-1-yl]-1-
[(3*S*)-tetrahydrofuran-3-yl]-6,7-dihydro-4*H*-pyrazolo[4,3-*c*]pyridin-5-yl]ethanone
(9)**

11
12
13

Step 1:

14
15
16

6-bromo-7-(trifluoromethyl)-1,2,3,4-tetrahydroquinoline (51)

17
18
19
20
21
22
23
24
25
26
27
28
29
30
31
32
33
34
35

To a solution of 7-(trifluoromethyl)-1,2,3,4-tetrahydroquinoline (**48**, 800 mg, 3.98 mmol) in DCM (50 mL) at 0 °C was added *N*-bromosuccinimide (637 mg, 3.58 mmol) portionwise over 20 min. The mixture was stirred at room temperature for 1 h. The reaction was concentrated in vacuo. The crude residue was purified by silica gel chromatography (petroleum ether / EtOAc = 10 : 1) to give the presumed title compound (**51**, 430 mg, 39%) as yellow oil.

36
37
38

Step 2:

39
40
41

6-(1-methyl-1*H*-pyrazol-4-yl)-7-(trifluoromethyl)-1,2,3,4-tetrahydroquinoline (54)

42
43
44
45
46
47
48
49
50
51
52
53
54
55
56
57
58
59
60

To a solution of 6-bromo-7-(trifluoromethyl)-1,2,3,4-tetrahydroquinoline (**51**, 430 mg, 1.54 mmol) in dioxane (20 mL) and H₂O (4 mL) was added Na₂CO₃ (488 mg, 4.61 mmol), chloro(2-dicyclohexylphosphino-2',4',6'-tri-*i*-propyl-1,1'-biphenyl)(2'-amino-1,1'-biphenyl-2-yl) palladium(II) (121 mg, 0.150 mmol), 2-(dicyclohexylphosphino)-2',4',6'-triiisopropylbiphenyl (73 mg, 0.15 mmol) and 1-methyl-4-(4,4,5,5-tetramethyl-1,3,2-dioxaborolan-2-yl)-1*H*-pyrazole (383 mg, 1.84 mmol). The mixture was heated to 80 °C for 3 h under a nitrogen atmosphere. After cooling to room temperature, the mixture was

1
2
3 concentrated in vacuo. The crude residue was purified by silica gel chromatography
4 (petroleum ether / EtOAc = 3 : 1) to give the presumed title compound (**54**, 300 mg,
5
6 70%) as a white solid.
7
8
9

10
11
12
13
14 **Step 3:**
15

16
17
18 **1-[3-[6-(1-methylpyrazol-4-yl)-7-(trifluoromethyl)-3,4-dihydro-2*H*-quinolin-1-yl]-1-**
19
20 **[(3*S*)-tetrahydrofuran-3-yl]-6,7-dihydro-4*H*-pyrazolo[4,3-*c*]pyridin-5-yl]ethanone**
21

22
23 **(9)**
24

25
26 To a solution of (*S*)-1-(3-bromo-1-(tetrahydrofuran-3-yl)-6,7-dihydro-1*H*-pyrazolo[4,3-
27
28 *c*]pyridin-5(4*H*)-yl)ethanone (**33**, 112 mg, 0.360 mmol), 6-(1-methyl-1*H*-pyrazol-4-yl)-7-
29
30 (trifluoromethyl)-1,2,3,4-tetrahydroquinoline (**54**, 100 mg, 0.36 mmol) and *t*-BuONa
31
32 (103 mg, 1.07 mmol) in 1,4-dioxane (2 mL) was added dichloro[1,3-bis(2,6-di-3-
33
34 pentylphenyl)imidazol-2-ylidene](3-chloropyridyl)palladium(II) (28 mg, 0.040 mmol).
35
36 The mixture was irradiated in a microwave at 150 °C for 1 h. After cooling to room
37
38 temperature, water (40 mL) was added and extracted with EtOAc (30 mL x 3). The
39
40 combined organic layers were washed with brine (50 mL), dried over anhydrous Na₂SO₄,
41
42 filtered and concentrated in vacuo. The crude residue was purified by reverse phase
43
44 chromatography (acetonitrile 40–70% / 0.225 % formic acid in water) to give the title
45
46 compound (**9**, 39 mg, 21%) as a white solid. ¹H NMR (400 MHz, CDCl₃) δ 7.53 (d, *J* =
47
48 2.8 Hz, 1H), 7.41 (d, *J* = 7.2 Hz, 1H), 7.07–7.02 (m, 1H), 6.90 (d, *J* = 7.6 Hz, 1H), 4.78–
49
50 4.76 (m, 1H), 4.27–4.13 (m, 4H), 4.00–3.91 (m, 3H), 3.93 (s, 3H), 3.76–3.70 (m, 3H),
51
52 2.88–2.84 (m, 4H), 2.43–2.39 (m, 2H), 2.18–2.06 (m, 5H). LCMS M/Z (M+H) 515.
53
54
55
56
57
58
59
60

1
2
3
4
5
6
7
8
9
10
11
12
13
14
15
16
17
18
19
20
21
22
23
24
25
26
27
28
29
30
31
32
33
34
35
36
37
38
39
40
41
42
43
44
45
46
47
48
49
50
51
52

1-[3-[7-methyl-6-(1-methylpyrazol-4-yl)-3,4-dihydro-2*H*-quinolin-1-yl]-1-(3*S*)-tetrahydrofuran-3-yl]-6,7-dihydro-4*H*-pyrazolo[4,3-*c*]pyridin-5-yl]ethanone (5)

To a solution of 1-[3-[7-chloro-6-(1-methylpyrazol-4-yl)-3,4-dihydro-2*H*-quinolin-1-yl]-1-(3*S*)-tetrahydrofuran-3-yl]-6,7-dihydro-4*H*-pyrazolo[4,3-*c*]pyridin-5-yl]ethanone (6, 150 mg, 0.313 mmol) in toluene (3 mL) and H₂O (1 mL), was added MeBF₃K (116 mg, 0.939 mmol), palladium(II) acetate (7 mg, 0.03 mmol), Cs₂CO₃ (612 mg, 0.626 mmol) and di(adamantan-1-yl)(butyl)phosphine (23 mg, 0.0616 mmol). The mixture was heated to 100 °C for 18 h under a nitrogen atmosphere. After cooling the reaction to room temperature, the mixture was concentrated in vacuo. The crude residue was purified by Prep-TLC (DCM / MeOH = 20 : 1) to give the title compound (5, 21 mg, 15%) as a white solid. ¹H NMR (400 MHz, DMSO-*d*₆) δ 7.76 (s, 1H), 7.52 (s, 1H), 6.99–6.98 (m, 1H), 6.36–6.34 (m, 1H), 4.90–4.85 (m, 1H), 4.14–4.05 (m, 2H), 4.04–3.93 (m, 2H), 3.87–3.66 (m, 7H), 3.58–3.52 (m, 2H), 2.84–2.67 (m, 4H), 2.34–2.21 (m, 2H), 2.15 (s, 3H), 2.09–1.81 (m, 5H). LCMS M/Z (M+H) 461.

43
44
45
46
47
48
49
50
51
52

1-(3-(7-(difluoromethyl)-6-(1-methyl-1*H*-pyrazol-4-yl)-3,4-dihydroquinolin-1(2*H*)-yl)-1-(tetrahydro-2*H*-pyran-4-yl)-1,4,6,7-tetrahydro-5*H*-pyrazolo[4,3-*c*]pyridin-5-yl)ethan-1-one (10)

53
54
55
56
57
58
59
60

To a solution of 7-(difluoromethyl)-6-(1-methyl-1*H*-pyrazol-4-yl)-1,2,3,4-tetrahydroquinoline (53, 251 mg, 0.950 mmol) in 2-methyl-2-butanol (8 mL) was added 1-(3-bromo-1-(tetrahydro-2*H*-pyran-4-yl)-6,7-dihydro-1*H*-pyrazolo[4,3-*c*]pyridin-5(4*H*)-

1
2
3 yl)ethanone (**34**, 500 mg, 1.52 mmol), (2-dicyclohexylphosphino-2,4,6-triisopropyl-1,1-
4 biphenyl)[2-(2-amino-1,1-biphenyl)]palladium(II) methanesulfonate (129 mg, 0.150
5 mmol) and K₃PO₄ (971 mg, 4.60 mmol). The mixture was heated to 95 °C for 42 h under
6 an argon atmosphere. After cooling the reaction to room temperature, the mixture was
7 concentrated in vacuo. The crude residue was purified by silica gel chromatography
8 (DCM / MeOH = 50:1) to give 1-[3-[7-(difluoromethyl)-6-(1-methylpyrazol-4-yl)-3,4-
9 dihydro-2*H*-quinolin-1-yl]-1-tetrahydrofuran-3-yl-6,7-dihydro-4*H*-pyrazolo[4,3-
10 *c*]pyridin-5-yl]ethanone (**10**, 360 mg, 74%) as a yellow solid. ¹H NMR (400 MHz,
11 DMSO-*d*₆) δ 7.75 (s, 1H), 7.50 (s, 1H), 7.10 (s, 1H), 6.96–6.63 (m, 2H), 4.33–4.25 (m,
12 1H), 4.20–4.09 (m, 2H), 3.99–3.90 (m, 2H), 3.86 (s, 3H), 3.78–3.66 (m, 2H), 3.63–3.55
13 (m, 2H), 3.49–3.41 (m, 2H), 2.89–2.66 (m, 4H), 2.11–1.90 (m, 7H), 1.85–1.80 (m, 2H);
14 ¹³C NMR (101 MHz, 360 K, DMSO-*d*₆) δ 169.3, 148.4, 142.7, 138.3, 137.7, 131.1,
15 129.7, 129.2 (t, *J* = 20.8 Hz), 126.4, 121.4, 119.1, 114.3 (t, *J* = 235.3 Hz), 110.7, 106.5,
16 66.5, 54.5, 49.6, 43.4, 39.0, 38.7, 32.8, 27.4, 22.5, 22.3, 21.7; HRMS *m/z* 511.2628 (M +
17 H⁺, C₂₇H₃₃F₂N₆O₂, requires 511.2633).

18
19
20
21
22
23
24
25
26
27
28
29
30
31
32
33
34
35
36
37
38
39
40
41
42
43 **1-[1-cyclohexyl-3-[7-(difluoromethyl)-6-(1-methylpyrazol-4-yl)-3,4-dihydro-2*H*-**
44 **quinolin-1-yl]-6,7-dihydro-4*H*-pyrazolo[4,3-*c*]pyridin-5-yl]ethanone (**11**)**

45
46
47
48
49 **Step 1:**

50
51
52 ***tert*-butyl 3-bromo-1-((2-(trimethylsilyl)ethoxy)methyl)-6,7-dihydro-1*H*-**
53 **pyrazolo[4,3-*c*]pyridine-5(4*H*)-carboxylate (**55**) and *tert*-butyl 3-bromo-2-((2-**
54
55
56
57
58
59
60

**(trimethylsilyl)ethoxy)methyl)-6,7-dihydro-2H-pyrazolo[4,3-c]pyridine-5(4H)-
carboxylate**

To a solution of *tert*-butyl 3-bromo-6,7-dihydro-1H-pyrazolo[4,3-c]pyridine-5(4H)-carboxylate (**26**, 80.0 g, 265 mmol) in THF (1.5 L) at 0 °C was added sodium hydride (60%, 12.71 g, 317.7 mmol) by portionwise. The mixture was stirred at room temperature for 0.5 h. 2-(Trimethylsilyl)ethoxymethyl chloride (52.97 g, 317.7 mmol) was added dropwise and the mixture stirred at room temperature for an additional 16 h. The mixture was quenched with water (1 L) and extracted with EtOAc (500 mL x 3). The combined organic layers were dried over anhydrous Na₂SO₄, filtered and concentrated in vacuo. The crude residue was purified by silica gel chromatography (petroleum ether / EtOAc = 5: 1) to give a mixture of the title compounds (**55**, 95 g, 83%) as yellow oil. LCMS M/Z (M+H) 434.

Step 2:

***tert*-butyl 3-(7-(difluoromethyl)-6-(1-methyl-1H-pyrazol-4-yl)-3,4-dihydroquinolin-
1(2H)-yl)-1-((2-(trimethylsilyl)ethoxy)methyl)-6,7-dihydro-1H-pyrazolo[4,3-
c]pyridine-5(4H)-carboxylate (**56**)**

To a solution of *tert*-butyl 3-bromo-1-((2-(trimethylsilyl)ethoxy)methyl)-6,7-dihydro-1H-pyrazolo[4,3-c]pyridine-5(4H)-carboxylate and *tert*-butyl 3-bromo-2-((2-(trimethylsilyl)ethoxy)methyl)-6,7-dihydro-2H-pyrazolo[4,3-c]pyridine-5(4H)-carboxylate (**55**, 65.7 g, 152 mmol) in 1,4-dioxane (200 mL) was added chloro(2-dicyclohexylphosphino-2',6'-di-*i*-propoxy-1,1'-biphenyl)(2'-amino-1,1'-biphenyl)-2-

1
2
3 yl)palladium(II) (5.9 g, 7.6 mmol), 2-dicyclohexylphosphino-2',6'-di-*i*-propoxy-1,1'-
4 biphenyl (3.54 g, 7.6 mmol), 7-(difluoromethyl)-6-(1-methyl-1*H*-pyrazol-4-yl)-1,2,3,4-
5 tetrahydroquinoline (20 g, 75.96 mmol) and *t*-BuONa (21.9 g, 227.89 mmol). The
6 mixture was heated to 120 °C for 16 h under an argon atmosphere. After cooling the
7 reaction to room temperature, water (800 mL) was added and extracted with EtOAc (500
8 mL x 3). The combined organic layers were washed with brine (500 mL x 3), dried over
9 anhydrous Na₂SO₄, filtered and concentrated in vacuo. The crude residue was purified by
10 silica gel chromatography (DCM / MeOH = 50 : 1) to give the title compound (**56**, 9.1 g,
11 20%) as a yellow oil. ¹H NMR (400 MHz, CDCl₃) δ 7.54 (s, 1H), 7.41 (s, 1H), 7.03 (s,
12 1H), 6.88 (s, 1H), 6.52 (t, *J* = 55.6 Hz, 1H), 5.33 (s, 2H), 4.10 (s, 2H), 3.96 (s, 3H), 3.73–
13 3.70 (m, 4H), 3.64 (t, *J* = 8.0 Hz, 2H), 2.87–2.80 (m, 4H), 2.09–2.07 (m, 2H), 1.45 (s,
14 9H), 0.93 (t, *J* = 8.0 Hz, 2H), 0.00 (s, 9H). LCMS M/Z (M+H) 615.

Step 3:

***tert*-butyl 3-(7-(difluoromethyl)-6-(1-methyl-1*H*-pyrazol-4-yl)-3,4-dihydroquinolin- 1(2*H*)-yl)-6,7-dihydro-1*H*-pyrazolo[4,3-*c*]pyridine-5(4*H*)-carboxylate (**57**)**

15
16
17
18
19
20
21
22
23
24
25
26
27
28
29
30
31
32
33
34
35
36
37
38
39
40
41
42
43
44
45 To a solution of *tert*-butyl 3-(7-(difluoromethyl)-6-(1-methyl-1*H*-pyrazol-4-yl)-3,4-
46 dihydroquinolin-1(2*H*)-yl)-1-((2-(trimethylsilyl)ethoxy)methyl)-6,7-dihydro-1*H*-
47 pyrazolo[4,3-*c*]pyridine-5(4*H*)-carboxylate (**56**, 8.5 g, 14 mmol) in THF (50 mL) was
48 added tetrabutylammonium fluoride (1.0 M in THF, 40 mL, 40 mmol). The mixture was
49 heated to 60 °C for 16 h under a nitrogen atmosphere. After cooling the reaction to room
50 temperature, EtOAc (200 mL) was added and washed with brine (100 mL x 3). The
51
52
53
54
55
56
57
58
59
60

1
2
3 organic layer was dried over anhydrous Na₂SO₄, filtered and concentrated in vacuo. The
4
5 crude residue was purified by silica gel chromatography (DCM / MeOH = 20 : 1) to give
6
7 the title compound (**57**, 4.4 g, 66%) as a yellow solid. ¹H NMR (400 MHz, CDCl₃) δ 7.54
8
9 (s, 1H), 7.42 (s, 1H), 7.03 (s, 1H), 6.87 (s, 1H), 6.52 (t, *J* = 55.6 Hz, 1H), 4.12 (s, 2H),
10
11 3.96 (s, 3H), 3.72–3.69 (m, 4H), 2.86–2.76 (m, 4H), 2.08–2.05 (m, 2H), 1.45 (s, 9H).
12
13 LCMS M/Z (M+H) 485.
14
15
16
17
18
19
20
21

22 **Step 4:**

23
24 **7-(difluoromethyl)-6-(1-methyl-1*H*-pyrazol-4-yl)-1-(4,5,6,7-tetrahydro-1*H*-**
25
26 **pyrazolo[4,3-*c*]pyridin-3-yl)-1,2,3,4-tetrahydroquinoline (**58**)**
27
28
29

30 To a solution of *tert*-butyl 3-(7-(difluoromethyl)-6-(1-methyl-1*H*-pyrazol-4-yl)-3,4-
31
32 dihydroquinolin-1(2*H*)-yl)-6,7-dihydro-1*H*-pyrazolo[4,3-*c*]pyridine-5(4*H*)-carboxylate
33
34 (**57**, 2.0 g, 4.13 mmol) in DCM (5 mL) at 0 °C was added trifluoroacetic acid (4.0 mL,
35
36 4.13 mmol). The mixture was stirred at 20 °C for 16 h and concentrated in vacuo to give
37
38 the title compound (**58**, 2.0 g, crude) as brown oil that required no further purification.
39
40
41
42 LCMS M/Z (M+H) 385.
43
44
45
46
47
48

49 **Step 5:**

50
51 **1-[3-[7-(difluoromethyl)-6-(1-methylpyrazol-4-yl)-3,4-dihydro-2*H*-quinolin-1-yl]-**
52
53 **1,4,6,7-tetrahydropyrazolo[4,3-*c*]pyridin-5-yl]ethanone (**59**)**
54
55
56
57
58
59
60

To a solution of 7-(difluoromethyl)-6-(1-methyl-1*H*-pyrazol-4-yl)-1-(4,5,6,7-tetrahydro-1*H*-pyrazolo[4,3-*c*]pyridin-3-yl)-1,2,3,4-tetrahydroquinoline (**58**, 120 mg, 0.310 mmol) in DCM (5 mL) at 0 °C was added triethylamine (0.09 mL, 0.6 mmol) and acetic anhydride (0.04 mL, 0.62 mmol). The mixture was stirred at 20 °C for 1 h. DCM (50 mL) was added, washed with water (30 mL x 3) and brine (30 mL). The organic layer was dried over anhydrous Na₂SO₄, filtered and concentrated in vacuo. The crude residue was purified by reverse phase chromatography (acetonitrile 26–56% / 0.05% NH₄OH in water) to give the title compound (**59**, 19 mg, 14%) as a white solid. ¹H NMR (400 MHz, DMSO-*d*₆) δ 12.42–12.31 (m, 1H), 7.75 (s, 1H), 7.50 (s, 1H), 7.10 (s, 1H), 6.96–6.62 (m, 1H), 6.73 (s, 1H), 4.21–4.04 (m, 2H), 3.86 (s, 3H), 3.76–3.51 (m, 4H), 2.88–2.66 (m, 4H), 2.07–1.87 (m, 5H). LCMS M/Z (M+H) 427.

Step 6:

1-[1-cyclohexyl-3-[7-(difluoromethyl)-6-(1-methylpyrazol-4-yl)-3,4-dihydro-2*H*-quinolin-1-yl]-6,7-dihydro-4*H*-pyrazolo[4,3-*c*]pyridin-5-yl]ethanone (11)

To a solution of 1-[3-[7-(difluoromethyl)-6-(1-methylpyrazol-4-yl)-3,4-dihydro-2*H*-quinolin-1-yl]-1,4,6,7-tetrahydropyrazolo[4,3-*c*]pyridin-5-yl]ethanone (**59**, 50 mg, 0.12 mmol) in DMF (5 mL) was added Cs₂CO₃ (69 mg, 0.21 mmol) and bromocyclohexane (0.03 mL, 0.23 mmol). The mixture was heated to 80 °C for 24 h. After cooling to room temperature, the mixture was filtered and concentrated in vacuo. The crude residue was purified by reverse phase chromatography (acetonitrile 42–72% / 0.2% formic acid in water) to give the title compound (**11**, 3 mg, 5%) as a white solid. ¹H NMR (400 MHz,

1
2
3
4
5
6
7
8
9
10
11
12
13
14
15
16
17
18
19
20
21
22
23
24
25
26
27
28
29
30
31
32
33
34
35
36
37
38
39
40
41
42
43
44
45
46
47
48
49
50
51
52
53
54
55
56
57
58
59
60

CDCl₃) δ 7.52 (d, *J* = 5.6 Hz, 1H), 7.40 (d, *J* = 6.4 Hz, 1H), 7.06–6.96 (m, 1H), 6.86 (d, *J* = 2.4 Hz, 1H), 6.68–6.34 (m, 1H), 4.30–4.10 (m, 2H), 3.96 (s, 3H), 3.92–3.83 (m, 2H), 3.76–3.66 (m, 3H), 2.90–2.72 (m, 4H), 2.19–2.02 (m, 7H), 1.96–1.88 (m, 6H), 1.44–1.22 (m, 2H). LCMS M/Z (M+H) 509.

1-[3-[7-(difluoromethyl)-6-(1-methylpyrazol-4-yl)-3,4-dihydro-2*H*-quinolin-1-yl]-1-(1-methylsulfonyl-4-piperidyl)-6,7-dihydro-4*H*-pyrazolo[4,3-*c*]pyridin-5-yl]ethanone (15)

In a similar manner to **11**, compound **15** was prepared from 1-(methylsulfonyl)piperidin-4-yl methanesulfonate to provide the title compound (**15**, 7%). ¹H NMR (400 MHz, CDCl₃) δ 7.57–7.54 (m, 1H), 7.44–7.39 (m, 1H), 7.07–7.01 (m, 1H), 6.90–6.87 (m, 1H), 6.71–6.37 (m, 1H), 4.28–4.13 (m, 2H), 4.10–4.02 (m, 1H), 3.99–3.91 (m, 3H), 3.96 (s, 3H), 3.75–3.69 (m, 3H), 3.02–2.92 (m, 2H), 2.90–2.83 (m, 5H), 2.81–2.71 (m, 2H), 2.39–2.24 (m, 2H), 2.17–2.05 (m, 7H). LCMS M/Z (M+H) 588.

1-[3-[7-(difluoromethyl)-6-(1-methylpyrazol-4-yl)-3,4-dihydro-2*H*-quinolin-1-yl]-1-(4-piperidyl)-6,7-dihydro-4*H*-pyrazolo[4,3-*c*]pyridin-5-yl]ethanone (13)

Step 1:

***tert*-butyl 4-(5-acetyl-3-(7-(difluoromethyl)-6-(1-methyl-1*H*-pyrazol-4-yl)-3,4-dihydroquinolin-1(2*H*)-yl)-4,5,6,7-tetrahydro-1*H*-pyrazolo[4,3-*c*]pyridin-1-yl)piperidine-1-carboxylate (60)**

1
2
3 In a similar manner to **11**, compound **60** was prepared from *tert*-butyl 4-
4 ((methylsulfonyl)oxy)piperidine-1-carboxylate to provide the title compound (**60**, 17%)
5 as a white solid. ¹H NMR (400 MHz, CDCl₃) δ 7.55–7.53 (m, 1H), 7.42–7.40 (m, 1H),
6 7.06–7.00 (m, 1H), 6.86 (s, 1H), 6.68–6.37 (m, 1H), 4.38–4.12 (m, 3H), 4.08–3.99 (m,
7 1H), 3.96 (s, 3H), 3.95–3.89 (m, 2H), 3.75–3.67 (m, 3H), 2.89–2.70 (m, 6H), 2.17–2.03
8 (m, 7H), 1.92–1.88 (m, 2H), 1.48 (s, 9H). LCMS M/Z (M+H) 610.
9
10
11
12
13
14
15
16
17
18
19
20
21

22 Step 2:

23 24 25 **1-[3-[7-(difluoromethyl)-6-(1-methylpyrazol-4-yl)-3,4-dihydro-2*H*-quinolin-1-yl]-1-** 26 27 **(4-piperidyl)-6,7-dihydro-4*H*-pyrazolo[4,3-*c*]pyridin-5-yl]ethanone (12)** 28 29

30 To a solution of *tert*-butyl 4-(5-acetyl-3-(7-(difluoromethyl)-6-(1-methyl-1*H*-pyrazol-4-
31 yl)-3,4-dihydroquinolin-1(2*H*)-yl)-4,5,6,7-tetrahydro-1*H*-pyrazolo[4,3-*c*]pyridin-1-
32 yl)piperidine-1-carboxylate (**60**, 50 mg, 0.090 mmol) in DCM (2 mL) at 0 °C was added
33 trifluoroacetic acid (0.07 mL, 0.9 mmol). The mixture was stirred at room temperature for
34 1 h and concentrated in vacuo. The mixture was diluted with DCM (10 mL) and washed
35 with sat. aq. NaHCO₃ (10 mL x 2), brine (10 mL). The organic layer was dried over
36 anhydrous Na₂SO₄, filtered and concentrated in vacuo. The crude residue was resolved in
37 MeOH (1 mL), added water (10 mL), and lyophilized to give the title compound (**12**, 22
38 mg, 49%) as a white solid. ¹H NMR (400 MHz, CDCl₃) δ 7.54 (d, *J* = 6.0 Hz, 1H), 7.41
39 (d, *J* = 6.8 Hz, 1H), 7.08–6.97 (m, 1H), 6.88 (d, *J* = 3.6 Hz, 1H), 6.68–6.37 (m, 1H), 4.27–
40 4.11 (m, 2H), 4.10–4.01 (m, 1H), 3.96 (s, 3H), 3.93–3.87 (m, 1H), 3.79–3.68 (m, 3H),
41 3.37–3.26 (m, 2H), 2.93–2.71 (m, 6H), 2.19–1.93 (m, 9H). LCMS M/Z (M+H) 510.
42
43
44
45
46
47
48
49
50
51
52
53
54
55
56
57
58
59
60

1
2
3
4
5
6
7
8
9
10
11
12
13
14
15
16
17
18
19
20
21
22
23
24
25
26
27
28
29
30
31
32
33
34
35
36
37
38
39
40
41
42
43
44
45

1-[3-[7-(difluoromethyl)-6-(1-methylpyrazol-4-yl)-3,4-dihydro-2*H*-quinolin-1-yl]-1-(1-methyl-4-piperidyl)-6,7-dihydro-4*H*-pyrazolo[4,3-*c*]pyridin-5-yl]ethanone (13)

To a solution of 1-(3-(7-(difluoromethyl)-6-(1-methyl-1*H*-pyrazol-4-yl)-3,4-dihydroquinolin-1(2*H*)-yl)-1-(piperidin-4-yl)-6,7-dihydro-1*H*-pyrazolo[4,3-*c*]pyridin-5(4*H*)-yl)ethanone (**12**, 80 mg, 0.16 mmol) in DCE (2 mL) was added sodium cyanoborohydride (30 mg, 0.47 mmol), AcOH (0.05 mL, 0.9 mmol) and formaldehyde (37% in water, 0.035 mL, 0.47 mmol). The mixture was stirred at room temperature for 1 h. The reaction was quenched with sat. aq. NaHCO₃ (10 mL) and extracted with DCM (10 mL x 3). The combined organic layers were dried over anhydrous Na₂SO₄, filtered and concentrated in vacuo. The crude residue was purified by reverse phase chromatography (acetonitrile 24–54% / 0.05% NH₄OH in water) to give the title compound (**13**, 19 mg, 23%) as a white solid. ¹H NMR (400 MHz, DMSO-*d*₆) δ 7.73 (s, 1H), 7.48 (s, 1H), 7.08 (s, 1H), 6.92–6.62 (m, 2H), 4.15–4.10 (m, 2H), 4.02–3.94 (m, 1H), 3.85 (s, 3H), 3.72–3.65 (m, 2H), 3.60–3.55 (m, 2H), 2.83–2.71 (m, 6H), 2.18 (s, 3H), 2.05–1.90 (m, 9H), 1.84–1.75 (m, 2H). LCMS M/Z (M+H) 524.

46
47
48
49
50
51
52
53
54
55
56
57
58
59
60

1-[4-[5-acetyl-3-[7-(difluoromethyl)-6-(1-methylpyrazol-4-yl)-3,4-dihydro-2*H*-quinolin-1-yl]-6,7-dihydro-4*H*-pyrazolo[4,3-*c*]pyridin-1-yl]-1-piperidyl]ethanone (14)

Step 1:

***tert*-butyl 1-(1-acetylpiperidin-4-yl)-3-(7-(difluoromethyl)-6-(1-methyl-1*H*-pyrazol-4-yl)-3,4-dihydroquinolin-1(2*H*)-yl)-6,7-dihydro-1*H*-pyrazolo[4,3-*c*]pyridine-5(4*H*)-carboxylate (61)**

To a solution of *tert*-butyl 1-(1-acetylpiperidin-4-yl)-3-bromo-6,7-dihydro-1*H*-pyrazolo[4,3-*c*]pyridine-5(4*H*)-carboxylate (**30**, 500 mg, 1.20 mmol) in 1,4-dioxane (3 mL) was added 7-(difluoromethyl)-6-(1-methyl-1*H*-pyrazol-4-yl)-1,2,3,4-tetrahydroquinoline (**53**, 370 mg, 1.40 mmol), *t*-BuONa (562 mg, 5.9 mmol) and dichloro[1,3-bis(2,6-di-*i*-pentylphenyl)imidazol-2-ylidene](3-chloropyridyl)palladium(II) (93 mg, 0.12 mmol). The mixture was heated to 120 °C for 12 h under a nitrogen atmosphere. After cooling the reaction to room temperature, DCM (50 mL) was added and washed with water (40 mL x 2), brine (40 mL). The organic layer was dried over anhydrous Na₂SO₄, filtered and concentrated in vacuo. The crude residue was purified by silica gel chromatography (DCM / MeOH = 20 : 1) to give the title compound (**61**, 300 mg, 42%) as a white solid. ¹H NMR (400 MHz, DMSO-*d*₆) δ 7.75 (s, 1H), 7.49 (s, 1H), 7.10 (s, 1H), 6.79 (s, 1H), 6.78 (t, *J* = 55.2 Hz, 1 H), 4.48–4.41 (m, 1H), 4.39–4.28 (m, 2H), 4.08–3.98 (m, 2H), 3.94–3.90 (m, 1H), 3.86 (s, 3H), 3.61–3.56 (m, 2H), 3.24–3.09 (m, 1H), 2.84–2.74 (m, 4H), 2.74–2.63 (m, 2H), 2.02 (s, 3H), 1.98–1.85 (m, 6H), 1.41–1.37 (m, 9H). LCMS M/Z (M+H) 610.

Step 2:

1
2
3
4
5
6
7
8
9
10
11
12
13
14
15
16
17
18
19
20
21
22
23
24
25
26
27
28
29
30
31
32
33
34
35
36
37
38
39
40
41
42
43
44
45
46
47
48
49
50
51
52
53
54
55
56
57
58
59
60

1-(4-(3-(7-(difluoromethyl)-6-(1-methyl-1*H*-pyrazol-4-yl)-3,4-dihydroquinolin-1(2*H*)-yl)-4,5,6,7-tetrahydro-1*H*-pyrazolo[4,3-*c*]pyridin-1-yl)piperidin-1-yl)ethanone
(63)

To a solution of *tert*-butyl 1-(1-acetylpiperidin-4-yl)-3-(7-(difluoromethyl)-6-(1-methyl-1*H*-pyrazol-4-yl)-3,4-dihydroquinolin-1(2*H*)-yl)-6,7-dihydro-1*H*-pyrazolo[4,3-*c*]pyridine-5(4*H*)-carboxylate (**61**, 300 mg, 0.500 mmol) in DCM (2 mL) was added trifluoroacetic acid (0.4 mL, 5 mmol). The reaction was stirred at room temperature for 1 h and concentrated in vacuo. The crude residue was diluted with DCM (50 mL), washed with sat. aq. NaHCO₃ (30 mL x 2) and water (30 mL), brine (40 mL). The organic layer was dried over anhydrous Na₂SO₄, filtered and concentrated in vacuo to give the title compound (**63**, 200 mg, crude) as a white solid that required no further purification. LCMS M/Z (M+H) 510.

Step 3:

1
2
3
4
5
6
7
8
9
10
11
12
13
14
15
16
17
18
19
20
21
22
23
24
25
26
27
28
29
30
31
32
33
34
35
36
37
38
39
40
41
42
43
44
45
46
47
48
49
50
51
52
53
54
55
56
57
58
59
60

1-[4-[5-acetyl-3-[7-(difluoromethyl)-6-(1-methylpyrazol-4-yl)-3,4-dihydro-2*H*-quinolin-1-yl]-6,7-dihydro-4*H*-pyrazolo[4,3-*c*]pyridin-1-yl]-1-piperidyl]ethanone
(14)

To a solution of 1-(4-(3-(7-(difluoromethyl)-6-(1-methyl-1*H*-pyrazol-4-yl)-3,4-dihydroquinolin-1(2*H*)-yl)-4,5,6,7-tetrahydro-1*H*-pyrazolo[4,3-*c*]pyridin-1-yl)piperidin-1-yl)ethanone (**63**, 100 mg, 0.17 mmol) in DCM (2 mL) at 0 °C was added triethylamine (0.07 mL, 0.5 mmol) and acetic anhydride (0.02 mL, 0.2 mmol). The mixture was stirred at room temperature for 1 h. DCM (50 mL) was added, washed with water (40 mL) and

1
2
3
4
5
6
7
8
9
10
11
12
13
14
15
16
17
18
19
20
21
22
23
24
25
26
27
28
29
30
31
32
33
34
35
36
37
38
39
40
41
42
43
44
45
46
47
48
49
50
51
52
53
54
55
56
57
58
59
60

brine (40 mL). The organic layer was dried over anhydrous Na₂SO₄, filtered and concentrated in vacuo. The crude residue was purified by Prep-TLC (DCM / MeOH = 20 : 1) to give the title compound (**14**, 53 mg, 52%) as a white solid. ¹H NMR (400 MHz, DMSO-*d*₆) δ 7.75 (s, 1H), 7.50 (s, 1H), 7.10 (s, 1H), 6.94 - 6.64 (m, 2H), 4.46–4.42 (m, 1H), 4.39–4.26 (m, 1H), 4.21–4.08 (m, 2H), 3.93–3.89 (m, 1H), 3.86 (s, 3H), 3.79–3.65 (m, 2H), 3.63–3.52 (m, 2H), 3.25–3.11 (m, 1H), 2.90–2.83 (m, 3H), 2.80–2.64 (m, 2H), 2.08–1.96 (m, 6H), 1.95–1.83 (m, 5H), 1.80–1.67 (m, 1H). LCMS M/Z (M+H) 552.

1-[3-[7-(difluoromethyl)-6-(1-methylpyrazol-4-yl)-3,4-dihydro-2H-quinolin-1-yl]-1-(1,1-dioxothian-4-yl)-6,7-dihydro-4H-pyrazolo[4,3-*c*]pyridin-5-yl]ethanone (16)

In a similar manner to **14**, compound **16** was prepared from *tert*-butyl 3-bromo-1-(1,1-dioxidotetrahydro-2H-thiopyran-4-yl)-6,7-dihydro-1H-pyrazolo[4,3-*c*]pyridine-5(4H)-carboxylate (**35**) to provide the title compound (**16**, 40%) as a white solid. ¹H NMR (400 MHz, DMSO-*d*₆) δ 7.76 (s, 1H), 7.50 (s, 1H), 7.11 (s, 1H), 6.94–6.65 (m, 2H), 4.52–4.48 (m, 1H), 4.16–4.11 (m, 2H), 3.86 (s, 3H), 3.75–3.69 (m, 2H), 3.60–3.58 (m, 2H), 3.35–3.30 (m, 2H), 3.25–3.22 (m, 2H), 2.84v2.73 (m, 4H), 2.43–2.41 (m, 2H), 2.23–2.20 (m, 2H), 2.07–1.96 (m, 5H). LCMS M/Z (M+H) 559.

3-[7-(difluoromethyl)-6-(1-methylpyrazol-4-yl)-3,4-dihydro-2H-quinolin-1-yl]-1-tetrahydropyran-4-yl-6,7-dihydro-4H-pyrazolo[4,3-*c*]pyridine-5-carboxamide (18)

Step 1:

***tert*-butyl 3-(7-(difluoromethyl)-6-(1-methyl-1*H*-pyrazol-4-yl)-3,4-dihydroquinolin-1(2*H*)-yl)-1-(tetrahydro-2*H*-pyran-4-yl)-6,7-dihydro-1*H*-pyrazolo[4,3-*c*]pyridine-5(4*H*)-carboxylate (65)**

To a solution of 7-(difluoromethyl)-6-(1-methyl-1*H*-pyrazol-4-yl)-1,2,3,4-tetrahydroquinoline (**53**, 3.41 g, 13 mmol) in dioxane (100 mL) was added *tert*-butyl 3-bromo-1-(tetrahydro-2*H*-pyran-4-yl)-6,7-dihydro-1*H*-pyrazolo[4,3-*c*]pyridine-5(4*H*)-carboxylate (**29**, 5.0 g, 12.9 mmol), chloro(2-dicyclohexylphosphino-2',6'-di-*i*-propoxy-1,1'-biphenyl)[2-(2-aminoethylphenyl)]palladium(II), methyl-*tert*-butylether adduct (1.01 g, 1.30 mmol), 2-dicyclohexylphosphino-2',6'-di-*i*-propoxy-1,1'-biphenyl (0.60 g, 1.3 mmol) and *t*-BuONa (3.70 g, 38.8 mmol). The mixture was heated to 120 °C for 16 h under an argon atmosphere. After cooling the reaction to room temperature, the mixture was concentrated in vacuo. The crude residue was purified by silica gel chromatography (DCM / MeOH = 100 : 1) to give the title compound (**65**, 5.4 g, 73%) as a light yellow solid. LCMS M/Z (M+H) 569.

Step 2:

7-(difluoromethyl)-6-(1-methyl-1*H*-pyrazol-4-yl)-1-(1-(tetrahydro-2*H*-pyran-4-yl)-4,5,6,7-tetrahydro-1*H*-pyrazolo[4,3-*c*]pyridin-3-yl)-1,2,3,4-tetrahydroquinoline (66)

To a solution of *tert*-butyl 3-(7-(difluoromethyl)-6-(1-methyl-1*H*-pyrazol-4-yl)-3,4-dihydroquinolin-1(2*H*)-yl)-1-(tetrahydro-2*H*-pyran-4-yl)-6,7-dihydro-1*H*-pyrazolo[4,3-*c*]pyridine-5(4*H*)-carboxylate (**65**, 6.3 g, 11 mmol) in DCM (20 mL) was added trifluoroacetic acid (20 mL). The mixture was stirred at 30 °C for 3 h. The reaction was

1
2
3 concentrated in vacuo to give the title compound (**66**, 10.8 g, crude) as brown oil which
4
5 was used to the next step without further purification. LCMS M/Z (M+H) 469.
6
7
8
9
10

11
12 **Step 3:**
13

14
15 **3-[7-(difluoromethyl)-6-(1-methylpyrazol-4-yl)-3,4-dihydro-2H-quinolin-1-yl]-1-**
16
17 **tetrahydropyran-4-yl-6,7-dihydro-4H-pyrazolo[4,3-c]pyridine-5-carboxamide (18)**
18
19

20
21 To a solution of 7-(difluoromethyl)-6-(1-methylpyrazol-4-yl)-1-(1-tetrahydropyran-4-yl-
22
23 4,5,6,7-tetrahydropyrazolo[4,3-c]pyridin-3-yl)-3,4-dihydro-2H-quinoline (**66**, 200 mg,
24
25 0.430 mmol) in DCM (2 mL) was added trimethylsilyl isocyanate (0.12 mL, 0.85 mmol).
26
27 The mixture was stirred at room temperature for 3 h and concentrated in vacuo. The
28
29 crude residue was purified by reverse phase chromatography (acetonitrile 18–48% / 0.1%
30
31 NH₄OH in water) to give the title compound (**18**, 44 mg, 20%) as a white solid. ¹H NMR
32
33 (400 MHz, DMSO-*d*₆) δ 7.75 (s, 1H), 7.50 (s, 1H), 7.09 (s, 1H), 6.83 (s, 1H), 6.78 (t, *J* =
34
35 55.2 Hz, 1H), 6.08 (s, 2H), 4.31–4.26 (m, 1H), 4.02 (s, 2H), 3.97–3.94 (m, 2H), 3.86 (s,
36
37 3H), 3.60–3.55 (m, 4H), 3.48–3.42 (m, 2H), 2.84–2.67 (m, 4H), 2.00–1.94 (m, 4H), 1.83–
38
39 1.80 (m, 2H). LCMS M/Z (M+H) 512.
40
41
42
43
44
45
46
47
48
49
50
51
52
53
54
55
56
57
58
59
60

51
52 **3-[7-(difluoromethyl)-6-(1-methylpyrazol-4-yl)-3,4-dihydro-2H-quinolin-1-yl]-N-**
53
54 **methyl-1-tetrahydropyran-4-yl-6,7-dihydro-4H-pyrazolo[4,3-c]pyridine-5-**
55
56 **carboxamide (19)**
57
58
59
60

To a solution of 7-(difluoromethyl)-6-(1-methylpyrazol-4-yl)-1-(1-tetrahydropyran-4-yl)-4,5,6,7-tetrahydropyrazolo[4,3-*c*]pyridin-3-yl)-3,4-dihydro-2*H*-quinoline (**66**, 10.8 g, 23.0 mmol), triethylamine (8.1 g, 80 mmol) in DCM (20 mL) was added *N*-methylimidazole-1-carboxamide (4.0 g, 32 mmol). The reaction was stirred at 25 °C for 36 h. Water (20 mL) was added and extracted with DCM (20 mL x 3). The combined organic layers were dried over anhydrous Na₂SO₄, filtered and concentrated in vacuo. The crude residue was purified by silica gel chromatography (DCM / MeOH = 100 : 1) to give the title compound (**19**, 2.7 g, 22%) as a light yellow solid. ¹H NMR (400 MHz, DMSO-*d*₆) δ 7.76–7.75 (m, 1H), 7.49 (s, 1H), 7.10 (s, 1H), 6.83 (s, 1H), 6.92–6.78 (t, *J* = 55.2 Hz, 1H), 6.65–6.53 (m, 1H), 4.31–4.28 (m, 1H), 4.13–3.93 (m, 4H), 3.86 (s, 3H), 3.69–3.58 (m, 4H), 3.48–3.42 (m, 2H), 2.84–2.74 (m, 4H), 2.54–2.53 (m, 3H), 1.97–1.80 (m, 6H). ¹³C NMR (101 MHz, DMSO-*d*₆) δ 158.3, 148.0, 142.5, 138.2, 137.9, 131.0, 129.7, 128.9 (t, *J* = 20.5 Hz), 126.0, 121.0 (t, *J* = 5.1 Hz), 119.0, 114.2 (t, *J* = 235.8 Hz), 110.2 (t, *J* = 6.1 Hz), 106.8, 66.5, 54.0, 49.4, 40.8, 40.7, 39.0, 32.8, 27.6, 27.4, 22.1, 21.9. HRMS *m/z* 526.2718 (M + H⁺, C₂₇H₃₄F₂N₇O₂, requires 526.2742).

3-[7-(difluoromethyl)-6-(1-methylpyrazol-4-yl)-3,4-dihydro-2*H*-quinolin-1-yl]-*N*-ethyl-1-tetrahydropyran-4-yl-6,7-dihydro-4*H*-pyrazolo[4,3-*c*]pyridine-5-carboxamide (20**)**

To a solution of pyridine (0.37 mL, 4.6 mmol), 7-(difluoromethyl)-6-(1-methylpyrazol-4-yl)-1-(1-tetrahydropyran-4-yl)-4,5,6,7-tetrahydropyrazolo[4,3-*c*]pyridin-3-yl)-3,4-dihydro-2*H*-quinoline (**66**, 362 mg, 0.770 mmol) in DMF (5 mL) was added 4-nitrophenyl chloroformate (467 mg, 2.32 mmol). The reaction was stirred at room

1
2
3 temperature for 2 h. Ethanamine (12 mL, 24 mmol) was added to the reaction mixture.
4
5 The reaction was heated to 80 °C for 12 h in a sealed tube. After cooling to room
6
7 temperature, the reaction mixture was concentrated in vacuo. The crude residue was
8
9 purified by reverse phase chromatography (acetonitrile 33–51% / 0.2% formic acid in
10
11 water) to give the title compound (**20**, 57 mg, 14%) as a white solid. ¹H NMR (400 MHz,
12
13 DMSO-*d*₆) δ 7.75 (s, 1H), 7.49 (s, 1H), 7.09 (s, 1H), 6.83 (s, 1H), 6.78 (t, *J* = 55.6 Hz,
14
15 1H), 6.60 (t, *J* = 5.6 Hz, 1H), 4.37–4.20 (m, 1H), 4.01 (s, 2H), 4.00–3.91 (m, 2H), 3.86 (s,
16
17 3H), 3.66–3.56 (m, 4H), 3.51–3.39 (m, 2H), 3.02 (q, *J* = 6.8 Hz, 2H), 2.88–2.82 (m, 2H),
18
19 2.77–2.72 (m, 2H), 2.07–1.89 (m, 4H), 1.86–1.78 (m, 2H), 0.97 (t, *J* = 6.8 Hz, 3H).
20
21 LCMS M/Z (M+H) 540.
22
23
24
25
26
27
28
29

30
31 **3-[7-(difluoromethyl)-6-(1-methylpyrazol-4-yl)-3,4-dihydro-2*H*-quinolin-1-yl]-*N,N*-**
32
33 **dimethyl-1-tetrahydropyran-4-yl-6,7-dihydro-4*H*-pyrazolo[4,3-*c*]pyridine-5-**
34
35 **carboxamide (21)**
36
37

38 To a solution of triethylamine (0.31 mL, 2.3 mmol), 7-(difluoromethyl)-6-(1-
39
40 methylpyrazol-4-yl)-1-(1-tetrahydropyran-4-yl)-4,5,6,7-tetrahydropyrazolo[4,3-*c*]pyridin-
41
42 3-yl)-3,4-dihydro-2*H*-quinoline (**66**, 211 mg, 0.450 mmol) in DMF (2 mL) was added
43
44 dimethylcarbonyl chloride (0.04 mL, 0.45 mmol). The reaction was stirred at room
45
46 temperature for 16 h. EtOAc (5 mL) was added and washed with water (5 mL). The
47
48 organic layer was concentrated in vacuo. The crude residue was purified by reverse phase
49
50 chromatography (acetonitrile 30–60% / 0.2% formic acid in water) to give the title
51
52 compound (**21**, 55 mg, 22%) as a white solid. ¹H NMR (400 MHz, DMSO-*d*₆) δ 7.76 (s,
53
54 1H), 7.50 (s, 1H), 7.10 (s, 1H), 6.81 (s, 1H), 6.79 (t, *J* = 55.2 Hz, 1H), 4.38–4.20 (m, 1H),
55
56
57
58
59
60

1
2
3 4.02–3.90 (m, 2H), 3.87 (s, 3H), 3.84–3.79 (m, 2H), 3.62–3.54 (m, 2H), 3.49–3.42 (m,
4
5 2H), 3.41–3.36 (m, 2H), 2.91–2.79 (m, 4H), 2.70 (s, 6H), 2.05–1.91 (m, 4H), 1.88–1.76
6
7 (m, 2H). LCMS M/Z (M+H) 540.
8
9

10
11 **Modeling Methods.** All crystal structure figures were made using PyMOL Molecular
12
13 Graphics System, Version 1.8 Schrödinger, LLC.
14

15 **Expression and purification of bromodomain proteins.** The expression and
16
17 purification of bromodomain proteins was carried out as previously described.^{11,32}
18
19

20
21 **Expression and purification of bromodomain proteins for crystallography.** The
22
23 expression and purification of CRBP and BRD4 bromodomains for crystallography have
24
25 been previously described.¹¹
26
27

28
29 **Time-Resolved Fluorescence Resonance Energy Transfer Assays.** Compound
30
31 potencies were evaluated in a panel of biochemical bromodomain binding assays.
32
33 Binding of biotinylated small-molecule ligands to recombinant His-tagged
34
35 bromodomains was assessed by time-resolved fluorescence resonance energy transfer
36
37 (TR-FRET). Test compounds that compete with the biotinylated ligand for bromodomain
38
39 binding reduce the TR-FRET signal. All biochemical assay protocols were carried out as
40
41 previously described.^{11,32,33}
42
43
44
45

46
47 **Cellular assay protocols.** The CBP BRET assay was carried out as previously
48
49 described.¹¹ To determine the inhibition of *MYC* expression, MV-4-11 cells (ATCC)
50
51 were plated at 10,000 cells per well in 96-well plates in RPMI1640 media supplemented
52
53 with 10% fetal bovine serum and 2 mM L-glutamine. Test compounds diluted in DMSO
54
55 were transferred to the cell plates, keeping final DMSO concentration consistent at 0.1%,
56
57
58
59
60

1
2
3 and incubated for 4 h at 37 °C. Lysis and analysis for *MYC* expression were carried out
4
5 using QuantiGene 2.0 reagents (Affymetrix/eBioscience, probe set cat # SA-50182) and
6
7 following the vendor's instructions. Luminescence was read using an EnVision plate
8
9 reader (PerkinElmer) and EC₅₀s generated in XLFit using a 4-parameter non-linear
10
11 regression fit.
12
13

14
15
16 **In vitro metabolic stability experiments, MDCK permeability experiments, protein**
17
18 **binding experiments and CYP inhibition assessment.** Experiments were carried out as
19
20 previously described.¹²
21
22

23
24 **In vivo PK of 10 & 19.** Mouse PK: Twelve female CD-1 mice were obtained from Vital
25
26 River Laboratory Animal Co., Ltd., Beijing, P.R. China. All animals were 6–9 weeks old
27
28 at the time of study and weighed between 20 to 35 g. Animals (n = 3 per dosing route)
29
30 were dosed with **10** or **19** at 1 mg/kg i.v. (in propyl ethylene glycol 400 (35% v/v) and
31
32 water (65% v/v)) or 5 mg/kg p.o. (suspended in 0.5% w/v methylcellulose, 0.2% w/v
33
34 Tween 80). Food and water were available ad libitum to all animals. Serial blood samples
35
36 (15 µL) were collected by tail nick at 0.033, 0.083, 0.25, 0.5, 1, 3, 8, and 24 h after the
37
38 intravenous administration and 0.083, 0.25, 0.5, 1, 3, 8, and 24 h after the oral
39
40 administration. All blood samples were diluted with 60 µL water containing 1.7 mg/mL
41
42 EDTA and kept at –80 °C until analysis.
43
44
45
46

47
48 Rat PK: Twelve male Sprague-Dawley rats were obtained from Shanghai SLAC
49
50 Laboratory Animal Co. Ltd., Shanghai, P.R. China. All animals were 6–9 weeks old at
51
52 the time of study and weighed between 200 to 300 g. Animals (n = 3 per dosing route)
53
54 were dosed with **10** or **19** at 1 mg/kg i.v. (in propyl ethylene glycol 400 (35% v/v) and
55
56
57
58
59
60

1
2
3 water (65% v/v)) or 5 mg/kg p.o. (suspended in 0.5% w/v methylcellulose, 0.2% w/v
4
5 Tween 80). Food and water were available ad libitum to animals in the i.v. groups.
6
7
8 Animals in p.o. groups were fasted overnight and food withheld until 4 hours post-dose.
9
10 Approximately 250 μ L of blood were collected via the catheter at 0.033, 0.083, 0.25, 0.5,
11
12 1, 2, 4, 8, and 24 h after the intravenous or oral administration. All blood samples were
13
14 collected into tubes containing 5 μ L of 0.5 M K₂EDTA and processed for plasma.
15
16 Samples were centrifuged (2500 x g for 15 minutes at 4 °C) within one hour of
17
18 collection, and plasma samples were kept at -80 °C until analysis.
19
20
21

22
23 Dog PK: Twelve non-naïve male beagle dogs were obtained from Marshall Bioresources,
24
25 Beijing, P.R. China. All animals were 6 months to 2 years old at the time of study and
26
27 weighed between 6 to 10 kg. Animals (n = 3 per dosing route) were dosed with **10** or **19**
28
29 at 1 mg/kg i.v. (in ethanol (20% v/v), propyl ethylene glycol 400 (15% v/v) and water
30
31 (65% v/v)) or 5 mg/kg p.o. (suspended in 0.5% w/v methylcellulose, 0.2% w/v Tween
32
33 80). Food and water were available ad libitum to animals in the i.v. groups. Animals in
34
35 p.o. groups were fasted overnight and food withheld until 4 hours post-dose.
36
37 Approximately 800 μ L of blood was collected from a peripheral vessel at pre-dose,
38
39 0.033, 0.083, 0.25, 0.5, 1, 3, 6, 9, and 24 h after the intravenous administration and pre-
40
41 dose, 0.083, 0.25, 0.5, 1, 3, 6, 9, and 24 h after the oral administration. All blood samples
42
43 were collected into tubes containing 10 μ L of 0.5 M K₂EDTA and processed for plasma.
44
45 Samples were centrifuged (3000 x g for 10 minutes at 4 °C) within one hour of
46
47 collection, and plasma samples were kept at -80 °C until analysis.
48
49
50
51
52

53
54
55 Monkey PK: Twelve non-naïve male cynomolgus monkeys were obtained from Hainan
56
57 Jingang Laboratory Animal Co. Ltd., Haikou Hainan Province, P.R. China. All animals
58
59
60

1
2
3 were at least 2 years old at the time of study and weighed between 2 to 5 kg. Animals (n
4 = 3 per dosing route) were dosed with **10** or **19** 1 mg/kg i.v. (in ethanol (20% v/v), propyl
5 ethylene glycol 400 (15% v/v) and water (65% v/v)) or 5 mg/kg p.o. (suspended in 0.5%
6 w/v methylcellulose, 0.2% w/v Tween 80). Food and water were available ad libitum to
7 animals in the i.v. groups. Animals in p.o. groups were fasted overnight and food
8 withheld until 4 hours post-dose. Approximately 800 μ L of blood was collected from a
9 peripheral vessel at pre-dose, 0.033, 0.083, 0.25, 0.5, 1, 3, 6, 9, and 24 h after the
10 intravenous administration and pre-dose, 0.083, 0.25, 0.5, 1, 3, 6, 9, and 24 h after the
11 oral administration. All blood samples were collected into tubes containing 10 μ L of 0.5
12 M K_2EDTA and processed for plasma. Samples were centrifuged (3000 x g for 10
13 minutes at 4 $^{\circ}C$) within one hour of collection, and plasma samples were kept at $-80^{\circ}C$
14 until analysis.
15
16
17
18
19
20
21
22
23
24
25
26
27
28
29
30
31

32 Bio-Analytical Method of PK Samples: Concentrations of **10** and **19** were determined by
33 a non-validated LC-MS/MS assay. The diluted blood samples were prepared for analysis
34 by placing a 25 μ l aliquot into a 96-well plate followed by the addition of 200 μ l of
35 acetonitrile containing an internal standard mixture (0.1 μ g/mL indomethacin). The
36 samples were vortexed and centrifuged at 4000 rpm for 10 minutes at 4 $^{\circ}C$; 50 μ L of the
37 supernatant was diluted with 150 μ L water and 10 μ L of the solution was injected onto an
38 analytical column. An Acquity UPLC System (Waters) coupled with an API 4000 mass
39 spectrometer (AB Sciex, Foster City, CA) was used for sample analysis. The mobile
40 phases were 0.025% FA & 1 mM NH_4OAc in water/ACN (v:v, 95:5) (A) and 0.025% FA
41 & 1 mM NH_4OAc in ACN/water (v:v, 95:5) (B). The gradient was as follows: starting at
42 10% B and increased to 65% B for 1.2 minutes, then to 95% for 0.6 minute, maintained
43
44
45
46
47
48
49
50
51
52
53
54
55
56
57
58
59
60

1
2
3 at 95% B for 0.2 minutes, then decreased to 10% B within 0.01 minute. The total flow
4 rate was 0.6 ml/min and samples were injected onto an ACE 3 AQ (2.1x100 mm, 3 μ m)
5 analytical column with a total run time of 2 minutes. Data were acquired using multiple
6 reactions monitoring (MRM) in positive ion electrospray mode with an operating source
7 temperature of 550 °C. The MRM transition was m/z 511.400 \rightarrow 471.400 for **10**, 526.400
8 \rightarrow 486.400 for **19**, and 357.900 \rightarrow 139.000 for indomethacin. The lower and upper limits
9 of quantitation of the assay for **10** were 0.002 and 13.1 μ M, respectively. The lower and
10 upper limits of quantitation of the assay for **19** were 0.002 and 12.7 μ M, respectively.
11
12
13
14
15
16
17
18
19
20
21
22

23 **In vivo evaluation of 19 in MOLM-16 AML PK/PD and anti-tumor efficacy model.**

24 RT-PCR was performed using TaqMan RNA-to-Ct 1-Step Kit and Taqman Gene
25 Expression Assays (Applied Biosystems, Carlsbad, CA, USA). The comparative Ct
26 method was used to estimate relative changes in gene expression using *MYC* Taqman
27 assay (Hs00153408_m1) and *ACTB* TaqMan assay (Hs01060665_g1) as housekeeping
28 gene.
29
30
31
32
33
34
35
36
37

38 All procedures were approved by and conformed to the guidelines and principles set by
39 the Institutional Animal Care and Use Committee of Genentech and were carried out in
40 an Association for the Assessment and Accreditation of Laboratory Animal Care
41 (AAALAC)-accredited facility. Female C.B-17 SCID.bg mice that were 8–9 weeks old
42 and weighed 20–24 g were obtained from Charles River Lab. They were inoculated with
43 five million MOLM-16 leukemia acute myelogenic cells (suspended in a 1:1 mixture of
44 Hank's Balanced Salt Solution containing Matrigel at a 1:1 ratio) in the right flank
45 subcutaneously. Tumors were monitored until they reached a mean tumor volume of
46 130–300 mm³. The mean tumor volume across all eight groups was 260 \pm 34.5 mm³
47
48
49
50
51
52
53
54
55
56
57
58
59
60

1
2
3 (mean \pm SD) at the initiation of dosing. Mice were given 0 (Vehicle - 0.5%
4 methylcellulose, 0.2% Tween-80), 3, 10, 30 mg/kg compound **19** by gavage, twice daily
5
6 (BID) for 21 days in a volume of 100 μ L. Tumor volumes were measured in two
7
8 dimensions (length and width) using Ultra Cal-IV calipers (model 54–10–111; Fred V.
9
10 Fowler Co.; Newton, MA) and analyzed using Excel, version 11.2 (Microsoft
11
12 Corporation; Redmond WA). The tumor volume was calculated with the following
13
14 formula: Tumor size (mm^3) = (longer measurement \times shorter measurement²) \times 0.5.
15
16 Animal body weights were measured using an Adventura Pro AV812 scale (Ohaus
17
18 Corporation; Pine Brook, NJ). Percent weight change was calculated using the following
19
20 formula: Group percent weight change = (new weight – initial weight) / initial weight) \times
21
22 100. Plasma, tumor, and brain samples were collected at 2 hours post-dose. To analyze
23
24 the repeated measurement of tumor volumes from the same animals over time, a
25
26 mixed-modeling approach was used. This approach addresses both repeated
27
28 measurements and modest dropouts due to any non-treatment related removal of animals
29
30 before the end of study. Cubic regression splines were used to fit a non-linear profile to
31
32 the time courses of log₂ tumor volume at each dose level. The non-linear profiles were
33
34 then related to dose within the mixed model. Tumor growth inhibition as a percentage of
35
36 vehicle was calculated as the percentage of the area under the fitted tumor volume–time
37
38 curve (AUC) per day for each dose group in relation to the vehicle, using the following
39
40 formula: %TGI = 100 \times [1 – (AUC_{dose} per day \div AUC_{vehicle} per day)].
41
42
43
44
45
46
47
48
49
50

51
52 Concentrations of **19** were determined by a nonvalidated LC-MS/MS assay. The plasma
53
54 samples were prepared for analysis by placing a 25 μ L aliquot into a 96-well plate. The
55
56 tumor samples were collected and weighed. Four volume of water by tissue weight was
57
58
59
60

1
2
3 added. Using a bead beating homogenizer, the tissue samples were homogenized and 25
4 μL of each was aliquoted into a 96-well plate. A volume of 200 μL of acetonitrile
5
6 containing an internal standard (labetalol) was added to the sample. The samples were
7
8 vortexed and centrifuged at 4000 rpm for 10 minutes, and 50 μL of the supernatant was
9
10 diluted with 150 μL of in water. A 10 μL injection volume was used for analysis on a
11
12 SIL-30ACMP autosampler system (Shimadzu, Columbia, MD) was linked to LC-30AD
13
14 pumps (Shimadzu), coupled with an API 5500 QTrap mass spectrometer (Sciex, Foster
15
16 City, CA) for was used for sample analysis. The mobile phases were 0.1% FA (formic
17
18 acid) in water (A) and 0.1% FA in MeCN (B). The gradient was as following: starting at
19
20 10% B and increased to 90% B in 0.6 minutes, maintained at 90% B for 0.2 minutes, then
21
22 decreased to 10% B within 0.1 minute. The total flow rate was 1.2 ml/min and column
23
24 for separation was Kinetex XB-C18 column (50x2.1mm, 2.6 μm) with a total run time of
25
26 1 minutes. Data were acquired using multiple reactions monitoring (MRM) in positive
27
28 ion electrospray mode with an operating source temperature of 550 $^{\circ}\text{C}$. The MRM
29
30 transition was m/z 526.1 \rightarrow 486.2 for **19** and 329.076 \rightarrow 294.1 for labetalol. The lower
31
32 and upper limits of quantitation of the assay for **19** were 0.002 and 39 μM , respectively.
33
34
35
36
37
38
39
40
41

42 **In vitro evaluation of 19 on T_{regs} .** Human naïve CD4⁺ T cells were isolated from
43
44 PBMCs of healthy donors using naïve CD4⁺T cell isolation kit II (Miltenyi Biotec) and
45
46 differentiated to iT_{regs} for 4 days using plate-bound anti-CD3 (5 $\mu\text{g}/\text{ml}$; eBioscience),
47
48 soluble anti-CD28 (3 $\mu\text{g}/\text{ml}$; eBioscience), plus rTGF β (5ng/ml; R&D Systems) and rIL-
49
50 2 (10 ng/ml; R&D Systems) in complete RPMI-1640 medium (10% FCS, 50 μM 2-
51
52 mercaptoethanol, 10% Penicillin /Streptomycin, 10% NEAA, 10% Sodium Pyruvate).
53
54
55
56
57
58
59
60
Compound **19** was used at 2 μM and titrated down at 2x dilution. This study followed the

1
2
3 principles of research ethics as set forth in the Belmont Report and was approved by the
4
5 Western Institutional Review Board (WIRB-Protocol number CEHS-CP 307.2).
6

7
8 iT_{regs} were stained using antibodies against surface markers CD4 FITC (clone OKT-4),
9
10 and CD25 Pacific Blue (clone BC96) (all from eBioscience), fixed/permeabilized with
11
12 the Foxp3 / Transcription Factor Staining Buffer Set (eBioscience) and labeled for
13
14 intracellular Foxp3 APC (clone 259D/C7; BD Biosciences). iT_{regs} were stained for
15
16 viability using fixable viability dye efluor® 781. Samples were acquired on a BD LSR
17
18 Fortessa using FACSDiva software (BD Biosciences). Data were analyzed using the
19
20 FlowJo software (TreeStar, FLOWJO, LLC).
21
22

23
24 Total RNA was isolated from iT_{regs} using RNeasy (Qiagen), including an on-column
25
26 DNase I digestion. cDNA was prepared using High Capacity cDNA Reverse
27
28 Transcriptase Kit (Life Technologies). Quantitative RT-PCR was performed to determine
29
30 Foxp3 gene expression levels with the ABI 7900 HT Fast Real-Time PCR System
31
32 (Applied Biosystems). Gene expression data was normalized to B2M as a housekeeping
33
34 gene.
35
36
37

38 **Kinetic solubility assay.** Kinetic solubility assay starts with compound DMSO stock
39
40 solutions. This assay uses Millipore Multiscreen 96-well filter plates for the 24 hour
41
42 equilibration shaking. For routine equilibrium solubility determination of discovery
43
44 chemistry compounds, samples are prepared by adding 4 μL of the 10 mM DMSO stock
45
46 solution into 196 μL of PBS buffer pH 7.4 in the 96-well filter plates, yielding a
47
48 compound concentration of 200 μM and 2% DMSO. The PBS buffer pH7.4 was
49
50 prepared by Genentech media lab. The filter plate is sealed with aluminum sealing film
51
52 and shaken at room temperature for 24 hours at 1000 rpm. When shaking has completed,
53
54
55
56
57
58
59
60

1
2
3 the solutions are filtered into a clean 96-well plate utilizing a vacuum manifold. After
4
5 filtration some precipitate is often observed at the bottom of the filtration plate wells. The
6
7 filtrate samples are diluted by a factor of 2 using PBS pH7.4 buffer and then transferred
8
9 to a 384-well plate for analysis by LCMS-CLND (CLND: Chemiluminescence nitrogen
10
11 detector). 5 μ L of each sample was injected twice into the LCMS-CLND instrument for
12
13 repeat analysis. Samples are detected and analyzed using UV 254nm and CLND. UV
14
15 254nm is used primarily to confirm the sample purity but in rare cases, is also used to
16
17 quantify the concentration of compounds with no nitrogen, where additional work is done
18
19 to create a compound specific calibration curve. The identification of CLND target peaks
20
21 of each compound is confirmed by LCMS. Sample quantification is accomplished by
22
23 CLND peak intensity, the CLND calibration curve, and the number of nitrogen contained
24
25 in the compound. One calibration curve of caffeine is used for solubility quantitative
26
27 determination. A fresh calibration curve is generated for every batch.
28
29
30
31
32
33
34
35
36
37

38 **Associated Content**

39 **Supporting Information**

40
41
42 The Supporting Information is available free of charge on the ACS Publications website
43
44 at DOI: .
45
46
47
48

49
50
51 Full experimental details and characterization for all reported compounds, BromoScan
52
53 data for **10** and **19**, Cerep off-target screening data for **19**, Invitrogen kinase data for **19**,
54
55
56
57
58
59
60

1
2
3 *Ab initio* torsion scan data for **8**, PK/PD data for **19**, crystallography methods for **3**-CBP,
4
5 **8**-CBP, **17**-CBP, **10**-CBP, **19**-CBP, **19**-BRD4(1) (PDF)
6
7

8
9 Molecular formula strings (CSV)
10

11 12 **Accession Codes**

13
14
15 PDB codes for the structures of the CBP bromodomain in complex with **3**, **8**, **17**, **10** and
16
17 **19** are 5W0F, 5W0I, 5W0L, 5W0Q and 5W0E, respectively. PDB code for the structure
18
19 of the BRD4(1) in complex with **19** is 5VZS. Authors will release the atomic coordinates
20
21 and experimental data upon article publication.
22
23
24
25
26
27

28 29 **Author Information**

30 31 32 **Corresponding Authors**

33
34
35 *F.A.R E-mail: anthony.romero@unitybiotechnology.com
36
37

38
39 *S.M. E-mail: magnuson.steven@gene.com
40
41
42
43
44

45 46 **Acknowledgements**

47
48 The authors thank Suzanne Brown, Ning Liu, Mika Kosaka, Emile Plise, and Jonathan
49
50 Cheong in the DMPK department. Mengling Wong, Michael Hayes, and Amber Guillen
51
52 for compound purification. Baiwei Lin, Deven Wang, and Yutao Jiang are acknowledged
53
54 for analytical support. Grady Howes, Jan Seerveld, Hao Zheng, and Gigi Yuen for help
55
56
57
58
59
60

1
2
3 with compound management and logistics are also recognized. This research used
4
5 resources of the Advanced Light Source, which is a DOE Office of Science User Facility
6
7
8 under contract no. DE-AC02-05CH11231. We would like to acknowledge the beamline
9
10 staff at ALS 5.0.2 for their help and support
11
12
13
14
15
16

17 **Abbreviations Used**

18
19
20 AML, acute myeloid leukemia; BAZ2B, bromodomain adjacent to zinc finger domain
21
22 2B; BET, bromodomain and extra terminal; Boc, *tert*-butyloxycarbonyl; BPTF,
23
24 bromodomain plant homeodomain finger transcription factor; BRD4(X), bromodomain X
25
26 (X = 1, 2) of the bromodomain-containing protein 4; BRD8, bromodomain-containing
27
28 protein 8; BRD9, bromodomain-containing protein 9; BRET, bioluminescence resonance
29
30 energy transfer BRPF1, bromodomain and plant homeodomain finger containing 1; CBP,
31
32 cyclic adenosine monophosphate response element binding protein, binding protein;
33
34 CECR2, cat eye syndrome chromosome region, candidate 2; Cl_{hep} , predicted hepatic
35
36 clearance; CNS, central nervous system; DBU, 1,8-Diazabicyclo[5.4.0]undec-7-ene;
37
38 DCE, dichloroethane; DCM, dichloromethane; DIEA, *N,N*-diisopropylethyl amine; DMF,
39
40 *N,N*-dimethylformamide; DMSO, dimethylsulfoxide; DNA, deoxyribonucleic acid;
41
42 Foxp3, forkhead box P3; GCN5L, general control of amino-acid synthesis 5-like 2; HAT,
43
44 histone acetyl transferase; HATU, 1-[bis(dimethylamino)methylene]-1*H*-1,2,3-
45
46 triazolo[4,5-*b*]pyridinium 3-oxid hexafluorophosphate, i.v., intravenous, KAc, acetylated
47
48 lysine, $K_{p,uu}$, ratio of the unbound drug concentration in brain to unbound drug
49
50 concentration in plasma; LE, ligand efficiency; LLE, lipophilic ligand efficiency; LM,
51
52
53
54
55
56
57
58
59
60

1
2
3 liver microsomes; MeCN, acetonitrile; NBS, *N*-bromosuccinimide; p.o., per os; P300,
4
5 adenoviral E1A binding protein; P_{app} A to B, apparent permeability apical-to-basolateral;
6
7
8 PBMCs, peripheral blood mononuclear cells; PCAF, P300/CBP-associated factor; PK,
9
10 pharmacokinetic; QD, one a day; q-RT-PCR, quantitative reverse transcriptase
11
12 polymerase chain reaction; SAR, structure-activity relationship; SEM, [2-
13
14 (Trimethylsilyl)ethoxy]methyl; SFC, supercritical fluid chromatography; TAF1(X),
15
16 bromodomain X (X = 1, 2) of the TATA-box binding protein associated factor 1; TEA,
17
18 triethylamine; TFA, trifluoroacetic acid; THF, tetrahydrofuran; THP, tetrahydropyran;
19
20 THQ, tetrahydroquinoline; *t*PSA, total polar surface area; TR-FRET, time-resolved
21
22 fluorescence energy transfer
23
24
25
26
27

28 References

- 29
30
31
32 (1) Bannister, A. J.; Kouzarides, T. The CBP Co-Activator Is a Histone
33
34 Acetyltransferase. *Nature* **1996**, *384*, 641–643.
35
36
37 (2) Delvecchio, M.; Gaucher, J.; Aguilar-Gurrieri, C.; Ortega, E.; Panne, D.
38
39 Structure of the P300 Catalytic Core and Implications for Chromatin Targeting
40
41 and HAT Regulation. *Nat. Struct. Mol. Biol.* **2013**, *20*, 1040–1046.
42
43
44 (3) Mujtaba, S.; He, Y.; Zeng, L.; Yan, S.; Plotnikova, O.; Sachchidanand; Sanchez,
45
46 R.; Zeleznik-Le, N. J.; Ronai, Z.; Zhou, M.-M. Structural Mechanism of the
47
48 Bromodomain of the Coactivator CBP in P53 Transcriptional Activation. *Mol.*
49
50 *Cell* **2004**, *13*, 251–263.
51
52
53 (4) Iyer, N. G.; Ozdag, H.; Caldas, C. p300/CBP and Cancer. *Oncogene* **2004**, *23*,
54
55 4225–4231.
56
57
58
59
60

- 1
2
3
4
5
6
7
8
9
10
11
12
13
14
15
16
17
18
19
20
21
22
23
24
25
26
27
28
29
30
31
32
33
34
35
36
37
38
39
40
41
42
43
44
45
46
47
48
49
50
51
52
53
54
55
56
57
58
59
60
- (5) Dutta, R.; Tiu, B.; Sakamoto, K. M. CBP/P300 Acetyltransferase Activity in Hematologic Malignancies. *Mol. Genet. Metab.* **2016**, *119*, 37–43.
- (6) Dekker, F. J.; Haisma, H. J. Histone Acetyl Transferases as Emerging Drug Targets. *Drug Discovery Today* **2009**, *14*, 942–948.
- (7) Fujisawa, T.; Filippakopoulos, P. Functions of Bromodomain-Containing Proteins and Their Roles in Homeostasis and Cancer. *Nat. Rev. Mol. Cell Biol.* **2017**, 246–262.
- (8) Liu, Y.; Wang, L.; Predina, J.; Han, R.; Beier, U. H.; Wang, L.-C. S.; Kapoor, V.; Bhatti, T. R.; Akimova, T.; Singhal, S.; Brindle, P. K.; Cole, P. A.; Albelda, S. M.; Hancock, W. W. Inhibition of P300 Impairs Foxp3⁺ T Regulatory Cell Function and Promotes Antitumor Immunity. *Nat. Med.* **2013**, *19*, 1173–1177.
- (9) Conery, A. R.; Centore, R. C.; Neiss, A.; Keller, P. J.; Joshi, S.; Spillane, K. L.; Sandy, P.; Hatton, C.; Pardo, E.; Zawadzke, L.; Bommi-Reddy, A.; Gascoigne, K. E.; Bryant, B. M.; Mertz, J. A.; Sims, R. J. Bromodomain Inhibition of the Transcriptional Coactivators CBP/EP300 as a Therapeutic Strategy to Target the IRF4 Network in Multiple Myeloma. *eLife* **2016**, *5*, e10483.
- (10) Ghosh, S.; Taylor, A.; Chin, M.; Huang, H.-R.; Conery, A. R.; Mertz, J. A.; Salmeron, A.; Dakle, P. J.; Mele, D.; Côté, A.; Jayaram, H.; Setser, J. W.; Poy, F.; Hatzivassiliou, G.; DeAlmeida-Nagata, D.; Sandy, P.; Hatton, C.; Romero, F. A.; Chiang, E.; Reimer, T.; Crawford, T.; Pardo, E.; Watson, V. G.; Tsui, V.; Cochran, A. G.; Zawadzke, L.; Harmange, J.-C.; Audia, J. E.; Bryant, B. M.; Cummings, R. T.; Magnuson, S. R.; Grogan, J. L.; Bellon, S. F.; Albrecht, B. K.; Sims, R. J., III; Lora, J. M. Regulatory T Cell Modulation by CBP/EP300

- 1
2
3 Bromodomain Inhibition. *J. Biol. Chem.* **2016**, *291*, 13014–13027.
- 4
5
6 (11) Taylor, A. M.; Côté, A.; Hewitt, M. C.; Pastor, R.; Leblanc, Y.; Nasveschuk, C.
7
8 G.; Romero, F. A.; Crawford, T. D.; Cantone, N.; Jayaram, H.; Setser, J.;
9
10 Murray, J.; Beresini, M. H.; de Leon Boenig, G.; Chen, Z.; Conery, A. R.;
11
12 Cummings, R. T.; Dakin, L. A.; Flynn, E. M.; Huang, O. W.; Kaufman, S.;
13
14 Keller, P. J.; Kiefer, J. R.; Lai, T.; Li, Y.; Liao, J.; Liu, W.; Lu, H.; Pardo, E.;
15
16 Tsui, V.; Wang, J.; Wang, Y.; Xu, Z.; Yan, F.; Yu, D.; Zawadzke, L.; Zhu, X.;
17
18 Zhu, X.; Sims, R. J., III; Cochran, A. G.; Bellon, S.; Audia, J. E.; Magnuson, S.;
19
20 Albrecht, B. K. Fragment-Based Discovery of a Selective and Cell-Active
21
22 Benzodiazepinone CBP/EP300 Bromodomain Inhibitor (CPI-637). *ACS Med.*
23
24 *Chem. Lett.* **2016**, *7*, 531–536.
- 25
26
27 (12) Crawford, T. D.; Romero, F. A.; Lai, K. W.; Tsui, V.; Taylor, A. M.; de Leon
28
29 Boenig, G.; Noland, C. L.; Murray, J.; Ly, J.; Choo, E. F.; Hunsaker, T. L.; Chan,
30
31 E. W.; Merchant, M.; Kharbanda, S.; Gascoigne, K. E.; Kaufman, S.; Beresini,
32
33 M. H.; Liao, J.; Liu, W.; Chen, K. X.; Chen, Z.; Conery, A. R.; Côté, A.;
34
35 Jayaram, H.; Jiang, Y.; Kiefer, J. R.; Kleinheinz, T.; Li, Y.; Maher, J.; Pardo, E.;
36
37 Poy, F.; Spillane, K. L.; Wang, F.; Wang, J.; Wei, X.; Xu, Z.; Xu, Z.; Yen, I.;
38
39 Zawadzke, L.; Zhu, X.; Bellon, S.; Cummings, R.; Cochran, A. G.; Albrecht, B.
40
41 K.; Magnuson, S. Discovery of a Potent and Selective in Vivo Probe (GNE-272)
42
43 for the Bromodomains of CBP/EP300. *J. Med. Chem.* **2016**, *59*, 10549–10563.
- 44
45
46 (13) Popp, T. A.; Tallant, C.; Rogers, C.; Fedorov, O.; Brennan, P. E.; Müller, S.;
47
48 Knapp, S.; Bracher, F. Development of Selective CBP/P300 Benzoxazepine
49
50 Bromodomain Inhibitors. *J. Med. Chem.* **2016**, *59*, 8889–8912.
- 51
52
53
54
55
56
57
58
59
60

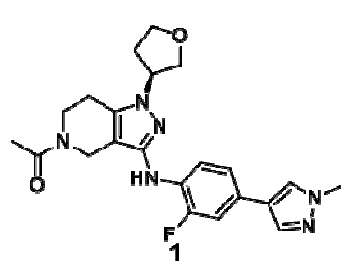
- 1
2
3
4
5
6
7
8
9
10
11
12
13
14
15
16
17
18
19
20
21
22
23
24
25
26
27
28
29
30
31
32
33
34
35
36
37
38
39
40
41
42
43
44
45
46
47
48
49
50
51
52
53
54
55
56
57
58
59
60
- (14) Rooney, T. P. C.; Filippakopoulos, P.; Fedorov, O.; Picaud, S.; Cortopassi, W. A.; Hay, D. A.; Martin, S.; Tumber, A.; Rogers, C. M.; Philpott, M.; Wang, M.; Thompson, A. L.; Heightman, T. D.; Pryde, D. C.; Cook, A.; Paton, R. S.; Müller, S.; Knapp, S.; Brennan, P. E.; Conway, S. J. A Series of Potent CREBBP Bromodomain Ligands Reveals an Induced-Fit Pocket Stabilized by a Cation- Π Interaction. *Angew. Chem. Int. Ed.* **2014**, *53*, 6126–6130.
- (15) Hay, D. A.; Fedorov, O.; Martin, S.; Singleton, D. C.; Tallant, C.; Wells, C.; Picaud, S.; Philpott, M.; Monteiro, O. P.; Rogers, C. M.; Conway, S. J.; Rooney, T. P. C.; Tumber, A.; Yapp, C.; Filippakopoulos, P.; Bunnage, M. E.; Müller, S.; Knapp, S.; Schofield, C. J.; Brennan, P. E. Discovery and Optimization of Small-Molecule Ligands for the CBP/P300 Bromodomains. *J. Am. Chem. Soc.* **2014**, *136*, 9308–9319.
- (16) Unzue, A.; Xu, M.; Dong, J.; Wiedmer, L.; Spiliotopoulos, D.; Caflisch, A.; Nevado, C. Fragment-Based Design of Selective Nanomolar Ligands of the CREBBP Bromodomain. *J. Med. Chem.* **2016**, *59*, 1350–1356.
- (17) Picaud, S.; Fedorov, O.; Thanasopoulou, A.; Leonards, K.; Jones, K.; Meier, J.; Olzscha, H.; Monteiro, O.; Martin, S.; Philpott, M.; Tumber, A.; Filippakopoulos, P.; Yapp, C.; Wells, C.; Che, K. H.; Bannister, A.; Robson, S.; Kumar, U.; Parr, N.; Lee, K.; Lugo, D.; Jeffrey, P.; Taylor, S.; Vecellio, M. L.; Bountra, C.; Brennan, P. E.; O'Mahony, A.; Velichko, S.; Müller, S.; Hay, D.; Daniels, D. L.; Urh, M.; La Thangue, N. B.; Kouzarides, T.; Prinjha, R.; Schwaller, J.; Knapp, S. Generation of a Selective Small Molecule Inhibitor of the CBP/P300 Bromodomain for Leukemia Therapy. *Cancer Res.* **2015**, *75*,

- 1
2
3 5106–5119.
4
5
6 (18) Hammitzsch, A.; Tallant, C.; Fedorov, O.; O'Mahony, A.; Brennan, P. E.; Hay,
7
8 D. A.; Martinez, F. O.; Al-Mossawi, M. H.; de Wit, J.; Vecellio, M.; Wells, C.;
9
10 Wordsworth, P.; Müller, S.; Knapp, S.; Bowness, P. CBP30, a Selective
11
12 CBP/P300 Bromodomain Inhibitor, Suppresses Human Th17 Responses. *Proc.*
13
14 *Natl. Acad. Sci. U. S. A.* **2015**, *112*, 10768–10773.
15
16
17 (19) Denny, R. A.; Flick, A. C.; Coe, J. W.; Langille, J.; Basak, A.; Liu, S.; Stock, I.
18
19 A.; Sahasrabudhe, P.; Bonin, P. D.; Hay, D. A.; Brennan, P. E.; Pletcher, M. T.;
20
21 Jones, L. H.; Chekler, E. L. P. Structure-Based Design of Highly Selective
22
23 Inhibitors of the CREB Binding Protein Bromodomain. *J. Med. Chem.* **2017**, *60*,
24
25 5349–5363.
26
27
28 (20) Romero, F. A.; Magnuson, S.; Pastor, R.; Tsui, V.; Murray, J.; Crawford, T.;
29
30 Albrecht, B. K.; Côté, A.; Taylor, A. M.; Lai, K. W.; Chen, K. X.; Bronner, S.;
31
32 Adler, M.; Egen, J.; Liao, J.; Wang, F.; Cyr, P.; Zhu, B.-Y.; Kauder, S. 4,5,6,7-
33
34 Tetrahydro-1H-Pyrazolo[4,3-C]Pyridin-3-Amine Compounds as CBP and/or
35
36 EP300 Inhibitors. WO2016086200. 2016.
37
38
39 (21) Romero, F. A.; Taylor, A. M.; Crawford, T. D.; Tsui, V.; Côté, A.; Magnuson, S.
40
41 Disrupting Acetyl-Lysine Recognition: Progress in the Development of
42
43 Bromodomain Inhibitors. *J. Med. Chem.* **2016**, *59*, 1271–1298.
44
45
46 (22) The (*S*) absolute stereochemistry of **8** was determined from the co-crystal
47
48 structure of **8** in the CBP bromodomain. In every instance the (*S*)-enantiomer
49
50 was always more potent than the (*R*)-enantiomer (data not shown). compounds **3**,
51
52
53 **5**, **6**, **7** and **9** were synthesized from (*R*)-tetrahydrofuran-3-ol and thus the
54
55
56
57
58
59
60

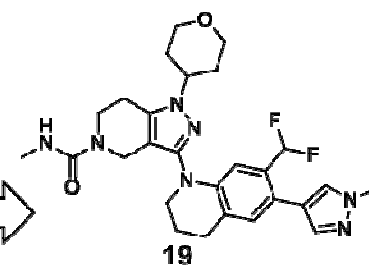
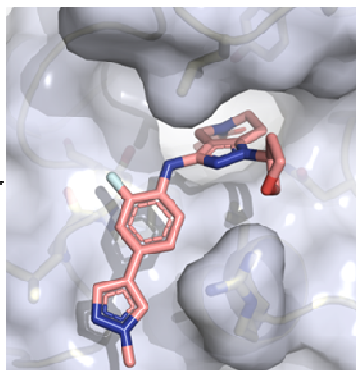
- 1
2
3 absolute stereochemistry is unambiguously that of the (*S*)-configuration.
4
5
6 (23) MoKa Molecular Discovery, Perugia. www.Moldiscovery.com/Software/Moka/
7
8 (Accessed July 27, 2017).
9
10
11 (24) Leeson, P. D.; Springthorpe, B. The Influence of Drug-Like Concepts on
12 Decision-Making in Medicinal Chemistry. *Nat. Rev. Drug Discovery* **2007**, *6*,
13 881–890.
14
15
16
17 (25) Hopkins, A. L.; Groom, C. R.; Alex, A. Ligand Efficiency: A Useful Metric for
18 Lead Selection. *Drug Discovery Today* **2004**, *9*, 430–431.
19
20
21
22 (26) Chan, H. M.; La Thangue, N. B. P300/CBP Proteins: HATs for Transcriptional
23 Bridges and Scaffolds. *J. Cell Sci.* **2001**, *114*, 2363–2373.
24
25
26
27 (27) Sakaguchi, S.; Yamaguchi, T.; Nomura, T.; Ono, M. Regulatory T Cells and
28 Immune Tolerance. *Cell* **2008**, *133*, 775–787.
29
30
31
32 (28) Tanaka, A.; Sakaguchi, S. Regulatory T Cells in Cancer Immunotherapy. *Cell*
33 *Res.* **2017**, *27*, 109–118.
34
35
36
37 (29) Shimizu, J.; Yamazaki, S.; Sakaguchi, S. Induction of Tumor Immunity by
38 Removing CD25 +CD4+ T Cells: a Common Basis Between Tumor Immunity
39 and Autoimmunity. *J. Immunol.* **1999**, *163*, 5211–5218.
40
41
42
43 (30) Hori, S.; Nomura, T.; Sakaguchi, S. Control of Regulatory T Cell Development
44 by the Transcription Factor Foxp3. *Science* **2003**, *299*, 1057–1061.
45
46
47
48 (31) Liu, Y.; Wang, L.; Han, R.; Beier, U. H.; Akimova, T.; Bhatti, T.; Xiao, H.;
49 Cole, P. A.; Brindle, P. K.; Hancock, W. W. Two Histone/Protein
50 Acetyltransferases, CBP and P300, Are Indispensable for Foxp3+ T-Regulatory
51 Cell Development and Function. *Mol. Cell. Biol.* **2014**, *34*, 3993–4007.
52
53
54
55
56
57
58
59
60

- 1
2
3
4
5
6
7
8
9
10
11
12
13
14
15
16
17
18
19
20
21
22
23
24
25
26
27
28
29
30
31
32
33
34
35
36
37
38
39
40
41
42
43
44
45
46
47
48
49
50
51
52
53
54
55
56
57
58
59
60
- (32) Crawford, T. D.; Tsui, V.; Flynn, E. M.; Wang, S.; Taylor, A. M.; Côté, A.; Audia, J. E.; Beresini, M. H.; Burdick, D. J.; Cummings, R. T.; Dakin, L. A.; Duplessis, M.; Good, A. C.; Hewitt, M. C.; Huang, H.-R.; Jayaram, H.; Kiefer, J. R.; Jiang, Y.; Murray, J. M.; Nasveschuk, C. G.; Pardo, E.; Poy, F.; Romero, F. A.; Tang, Y.; Wang, J.; Xu, Z.; Zawadzke, L. E.; Zhu, X.; Albrecht, B. K.; Magnuson, S. R.; Bellon, S. F.; Cochran, A. G. Diving Into the Water: Inducible Binding Conformations for BRD4, TAF1(2), BRD9, and CECR2 Bromodomains. *J. Med. Chem.* **2016**, *59*, 5391–5402.
- (33) Albrecht, B. K.; Gehling, V. S.; Hewitt, M. C.; Vaswani, R. G.; Côté, A.; Leblanc, Y.; Nasveschuk, C. G.; Bellon, S.; Bergeron, L.; Campbell, R.; Cantone, N.; Cooper, M. R.; Cummings, R. T.; Jayaram, H.; Joshi, S.; Mertz, J. A.; Neiss, A.; Normant, E.; O'Meara, M.; Pardo, E.; Poy, F.; Sandy, P.; Supko, J.; Sims, R. J., III; Harmange, J.-C.; Taylor, A. M.; Audia, J. E. Identification of a Benzoisoxazoloazepine Inhibitor (CPI-0610) of the Bromodomain and Extra-Terminal (BET) Family as a Candidate for Human Clinical Trials. *J. Med. Chem.* **2016**, *59*, 1330–1339.

Table of Contents Graphic



CBP IC_{50} = 0.02 μ M
CBP BRET IC_{50} = 0.41 μ M
BRD4(1) IC_{50} = 13 μ M



CBP IC_{50} = 0.0009 μ M
CBP BRET IC_{50} = 0.006 μ M
BRD4(1) IC_{50} = 5.1 μ M

